

**STUDIES TOWARDS THE EFFICIENT ISOLATION
AND PURIFICATION OF ANALOGUES OF
AMPHOTERICIN B FROM *STREPTOMYCES*
*NODOSUS***

Thesis submitted for the degree of
Doctor of Philosophy
at The University of Leicester

by

Odubunmi Olajumoke Ibrahim BSc (Hons), MSc

Department of Chemistry

University of Leicester

May 2013

Odubunmi Olajumoke Ibrahim

Studies towards the efficient isolation and purification of analogues of amphotericin B from *Streptomyces nodosus*

Abstract

Amphotericin B, produced by *Streptomyces nodosus*, is a medically important antifungal that is also active against *Leishmania* parasites. However, its use is severely limited by its toxicity. Treatment would be much more effective if non-toxic analogues of amphotericin B were available. Genetic manipulation of *S. nodosus* can provide access to such analogues potentially at clinically affordable cost.

Amphotericin B has been shown to be biosynthesised by a modular polyketide synthase (PKS) and three post PKS enzymes. Genetic disruption of one of the post PKS genes encoding a cytochrome P450 produces 16-descarboxyl-16-methyl-amphotericin B, which has been shown to be less toxic yet retains antifungal activity.

This thesis describes efforts to obtain improved characterisation and X-ray analysis of the PKS product, 8-deoxy-16-descarboxyl-16-methyl amphoteronolide B, by synthesising an octabenzoyl derivative. Results obtained show the derivatisation of the lactol gave the benzoyl ketone. Crystals were obtained but failed to diffract.

This thesis also describes the *in vivo* production, isolation, purification and characterisation of 16-descarboxyl-16-methyl-amphotericin B, 8-deoxy-16-descarboxyl-16-methyl amphotericin A and 16-descarboxyl-16-methyl-19-(O)-perosaminyl amphoteronolide B (pHap2). Evidence is also presented that the yield of extracts from various mutants of amphotericin B can be significantly improved by strain selection and optimising the growth conditions.

Improved purification protocols involving the intermediacy of less polar N-fluorenylmethoxycarbonyl (Fmoc) derivatives are also described. The use of Fmoc intermediates enabled partial purification by flash chromatography. However, derivatisation of very low purity samples (especially pHap2) resulted in low yields and formation of by-products.

The methodology reported in this thesis showed promise for assisting with large scale purification of a variety of glycosylated analogues of amphotericin B for extensive biological assays and assist with investigations into the mode of action of these antibiotics.

Acknowledgements

I will like to express my deepest appreciation to my supervisor, Dr Bernard Rawlings, for his patience, support, understanding and invaluable advice. I will also like to thank Dr Patrick Caffrey for providing the mutants I used for my research and Dr Barry Murphy for showing me the ropes and teaching me how to have 'green fingers'.

Furthermore, I will like to thank the staff and students in the Department of Chemistry, especially those in the Organic Group, for their support and for making my time at the university very memorable. Special mention goes to Kat Pugh, Helen Lewis, Sharifa Al Jabri, and Vicky Davison, for being there when I needed to vent frustrations and the few occasions when I needed to celebrate successes. Thanks to Mick Lee and Gerry Griffiths for their technical support.

Special thanks to my husband, Shehu, for being my greatest motivator and for being very understanding. I am grateful to my precious children for their patience and for always giving me a reason to smile. I will also like to thank my parents and siblings for their prayers and encouragement. Most importantly, thanks to God, for life and for being my hope.

Table of Contents

Abstract	2
Acknowledgements	3
Table of Contents	4
List of Figures	8
Abbreviations	14
Chapter one : Introduction	17
1.1 Amphotericin B	17
1.2 Clinical uses of amphotericin B	19
1.3 Mode of action	25
1.4 Semi-synthetic derivatives of amphotericin B	34
1.5 Biosynthesis of amphotericin B	36
1.6 Genetically engineered analogues	44
1.7 Aims of the project	56
Chapter two: Studies towards the efficient isolation and purification of 16-descarboxy-16-methyl-amphoterolide B from the “ΔamphNM+perDIDII” mutant	57
2.1 Introduction	57
2.2 Isolation, purification and derivatisation of 8-deoxy-16-descarboxy-16-methyl-amphoterolide B (21)	64
2.3 Derivatisation of aglycone (21) with benzoyl chloride	67
2.4 Crystallisation procedure for octabenzoyl aglycone	74
2.5 Variation and optimisation of benzoylation method	75
2.6 Conclusion	77

Chapter three: Isolation, purification and characterisation of 16- descarboxyl-16-methyl-amphotericin B and 8-deoxy-16-descarboxyl- 16-methyl-amphotericin A	78
3.1 Introduction	78
3.2 Extraction and purification of 16-descarboxyl-16-methyl- amphotericin B from the “ <i>Δ amphNM+perDIDI</i> ” mutant	79
3.3 Extraction and purification of 16-descarboxyl-16-methyl- amphotericin B (16) from the ‘ <i>amphNM</i> ’ mutant	95
3.4 8-Deoxy-16-descarboxyl-16-methyl-amphotericin A	102
3.5 Extraction of 8-deoxy-16-descarboxyl-16-methyl-amphotericin A (53)	103
3.6 Purification and analysis of 8-deoxy-16-descarboxyl-16-methyl- amphotericin A (53)	105
3.7 Conclusion	105
 Chapter four: Fmoc derivatisation	 107
4.1 Introduction	107
4.2 N-Fmoc derivatives of amphotericin analogues	108
4.3 N-Fmoc derivative of 16-descarboxyl-16-methyl-amphotericin B (16)	122
4.4 Variation and optimisation of Fmoc protection method	122
4.5 8-Deoxy-16-descarboxyl-N-fluorenylmethyloxycarbonyl-16-methyl- amphotericin A (62)	131
4.6 Deprotection of 16-descarboxyl-N-fluorenylmethyloxycarbonyl-16- methyl-amphotericin B (60)	136
4.7 Deprotection of 8-deoxy-16-descarboxyl-N- fluorenylmethyloxycarbonyl-16-methyl-amphotericin A (62)	143
4.8 Conclusion	144

**Chapter five: Isolation, purification and characterisation of 16-
descarboxyl-16-methyl-19-(O)-perosaminyl amphoteronolide B**

146

5.1	Introduction	146
5.2	extraction and purification of 16-descarboxyl-16-methyl-19-(O)- perosaminyl amphoteronolide B (66)	155
5.3	Fmoc derivatisation	176
5.4	Variation/optimisation of method used	179
5.5	Deprotection of 16-descarboxyl- <i>N</i> -fluorenylmethyloxycarbonyl-16- methyl-19-(O)-perosaminyl amphoteronolide B (68)	181
5.6	Conclusion/future work	183

Chapter six: Experimental 184

6.1	General conditions	184
6.2	Extraction of metabolites	190
6.3	8-Deoxy-16-descarboxyl-16-methyl-amphoteronolide B	191
6.4	(3R,5R,9S,11S,15R,17S,19S,35S)-Octabenzoyloxy-13-oxo- (16S,34S,36S)-trimethyl-(20E,22E,24E,26E,30E,32E)- octatriacontaheptaeno-(37S)-lactone (56)	192
6.5	16-Descarboxyl-16-methyl-amphotericin B (16)	197
6.6	8-Deoxy-16-descarboxyl-16-methyl-amphotericin A	203
6.7	16-Descarboxyl- <i>N</i> -fluorenylmethyloxycarbonyl-16-methyl- amphotericin B (60)	204
6.8	Optimisation of the method for the Fmoc derivatisation of 16- descarboxyl-16-methyl-amphotericin B (16)	208
6.9	8-Deoxy-16-descarboxyl- <i>N</i> -fluorenylmethyloxycarbonyl-16-methyl- amphotericin A (62)	210
6.10	Deprotection of 16-descarboxyl- <i>N</i> -fluorenylmethyloxycarbonyl-16- methyl-amphotericin B (60)	214
6.11	Deprotection of 8-Deoxy-16-descarboxyl- <i>N</i> - fluorenylmethyloxycarbonyl-16-methyl-amphotericin A (62)	217

6.12	Extraction of 16-descarboxyl-16-methyl-19-(<i>O</i>)-perosaminyl amphoteronolide B (62)	218
6.13	16-Descarboxyl- <i>N</i> -fluorenylmethyloxycarbonyl-16-methyl-19-(<i>O</i>)- perosaminyl amphoteronolide B (68)	223
6.14	Deprotection of 16-descarboxyl- <i>N</i> -fluorenylmethyloxycarbonyl-16- methyl-19-(<i>O</i>)-perosaminyl amphoteronolide B (68)	226
	Appendices	227
	References	243

List of Figures

- Figure 1.1 Structures of amphotericin B (**1**) and amphotericin A (**2**)
- Figure 1.2 Structures of Nystatin A1 (**3**) and Pimaricin (**4**)
- Figure 1.3 Structures of Ergosterol (**5**) and Cholesterol (**6**)
- Figure 1.4 Structures of Griseofulvin (**7**), Flucytosine (**8**) and Fluconazole (**9**)
- Figure 1.5 Structure of anidulafungin (**12**)
- Figure 1.6 Structure of Miltefosine (**13**)
- Figure 1.7 Hypothetical structure of a “barrel-stave” ion channel formed by 8 amphotericin Bs (**1**) and 8 sterols. Yellow and blue molecules represent **1** and sterol, respectively.
- Figure 1.8 Structure of N-acetyl amphotericin B (**14**)
- Figure 1.9 Structure of amphotericin B methyl ester (**15**)
- Figure 1.10 Open and Closed conformation of amphotericin B
- Figure 1.11 Structures of Intramolecular methylene bridged derivatives of amphotericin B
- Figure 1.12 Structure of the hypothetical conformation of amphotericin B with ergosterol
- Figure 1.13 Structure of 16-descarboxyl-16-methyl-amphotericin B (**17**)
- Figure 1.14 Structures of 13, 14-anhydro amphotericin B (**18**), 16-descarboxyl-16-hydroxymethyl-amphotericin B (**19**) and 13-methoxy-amphotericin B (**20**)
- Figure 1.15 Structure of *N*-methyl-*N*-D-fructosyl amphotericin B methyl ester (**21**)
- Figure 1.16 Structure of the PKS aglycone product of amphotericin B biosynthesis showing the role of Amph ABCIJK

- Figure 1.17 Structures of the PKS aglycone product of nystatin (**23**) and pimaricin (**24**) biosynthesis showing the role of NysABCDEFGHIJK and PimS01234 respectively
- Figure 1.18 Modular structures of polyene macrolide synthases with modules classified on the basis of the functional domains that they include
- Figure 1.19 Structures of 32,33-dihydro-33-hydroxy-nystatin A1 and 30,31-dihydro-31-hydroxy-nystatin A1
- Figure 1.20 Structures of S44HP (**27**) and BSG003 (**28**)
- Figure 1.21 Structures of BSG005 (**29**) and BSG018 (**30**)
- Figure 1.22 Structures of 8-deoxy-nystatin A1 (**31**), 8-deoxy-16-descarboxy-16-methyl-nystatin A1 (**32**), 8-deoxy-amphotericin B (**33**) and 8-deoxy-16-descarboxy-16-methyl-amphotericin B (**34**)
- Figure 1.23 Structures of 8-deoxy-amphoterolide B (**45**) and 8-deoxy-amphoterolide A (**46**)
- Figure 2.1 Structures of candicidin (**50**) and rimocidin (**51**)
- Figure 2.2 Structure of perimycin A (**52**)
- Figure 2.3 Structures of 8-deoxy-16-descarboxy-16-methyl-amphotericin B (**34**) and 8-deoxy-16-descarboxy-16-methyl-amphotericin A (**54**)
- Figure 2.4 Proton NMR showing the presence of lipids in aglycone (**22**) after purification
- Figure 2.5 NP-HPLC of octabenzoyl amphoterolide B showing traces of heptabenzoyl amphoterolide B (flash column product)

- Figure 2.6 Structure of 13, 14-anhydro derivative of octabenzoyl product
- Figure 2.7 ^{13}C -NMR of octabenzoyl amphoteronolide B showing no resonance at 153.5ppm
- Figure 2.8 ^{13}C -NMR for octabenzoyl amphoteronolide B in CDCl_3 showing resonance at 203 ppm and no acetal peak at 100 ppm.
- Figure 2.9 The possible conformation of the octabenzoyl derivative of **22**
- Figure 2.10 Suggested mechanism for the production of octabenzoyl lactol
- Figure 2.11 FAB-MS showing a mixture of heptabenzoyl and octabenzoyl amphoteronolide B
- Figure 2.12 Octabenzoyl amphoteronolide B (**45**)
- Figure 2.13 ESMS (+ve) showing presence of Octabenzoyl amphoteronolide B (**45**)
- Figure 3.1 Structure of 8-deoxy-16-descarboxyl-16-methyl-amphoteronolide B (**22**) and 16-descarboxyl-16-methyl-amphotericin B (**17**)
- Figure 3.2 RP-HPLC (405 nm) of the crude methanolic extract of '*amphNM+perDIDI*' grown with thiostrepton in the preculture and production media
- Figure 3.3 RP-HPLC (405 nm) of the crude methanolic extract of "*ΔamphNM+perDIDI*" grown with thiostrepton in the preculture but not in the production media

- Figure 3.4 RP-HPLC (405 nm) of the crude methanolic extract of “*ΔamphNM+perDIDI*” grown without thiostrepton in both the preculture and production media
- Figure 3.5 Comparison of the ratio of **17:22** isolated from “*ΔamphNM+perDIDI*” using different growth conditions
- Figure 3.6 Comparison of the amount of total heptaene isolated from “*amphNM+perDIDI*” mutant under the same growth conditions but with varying duration of incubation
- Figure 3.7 Proton NMR of **17** after water wash confirmed that the precipitate contains largely lipids
- Figure 3.8 An illustration of the preparation of preculture 1 (‘pc1’) and preculture 2 (‘pc2’) of the *amphNM* mutant
- Figure 3.9 Comparison of yield of **17** (as a percentage of the total heptaene) isolated from preculture 1 (‘pc1’) and preculture 2 (‘pc2’)
- Figure 3.10 Set-up for separation of mycelia and beads from broth
- Figure 3.11 Structure of 8-deoxy-16-descarboxyl-16-methyl-amphotericin A (**42**)
- Figure 3.12 RP-HPLC showing the crude extract of tetraenes present in *amphNM* disruptant
- Figure 3.13 Structure of 16-descarboxyl-16-methyl-amphotericin A (**58**)
- Figure 4.1 Structure of 14-fluoro-amphotericin B (**59**)

- Figure 4.2 Structure of amphotericin B (**1**), amphotericin B methyl ester (**15**) and 28-¹⁹F-amphotericin B methyl ester (**60**)
- Figure 4.3 Structure of 16-descarboxyl-*N*-fluorenylmethylcabonyl-16-methyl-amphotericin B (**61**)
- Figure 4.4 Positive ion ESMS showing the sodium adduct of **61**
- Figure 4.5 Proton NMR of **61** showing presence of lipids and aromatic impurity
- Figure 4.6 Structure of *N*-Fmoc derivative of **17** (**61**) and 13-methoxy-*N*-Fmoc derivative of **17** (**62**)
- Figure 4.7 NP-HPLC showing the hemi acetal and methyl ketal isomers from the *N*-Fmoc derivative of **17**
- Figure 4.8 Proton NMR showing precipitate and supernatant from crystals of *N*-Fmoc NM (**61**)
- Figure 4.9 Structure of *N*-Fmoc derivative of amphotercin A (**63**)
- Figure 4.10 Fmoc region of **63** showing C-9" and C-10"
- Figure 5.1 Structure of 8-deoxy-amphoterionolide A (**46**)
- Figure 5.2 Structure of perimycin A aglycone (**65**) and 8-deoxy-amphoterionolide B (**22**) showing similar glycosylation sites
- Figure 5.3 Structure of 19-(*O*)-perosaminyl-amphoterionolide B (**66**)
- Figure 5.4 Structure of 16-descarboxyl-16-methyl-19-(*O*)-perosaminyl-amphoterionolide B (**67**) and 8-deoxy-16-descarboxy-16-methyl-19-(*O*)-perosaminyl-amphoterionolide B (**68**)
- Figure 5.5 The effect of a change in the duration of incubation on the yield of **67**

- Figure 5.6 RP-HPLC showing combined methanolic extracts of **67** from muslin cloth (A) and Erlenmeyer method (B)
- Figure 5.7 RP-HPLC showing fourth extraction from the Erlenmeyer flask method (left) and third extraction from the muslin cloth method (right)
- Figure 5.8 RP-HPLC showing crude extract from the pHap2 mutant
- Figure 5.9 RP-HPLC showing a sample of the crude extract of the pHap2 mutant spiked with the crude extract from the *amphNM* mutant
- Figure 5.10 Proton NMR showing **67** after semi preparative HPLC
- Figure 5.11 UV spectra showing the wavelength of **67** at 403 nm and not 405 nm
- Figure 5.12 Structure of 8-deoxy-16-descarboxy-16-methyl-19-(O)-perosaminyl-amphoteronolide B (**68**)
- Figure 5.13 RP-HPLC showing precipitate and supernatant after ethyl acetate extraction of **67**
- Figure 5.14 Comparison of the position of the amino group in pHap2 (**67**) and *amphNM* (**17**)
- Figure 5.15 RP-HPLC showing deprotected **69** with traces of aglycone present

Abbreviations

Ac	Acetyl
ACP	Acyl carrier protein
AIDS	Acquired Immune Deficiency Syndrome
AME	Amphotericin B methyl ester
AT	Acyltransferase
Amph A	Amphotericin A
Amph B	Amphotericin B
Atm	Atmospheric pressure
Bz	Benzoyl
°C	Degrees Celsius
COSY	Correlation Spectroscopy
CSA	Camphorsulfonic acid
DEPT	Distortionless enhancement by polarisation transfer
DH	Dehydratase
DMSO	Dimethylsulfoxide
DMF	Dimethylformamide
Et	Ethyl
EtOAc	Ethylacetate
EtOH	Ethanol
ER	Enoylreductase
ESMS	Electrospray mass spectroscopy

eV	Electron volt
FD	Fructose-Dextrin
Fmoc-OSu	<i>N</i> -(9-Fluorenylmethoxy carbonyloxy) succinimide
Fmoc	Fluorenylmethoxycarbonyl
g	Gram
GDP	Guanine diphosphate
GT	Glycosyltransferase
GYE	Glucose-Yeast media
HPLC	High pressure liquid chromatography
Hz	Hertz
KR	ketoreductase
KS	Keto synthase
L	Litre
M	Molar
Me	Methyl
MeOH	Methanol
mg	Milligram
MHz	Megahertz
mmol	Millimole
m.p.	Melting point
m/z	Mass charge ratio
NMR	Nuclear magnetic resonance
PKS	Polyketide synthase

NFAME	<i>N</i> -methyl- <i>N</i> -D-fructosyl-amphotericin B methyl ester
NP-HPLC	Normal phase HPLC
PEG	Polyethylene glycol
ppm	Parts per million
rpm	Revolutions per minute
RP-HPLC	Reversed phase HPLC
RT	Room temperature
δ	Chemical shift relative to TMS
YG	Yeast-Glucose
TLC	Thin layer chromatography
TSE	Transmissible spongiform encephalopathies
UV	Ultraviolet

Chapter One: Introduction

1.1 Amphotericin B

Amphotericin B (Amph B) (**1**) is a polyene macrolide (Fig. 1.1) that was first isolated from the soil bacterium *Streptomyces nodosus* in 1955 along with its 'tetraene' 28,29-dihydro analogue, amphotericin A (**2**).¹

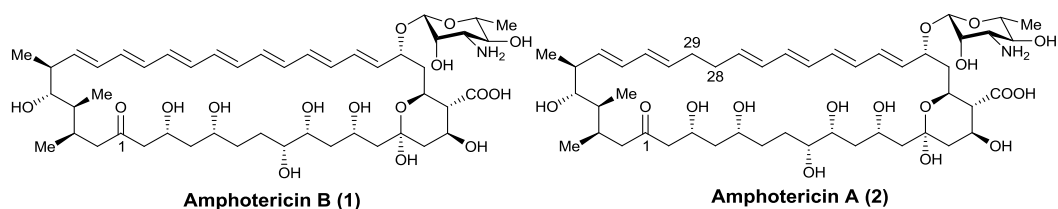


Figure 1.1 Structures of amphotericin B (**1**) and amphotericin A (**2**)

Amphotericin B (**1**) has been the most therapeutically effective antifungal agent for over five decades. It still serves as a point of reference for the potency of any new antifungal drug produced. In recent years, **1** has been used as a frontline treatment against leishmaniases.² Promising antiviral, and antiprion properties of **1** have also been reported.³ Other commercially important polyenes include the heptaene nystatin A1 (**3**) (also called fungicidin), that is used orally and topically as an antifungal,⁴ and the tetraene pimaricin (**4**) (also called natamycin), that is used in the food industry to prevent fungal growth on dried meat products and dairy products such as cottage cheese and yoghurt (Fig 1.2).⁵

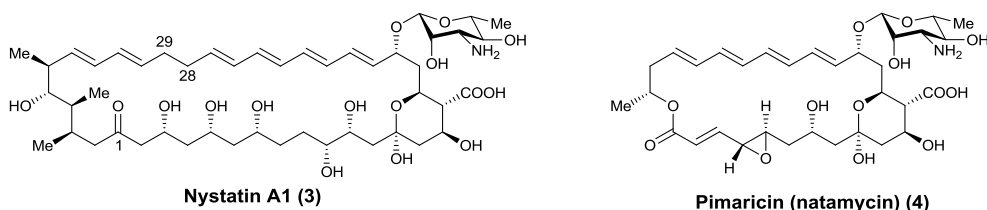


Figure 1.2 Structures of Nystatin A1 (**3**) and Pimaricin (**4**)

The primary mode of action of **1** is thought to be complexation with the fungal or trypanosomal steroid ergosterol (**5**) (Fig 1.3), followed by selective pore formation in fungal or trypanosomal membranes leading to uncontrolled loss of small metabolites and ions⁶ although other mechanisms may also be involved such as radical formation⁷ or binding to ergosterol making it unavailable for fungal use.⁸ The human toxicity is thought to be due to a combination of its general insolubility and tendency to aggregate leading to blockage of kidney vessels, along with less specific complexation with vertebrate steroid cholesterol, leading to some formation of transmembrane pores.⁹

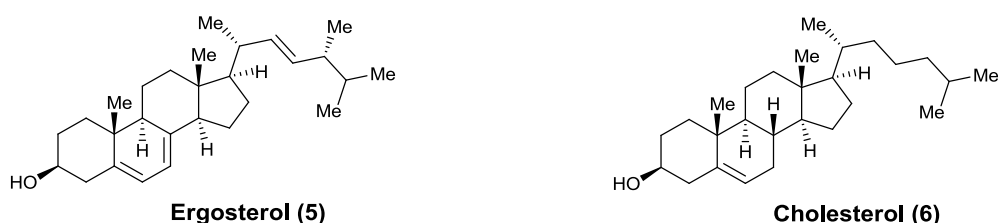


Figure 1.3 Structures of Ergosterol (**5**) and Cholesterol (**6**)

The overall structure of **1** comprises two rigid fragments, a macrolide ring and a mycosamine sugar moiety, which are linked by a rotatable β -glycosidic bond.^{10,11} The aglycone is composed of a hydrophilic polyhydroxyl chain along one side and a lipophilic polyene hydrocarbon chain on the other side, with a carboxyl group and 6-deoxyaminosugar

attached at one end. The amino group and carboxyl group can form a zwitterionic complex.^{12,13} Amphotericin B is poorly soluble in water (0.0017mg/mL).¹⁴ If the concentration of **1** is any higher, a mixture of soluble and insoluble aggregates is formed.¹³ The low solubility of **1** in other organic solvents has been attributed to the presence of so many free hydroxyl groups in the molecule.

1.2 Clinical uses of amphotericin B

1.2.1 Other antifungal agents

There are only a limited range of antifungal agents in therapy due to the close similarity of fungal and mammalian cells, they are both eukaryotes. The emergence of AIDS and the associated rise in fatal mycoses due to the use of immunosuppressant medical therapies stimulated the research into novel antifungal agents. Established antifungal agents include griseofulvin (**7**) (Fig. 1.4) that interferes with microtubule assembly (limited selectivity or fungal assembly)¹⁵; flucytosine (**8**) that is converted *in vivo* to 5-fluorouracil inhibiting thymidylate synthase.^{16,17}

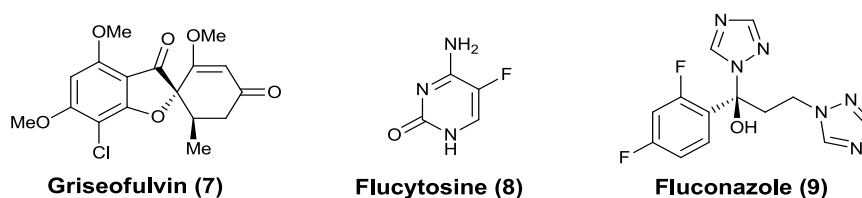
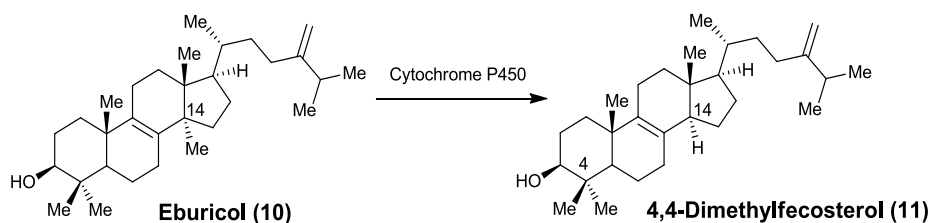


Figure 1.4 Structures of Griseofulvin (**7**), Flucytosine (**8**) and Fluconazole (**9**)

Many other established antifungal agents selectively target the biosynthesis of the fungal steroid, ergosterol.¹⁸ Both ergosterol (**5**) and cholesterol (**6**) are derived from lanosterol, but *via* different pathways.¹⁹ The principal target of the azoles such as fluconazole (**9**) is a cytochrome P450 enzyme responsible for oxidative removal of the 14 α -methyl group in **10** to give **11** (Scheme 1.1), a process specific to ergosterol biosynthesis.^{20,21} The azole's nitrogen binds to the haem iron inhibiting the enzyme. As the shape of the active site varies from fungal species to fungal species, different azoles are required to treat different species.²⁰ Resistance is increasing, mechanisms are thought to include

- i. efflux due to increased expression of membrane efflux pumps
- ii. overexpression of the demethylase or
- iii. mutations in the methylase reducing binding of the triazole.



Scheme 1.1 Oxidative demethylation of Eburicol (**10**)

More recently, the echinocandins, such as anidulafungin (**12**) (Fig. 1.5), have been used to treat azole resistant *Candida*.²² In contrast to the azoles, **12** targets the complex of membrane bound proteins that synthesise cell wall β -1,-3-D-glucan polysaccharides, an important component of the fungal cell wall.²⁰ It has been reported to be as effective as **1** against yeast infections, especially in invasive *Candida* and

antibacterial antibiotics on the assumption that an undiagnosed fungal infection is responsible.

Due to its poor solubility in most solvents, **1** was initially injected into the bloodstream as a DMSO solution. Later it was injected as a complex with cholic acid (fungizone) which is inexpensive and has been used for many years.⁶ Recent formulations such as liposomal formulation 'Ambisome' have greatly reduced toxicity and increased antifungal specificity.²⁷ In order to make these formulations, **1** is incorporated into a single liposomal bilayer composed of phospholipids and cholesterol. They are easier to administer, less toxic but very expensive, limiting their application.

1.2.3 Amphotericin B as an antileishmanial antibiotic

Leishmaniasis is a vector borne disease caused by various species of *Leishmania*, an obligate intra-macrophage protozoan parasite, and is fatal if left untreated.²⁸ The parasite is transmitted by the female phlebotomine sand fly.²⁹ Cutaneous leishmaniases gives rise to unsightly boils, and was referred to by British troops in Iraq as Baghdad boils. The mucocutaneous form is characterised by itchy lesion on an arm or leg or the face with possible swollen lymph nodes in the same area. Over a few months, the sore worsens and destroys surrounding tissue resulting in extreme disfigurement of the affected areas. However, the most fatal form is

visceral leishmaniasis (kala azar), whilst less visually horrific destroys internal organs resulting in death if left untreated.²

There are 500,000 new cases each year, with 50,000 fatalities, second only to malaria.^{30,31} Most (90%) of new cases occur in Bangladesh, India, Nepal and the Sudan. There are cases in Southern Europe, but due to the high level of health and nutrition, those infected rarely show symptoms.

For seventy years, the treatment was pentavalent antimonials such as sodium stibogluconate.² These are toxic drugs with life threatening side effects and resistance especially in Bihar and Nepal is now widespread. Whilst still used in some remote regions, the failure rate is now very high. Paromycin is an aminoglycoside with good antileishmanial activity^{32,33} that showed promising results in India, but is no longer manufactured.

Conventional amphotericin B (fungizone) is now the first line of treatment, but side effects coupled with the need for fifteen infusions over a month of hospitalisation is a complicated regime for these poor regions. However, efficacy is close to 100%. Miltefosine (**13**) is a new oral treatment that despite being teratogenic is entering clinical practice.

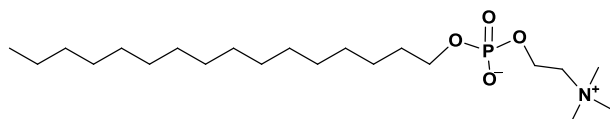


Figure 1.6 Structure of miltefosine (**13**)

The combination of miltefosine and **1** is showing promise. Liposomal amphotericin B (Ambisome), with its reduced toxicity, is considered the

best treatment,³⁴ and is used in First World countries, but costs \$3000 per treatment. In 2007, a subsidy was introduced by the WHO to reduce this to \$200 in poor areas. Progress towards developing a vaccine has been limited.³⁵

1.2.4 Prospective uses of Amphotericin B

1.2.4.1 Prion diseases

Prion diseases or transmissible spongiform encephalopathies (TSEs) are a group of neurodegenerative disorders that have the unique property of being infectious, sporadic and genetic in origin. They are associated with the conversion of a normal host protein, PrP^C into a pathogenic isoform PrP^{Sc}. In spite of years of research, there is no known cure for TSEs.³⁶

Compounds such as sulfated polyanions,³⁷ Congo red,³⁸ **1**³⁹ and the amphotericin B benzylidene derivative MS-8209,^{40,41} have prolonged survival in experimental models of scrapie. Of these compounds, only **1** and MS-8209 exerted an effect when administered late in disease.

Amphotericin B (**1**) has been shown to delay the accumulation of PrP^{Sc}⁴¹ and to increase the incubation time of the disease after experimental transmission in laboratory animals. Mange *et al.*, have shown that **1** interferes with the generation of abnormal PrP^C isoforms in culture.³⁹

Although amphotericin B's therapeutic action in TSEs is uncertain, it may relate to polyene complexes inhibiting conversion of PrP^C to PrP^{Sc}.

1.2.4.2 HIV treatment

Highly active antiretroviral therapy effectively suppresses HIV-1 replication but cannot eradicate the virus from infected patients. This therapy requires lifelong treatment which is hampered by side effects, development of drug resistance and high treatment costs.³

A prerequisite for the development of a curative treatment strategy for HIV-1 infection is the ability to eliminate HIV-1 infection from its latent reservoirs, these are unaffected by many current treatment regimes. HIV-1 latency develops primarily in memory T-cells and macrophages. Chemical compounds that reactivate latent HIV-1 infection include phorbol esters PMA,⁴² prostratin,^{43,44} histone deacetylase inhibitor trichostatin A^{45,46} and sodium butyrate.⁴⁷ Jones *et al.* have shown that **1** efficiently reactivates HIV-1 in a model of HIV-1 latent macrophage.⁴⁸ Although **1** does not directly reactivate latent HIV-1 infection in T-cells, amphotericin B-stimulated macrophages when co-cultured with T-cells can induce HIV-1 reactivation in these cells. It is assumed that trans-reactivation strategies hold promise to also reactivate latent HIV-1 infection *in vivo*.³

1.3 Mode of action

Over the last forty years there has been extensive work to understand the mode of action of **1**, but even to this day this is poorly understood.⁴⁹ It is clear that there is no 'one mechanism' and that many theories, whilst

intuitively attractive, are only part of the story. Whilst the focus of the work has been on the so-called 'barrel stave' model, half-pore and shuttle mechanisms are also feasible, these all potentially, contribute to its action, and usually, also its toxicity.⁵⁰

In 1965 Weber and Kinsky showed that cells grown in the absence of cholesterol were not inhibited by a polyene antibiotic, filipin.⁵¹ However, cells grown in the presence of cholesterol were lysed by the addition of polyene. In 1976, Ermishkin *et al.* observed transient formation of single ion channels by conductance through cholesterol containing 'black lipid membranes' after addition of **1** to both sides. They estimated the pores had a diameter of 0.4 nm.⁵²

The intimate nature of sterol and polyene in the complex was shown by Rychnovsky in 1992 when he showed that enantiomeric cholesterol would not participate in pore formation.⁵³ If the sterol was only required to be present in the bilayer and not part of the actual complex, then pore formation would still be expected.

At this time it was assumed that the mycosamine amino group and the carboxylate group would be in close proximity in any complex, as a zwitterion. However the previous observations that amphotericin B methyl ester, and amphotericin B amides retained activity did not fit with this 'common sense' assumption.⁵⁴

The dependence of pore formation on sterols has been explained as a direct interaction with varying binding affinity between **1** and sterols. This affinity is believed to be due to: the hydrogen bond between 3 β -OH of the sterol and the amino sugar moiety of **1**, or the Van der Waals force between the heptaene chromophore of **1** and the hydrophobic steroid ring.^{55,49,56}

1.3.1 The Barrel Stave

In 1974 De Kruiff and Demel proposed the formation of a circular arrangement of eight polyenes and eight steroids such that the outside of the circle is hydrophobic (in contact with the lipid bilayer, facing the ergosterol containing lipids) and the inside of the circle is hydrophilic, (the hydrophilic polyols faces the solvent exposed interior of the pore) forming a hydrophilic channel with a diameter of 0.8 nm.^{57,58} Two such pores would be needed to traverse the bilayer. DeKruiff also suggested that the C-35 hydroxyl groups would form hydrogen bonds from one half-pore to another half-pore, stabilising the trans-membrane pore formation. This requires a 22.5° rotation of one pore relative to the other, unlike the diagram below.

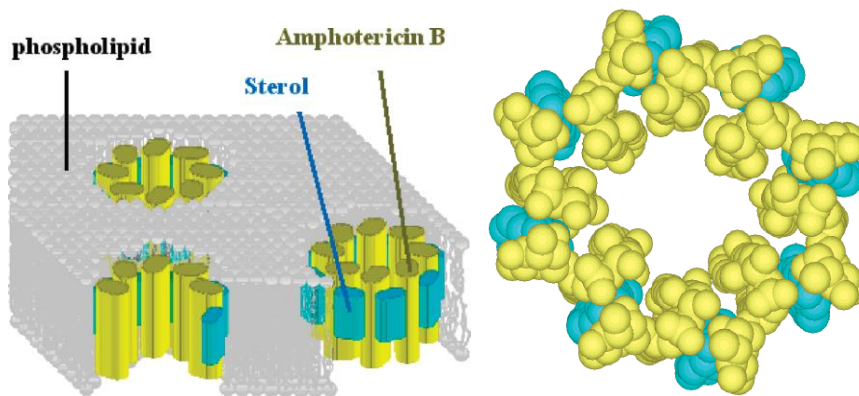


Figure 1.7 Hypothetical structure of a “barrel-stave” ion channel formed by 8 amphotericin Bs (**1**) and 8 sterols. Yellow and blue molecules represent **1** and sterol, respectively.⁵⁹

The mycosamine and C-41 carboxylate appendages of **1** have been predicted to be involved in binding sterol molecules found in the membranes of eukaryotic cells. There are three hypotheses regarding the roles played by the carboxylate at C-41 and mycosamine at C-19:

- i. the formation of intermolecular salt bridges and or hydrogen bonds between monomers of **1** are critical for channel self-assembly,
- ii. formation of polar interaction with phospholipid head groups are required to ‘anchor’ **1** to the membrane,

- iii. participation in hydrogen bonding interaction with membrane embedded ergosterol thereby promoting critical small molecule – small molecule interaction inside the lipid bilayer.

Deletion and/or derivatisation of appended functional groups in **1** represents a powerful approach for probing the still poorly understood activity of **1** and the various hypothesis regarding the roles of the functional groups.

Mazerski, Bolard and Borowski have shown that a substituted carboxyl group at C-41 retains the capacity to form charge-dipole interactions with the mycosamine amine, which could stabilise channel self-assembly.⁶⁰ This showed that the C-41 carboxylate is not required for the efficacy of **1**.

Mazerski *et al.*, and Matsumori *et al.*, showed that acylation of the C-3' amine on the mycosamine appendage caused a dramatic reduction in yeast permeabilising activity.^{60,61} This suggested that the amine on the mycosamine moiety is important for the activity of **1**.

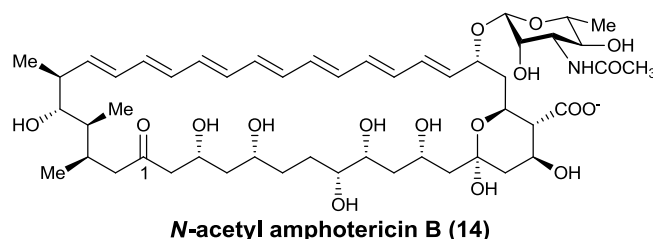


Figure 1.8 Structure of *N*-acetyl-amphotericin B (**14**)

In 2008, Szpilman *et al.*, synthesised 35-deoxy amphotericin B methyl ester (AME) and examined its ability to support efflux of potassium ions

from vesicles and found it was severely diminished.⁶² Gray *et al.* also showed that 35-deoxy-AME binds to ergosterol but lacks the capacity to permeabilise membrane.⁸ These results confirmed the importance of the hydroxyl group at C-35 of **1** in its role as a fungicide.

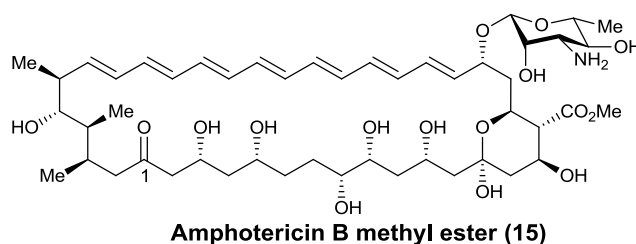


Figure 1.9 Structure of amphotericin B methyl ester (**15**)

Palacios *et al.*, reported a complete loss of both ion channel and antifungal activities of **1** when its mycosamine appendage was deleted.⁶³ Gray *et al.* recently determined that **1** directly binds ergosterol in a manner that requires the mycosamine appendage at C-19, thus explaining the inactivity of aglycone.⁸

In 2002, Baginski suggested that in the so called 'open conformation' (Fig. 1.9), the amino and carboxyl groups intermolecularly interact, favouring amphotericin B to amphotericin B interactions (aggregation), whilst in the closed conformation there was the intramolecular interaction (monomer).¹⁰

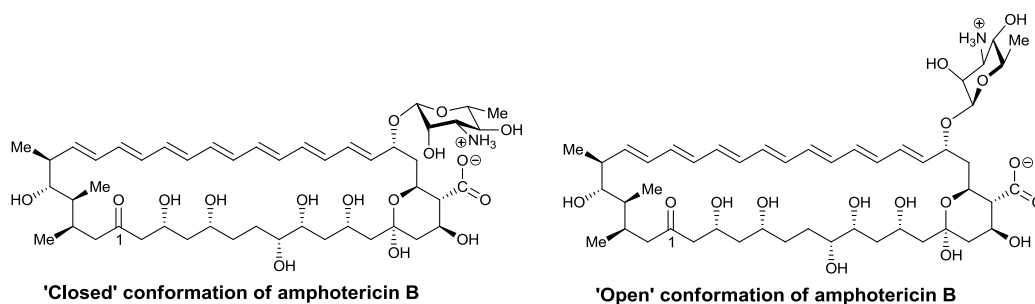


Figure 1.10 Structures showing the open and closed conformation of amphotericin B

Baginski *et al.*, also suggested an interaction between the sterol 3- β -OH and the mycosamine amino group on the basis of molecular dynamic simulations.⁶⁴ However, Mazerski suggested a hydrogen bond to the axial C-2'-OH group.⁶⁰

In 2005, Matsumori *et al.*, synthesised a series of analogues with different length methylene bridges linking the amino group and carboxyl group (15a-c).⁶⁵ This would restrict the free rotation about the glycosidic bond that occurs in **1**.

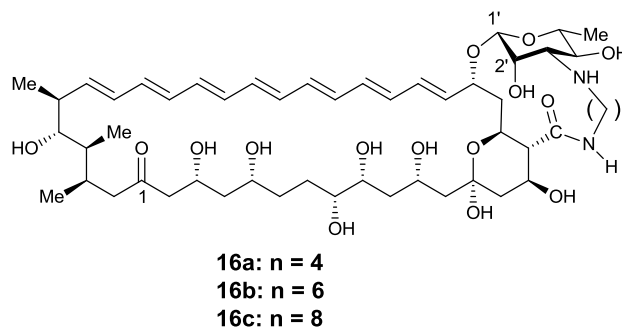


Figure 1.11 Structures of intramolecular methylene bridged derivatives of amphotericin B

In a potassium flux assay using ergosterol, **16b** was more active than **1** by a factor of two, both **16a** and **16c** were less active than **1**. Interestingly the use of cholesterol had little effect over sterol free liposomes. An

examination of the conformation of **16b** indicates that it is the axial C-2' OH that forms the hydrogen bonding to the sterol, in agreement with Mazerski's paper.⁶⁶ These results indicate the importance of mycosamine orientation in ergosterol selectivity. Conformational analysis suggests that there is a 30° rotation in sugar angle from **16a** to **16b**, but this may be optimum for sterol binding whilst in **16c** the rotation is too large. Previous n.O.e. NMR experiments have shown that half of the heptaene hydrogens are close to the polyol region. Hence any steroid should lie flat on top of (or below) the polyene area as shown in Fig 1.12. Hence only a small rotation of the mycosamine moiety would be necessary to obtain hydrogen bonding between the sterol 3-β-OH and the axial 2'-OH as depicted Fig 1.12.

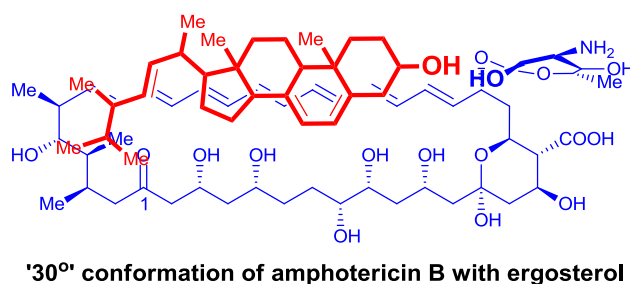


Figure 1.12 Structure of the hypothetical conformation of amphotericin B with ergosterol

The *in vivo* antifungal activities of **16a-c** did not agree with the model, but this may be because inactive (with the methylene bridge now disallowed) conformers are required to pass through the cell wall to get to the membrane, or due to the bridge affecting hydrophobicity or cell wall diffusion.

In 2007, Palacios *et al.*, synthesised 16-descarboxyl-16-methyl-amphotericin B (**17**) and found it retained similar antifungal activity to **1** with reduced toxicity, in agreement with results observed previously for a less pure biologically produced sample, reaffirming that the carboxyl group is not needed for activity.⁶³ In a later paper, Gray *et al.*, proposes that the binding of **1** to ergosterol, reducing its availability for use by the fungal cell, is the mechanism of antifungal activity.⁸

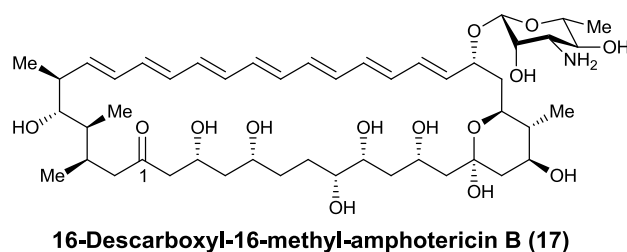


Figure 1.13 Structure of 16-descarboxyl-16-methyl-amphotericin B (**17**)

1.3.2 Other mechanisms

Gray *et al.*, has proposed that amphotericin B binds to free ergosterol, reducing the availability of ergosterol and thus reducing the viability of the fungal cells.⁸ A recent review discusses a multifaceted approach to both mode of action and toxicity, which in most literature has been neglected⁶⁷. The review covers literature that proposes that autoxidation of **1** leads to oxidative damage to cells via lipid peroxidation, or **1** acts as an electron transfer agent. It also proposes that **1** can stimulate the cells of the

immune system causing a respiratory burst in macrophages, this was inhibited by catalase. It is clear that **1** has a wide range of actions in both mammalian and fungal cells that are not yet clearly understood.

1.4 Semi-synthetic derivatives of amphotericin B

Total synthesis of **1** was achieved by Nicolaou *et al.* in 1988.⁶⁸ The complex multi-step synthetic route, is however, clearly not economically feasible or viable to make less toxic analogues. In any case, industrial strains of *S. nodosus* produce **1** at levels over 4 g/L and at these high levels, isolation is straightforward: extraction of whole cell broth with *n*-butanol is followed by reduced pressure evaporation and precipitation. A partition between ethyl acetate and acidic water enables separation from the co-metabolite **2**, with micro-crystallisation of **1** suitable for clinical use, and for generation of semi synthetic analogues.⁵⁴

Early synthetic derivatisation focussed on the amidation of the nitrogen, or esterification of the carboxyl group using simple chemistry not involving protecting steps.^{66,69} The amide derivative such as **14** retained surprising levels of activity.⁶⁰ The methyl ester (**15**) was investigated by Driver *et al.*,⁵⁴ At that time the interaction between the carboxyl group and amino group was thought important in the mode of action, but this methyl ester retained activity, with reduced conventional toxicity,⁵⁴ but was not further pursued due to other toxic properties. Driver and co-workers developed

elegant chemistry to generate 13,14-anhydroamphotericin B (**18**), 16-descarboxy-16-hydroxymethyl amphotericin B (**19**), and the methyl acetal (**20**).⁵⁴ Unfortunately this promising research programme was not continued further.

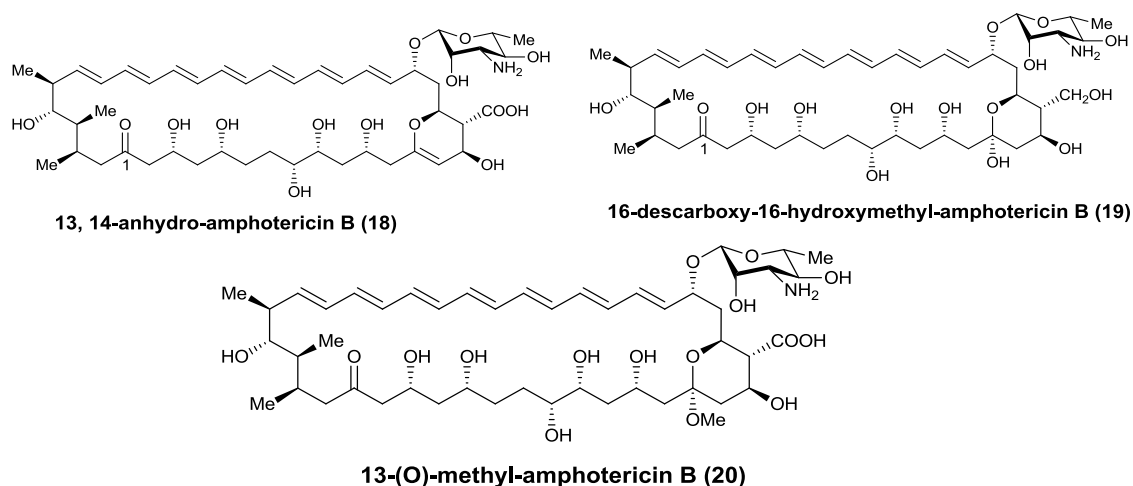


Figure 1.14 Structures of 13,14-anhydro amphotericin B (**18**), 16-descarboxyl-16-hydroxymethyl-amphotericin B (**19**) and 13-methoxy-amphotericin B (**20**)

Szlinger-Richert *et al.*, synthesised MFAME (**21**), which was reported to have much reduced nephrotoxicity and similar antifungal activity to **1**.⁷⁰ The successful synthesis showed that compounds exist in chemical space with much improved therapeutic properties than **1** albeit too expensive for clinical use.

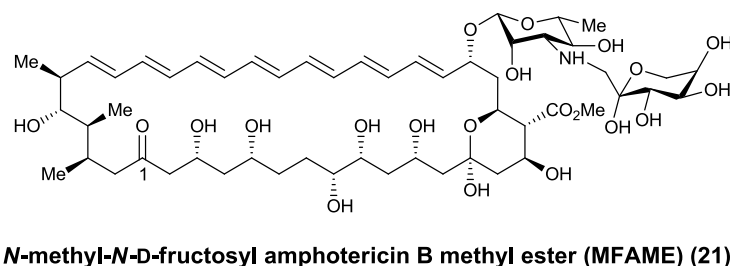


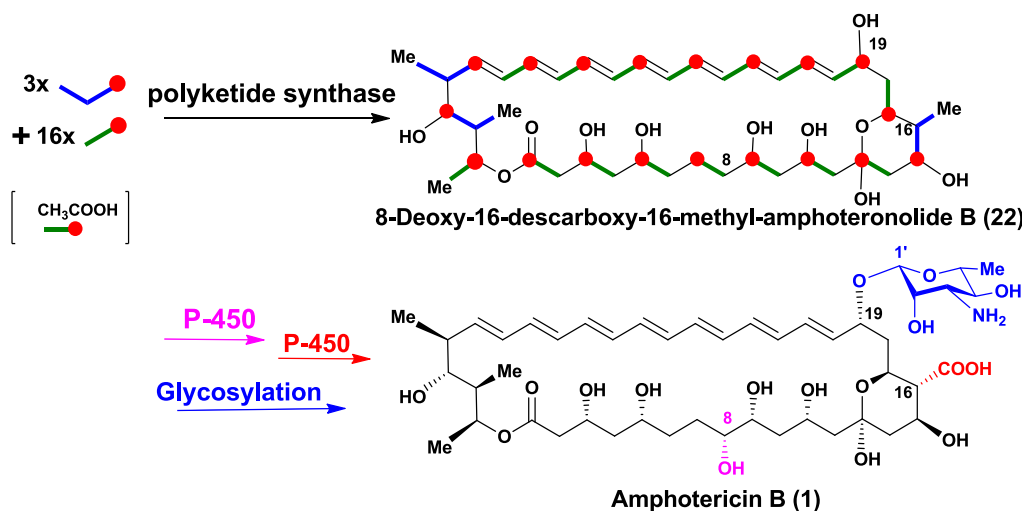
Figure 1.15 Structure of N-Methyl-N-D-fructosyl-amphotericin B methyl ester (**21**)

In 1999, Moribe *et al.*, generated the amino derivative with a long chain PEG derivative, and Blanc *et al.*, a peptide derivative.^{71,72} In recent work, Burke has developed a synthesis of the 16-descarboxyl-16-methyl derivative (**17**), which retained activity with reduced toxicity.⁶³

Whilst semi-synthesis has demonstrated that there are indeed much improved analogues out there in chemical space, the multistep nature of forming these derivatives, involving protection and deprotection steps, will pre-clude all of them from consideration as a clinically affordable analogue to **1**. However, if these, or related analogues, could be produced *in vivo*, this may enable their production and isolation at clinically affordable cost.

1.5 Biosynthesis of amphotericin B

The carbon chain of the macrolactone core is assembled from acetate and propionate units by a Type I modular polyketide synthase (PKS) followed by three post PKS modifications to give **1**.¹²



Scheme 1.2 Biosynthesis of amphotericin B (1)

The structure of amphotericin B suggests that the polyketide precursor is synthesised from the following sequence of starter and extender units: $\text{AP}_2\text{A}_8\text{PA}_7$, where A is acetate and P is propionate as shown in Scheme 1.2.¹² There are three domains always present in each extender module. These domains are acyltransferase (AT), 3-oxoacyl synthase (KS), and acyl carrier protein (ACP). These domains generate the 3-oxoacyl intermediate which can be reduced by a 3-oxoacyl reductase (KR) (if present and active) to a 3-hydroxyacyl group. Dehydratases (DH) dehydrate the 3-hydroxyacyl chain to 2-enoyl intermediate. This 2-enoyl intermediate is reduced to saturated intermediates by enoyl reductase (ER). When the acyl chain is assembled, lactonization occurs, forming the 8-deoxy-16-decarboxy-16-methyl-amphoteronolide B (22) (aglycone) above, and then the three post PKS modifications occur. The post PKS modifications are mediated by distinct oxidative and glycosylation enzymes. This modification involves:

- Oxidation of the methyl branch at C-16 to a carboxyl group using P450 gene (*amphN*).
- Addition of mycosaminyl sugar at C-19 by glycosylation with GDP-mycosamine by *amphDI*
- Hydroxylation at C-8 by cytochrome P450 (the final step) by *amphL*

The entire biosynthetic cluster has been sequenced by Caffrey *et al.*⁷³ The cluster contained six large PKS genes *amphABCDEFGHIJK*, two cytochrome P450 genes, *amphL* and *amphN*, *amphM* (a ferredoxin), sugar biosynthetic genes *amphDII* and *amphDIII*, and a glycosyl transferase *amphDI*, along with six regulatory and two ABC export genes. The large PKS genes each contained modules with individual enzyme components (DH, KR and ER) that correspond to the following functions in the aglycone assembly.

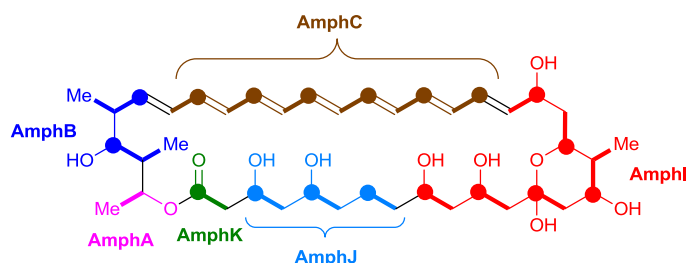


Figure 1.16 Structure of the PKS aglycone product of amphotericin B (**22**) biosynthesis showing the role of Amph ABCIJK

1.5.1 Biosynthesis of polyketides similar to amphotericin B

The nystatin (**3**) and pimaricin (**4**) gene clusters have also been sequenced.^{11,74} The DNA sequence encoding ten modules of the

candicidin PKS as well as some of the genes involved in the transport, regulation and post-PKS modification have also been disclosed.⁷⁵

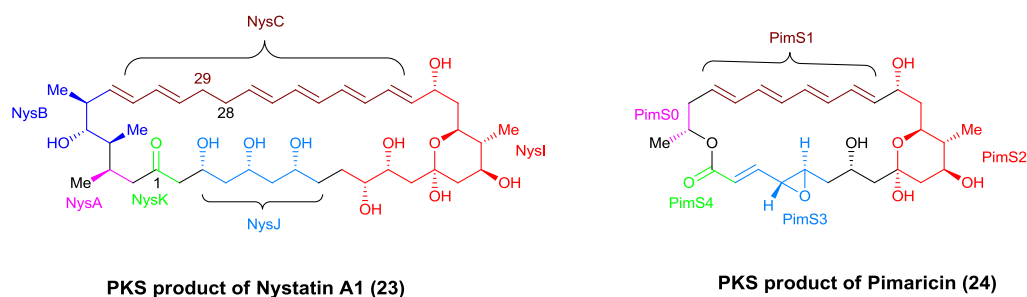


Figure 1.17 Structure of the PKS aglycone product of nystatin (23) and pimaricin (24) biosynthesis showing the role of NysABCDEFGHIJK and PimS01234 respectively.

The corresponding proteins in Nystatin (3) and amphotericin PKS show about 72% sequence identity. This is as might be expected from the structural similarity between these two polyenes. In the PKS of Pimaricin (4), the organisation of the modules are also similar except that certain modules are absent, in accordance with the contracted size of the macrolactone ring.¹¹

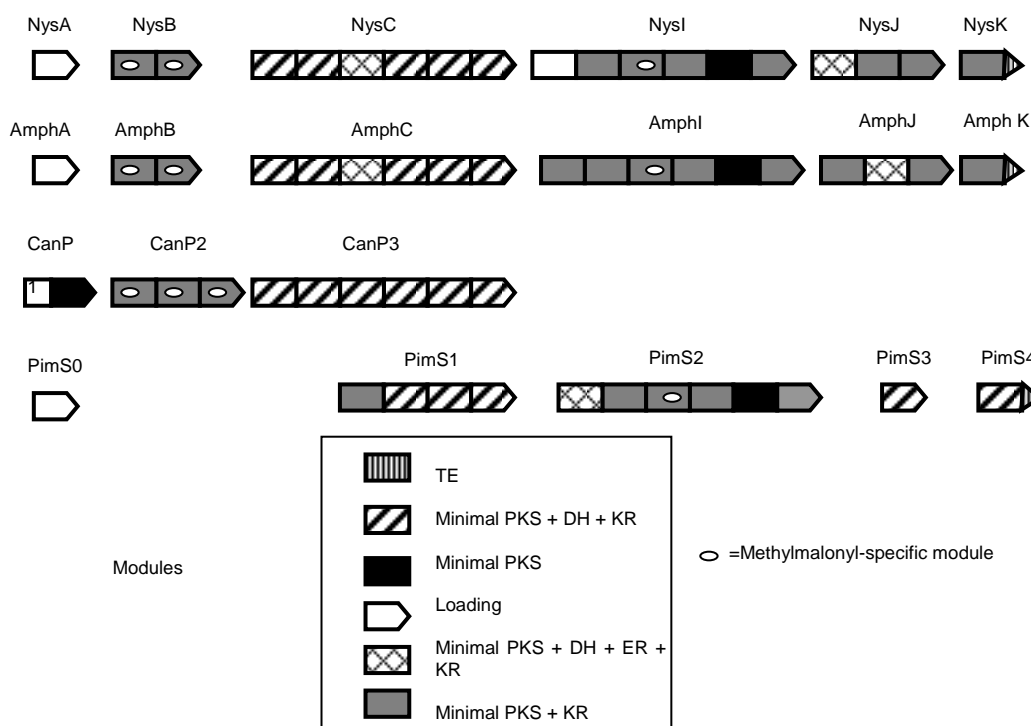


Figure 1.18 Modular structures of polyene macrolide synthases with modules classified on the basis of the functional domains that they include.

Minimal PKS refers to KS, AT, and ACP domains.

1.5.1.1 PKS loading modules

The PKS of **1**, **3** and **4**, all have discrete loading modules as shown in Figure 1.18. The AmphA and NysA proteins have the domain composition KS-AT-DH-ACP. The KS domains in these loading modules are almost identical to a regular KS domain except that a serine residue replaces the active site cysteine.¹¹

Within the AmphA and NysA proteins, it is thought that the AT domains (malonate-specific) acylate the ACP with malonate which are subsequently decarboxylated, by the KS, to provide an acetyl starter unit for the first extension module. The DH domains, is however, thought to be redundant.

The candicidin-loading module Can P1 as shown in Fig 1.18., consists of a CoA ligase (CoAL) domain and an ACP, and is fused to the first extension module.⁷⁵ The pimarin loading domain module PimS0 (as shown in fig 1.18) has the domain composition CoAL-ACP-KS-AT-ACP. It is possible that this loading module can also generate an acetyl starter unit by decarboxylation of a malonyl group.¹¹

1.5.1.2 PKS extension modules

The AmphB and NysB proteins catalyse the first two extension modules. The CanP2 protein incorporates three propionates in cycles 2, 3, and 4. In the biosynthesis of **4**, the acetate starter unit is transferred directly to the PimS1 protein that assembles most of the tetraene region of the polyketide chain.

AmphC, just like NysC, are hexamodular proteins that assemble most of the polyene unit.⁷⁶ Module 5 (contained in AmphC) actually also contains a partially active ER, resulting in the formation of some dihydro-co-metabolite, the tetraene amphotericin A (**2**).⁷³

The CanP3 protein catalyses six of the seven cycles that assemble the heptaene region. The organisation of the domain is identical to that of AmphC or NysC, however, no ER domain is present (as shown in fig 1.18).

AmphI, NysI and PimS2 are hexamodular proteins (shown in fig 1.18) in which each assemble another structural feature that is characteristic of polyene polyketides; the exocyclic carboxyl group and the hemiketal ring.

NysJ and AmphJ are trimodular proteins that catalyse cycles 15-17. The main difference between **3** and **1** PKSs is that the reductive loops are different in module 15 and 16.⁷³ In the NysJ protein, module 15 contains a complete reductive loop (DH-ER-KR) whereas module 16 contains only KR. In the AmphJ protein, module 15 contains DH-KR domain, but the DH appears to be non-functional, whereas module 16 contains a complete reductive loop. Both NysJ and AmphJ PKS contain a DH domain in module 17 even though it is inactive.

In pimaricin PKS, no trimodular protein is present. The penultimate cycle of chain extension is carried out by PimS3, which contains a functional DH

domain. This domain results in the formation of the pimaricinolide C-4 to C-5 double bond that is the substrate for PimD epoxidase.¹¹

NysK, AmphK and PimS4 catalyse the last cycle in the biosynthesis of **3**, **1** and **4** respectively. These unimodular proteins all have a thioesterase domain. It is however, not clear how each long precursor polyketide chain folds to allow the correct cyclisation.

1.5.1.3 Post-PKS modification

Polyenes, generally undergo relatively few post-PKS modifications. This usually involves the conversion of a methyl branch to a carboxyl group, and the hydroxylation in the polyol region of **1** and **3** and epoxidation of **4**. The majority of polyenes also contain only one sugar, mycosamine.

CanC, AmphN, NysL and PimD contain cytochrome P450, which oxidises the methyl side chain to an exocyclic group. Another cytochrome P450 contained in AmphL, NysL and PimD, introduces a hydroxyl group or epoxide.⁷⁷

AmphDIII, CanM, NysDIII, and PimJ have been found to contain a gene for a GDP-mannose-dehydratase. This suggests that the mycosamine sugar (3-amino-3,6-dideoxy-D-mannose) is synthesised from GDP-mannose.

Transaminases, AmphDII, CanA, NysDII, PimC, have been found in all four gene clusters, which is identical to the PLP-dependent transaminase that converts GDP-4-keto-6-deoxy-D-mannose to GDP-perosamine.

AmphDI, CanG, NysDI and Pimk proteins contain genes that are homologous to UDP-glucuronate transferases.

1.6 Genetically Engineered Analogues

A wide range of novel unnatural polyketides have been generated by disruption of polyketide genes.^{78,79,11}

Zotchev has disrupted several PKS genes in nystatin⁸⁰ and obtained a wide range of analogues. Borgos *et al.*, has inactivated DH domains with the polyene region, resulting in additional hydroxyl functionality.⁸¹ Disruption of DH3 and DH4 gave **25** and **26** respectively. These analogues had improved solubility, but did not retain biological activity, presumably due to the extra conformational flexibility and increased disorder in the structure.

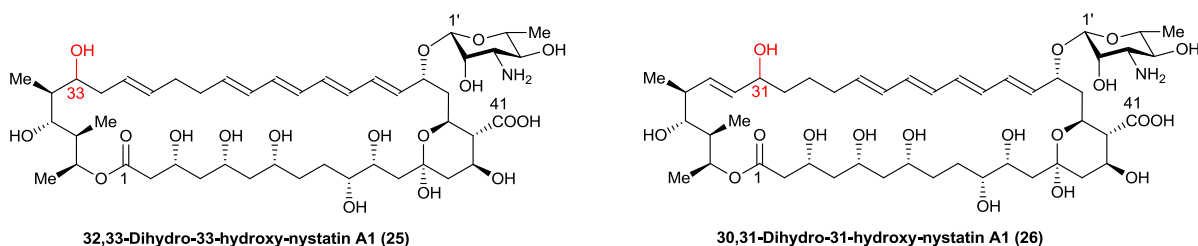


Figure 1.19 Structures of 32,33-dihydro-33-hydroxy-nystatin A1 (**25**) and 30,31-dihydro-31-hydroxy-nystatin A1 (**26**)

Brautesat *et al.*, reported on a series of nystatin analogues.⁸² Most of these had disruption at ER5 as an intact heptaene unit improves biological activity, as found in amphotericin. Disruption at ER5 resulted in S44HP (**27**) which showed considerably improved antifungal activity over nystatin A1 (**3**). Disruption at ER5 and DH15 gave BSG003 (**28**) by MS analysis, in which there is an additional hydroxyl at C-9 (stereochemistry undefined) but NysL has not oxidised at C-10. Interestingly, this swap of hydroxyl group from C-10 to C-9 considerably reduced both the antifungal activity and haemolytic activity.

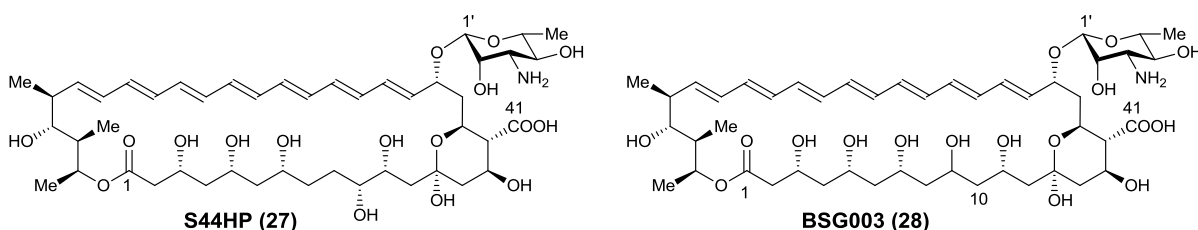


Figure 1.20 Structures of S44HP (**27**) and BSG003 (**28**)

Disruption of ER5 and NysN gave BSG005 (**29**) whilst ER5, DH15 and NysN have BSG018 (**30**). The C-16 methyl analogues were less toxic than their carboxyl counterparts

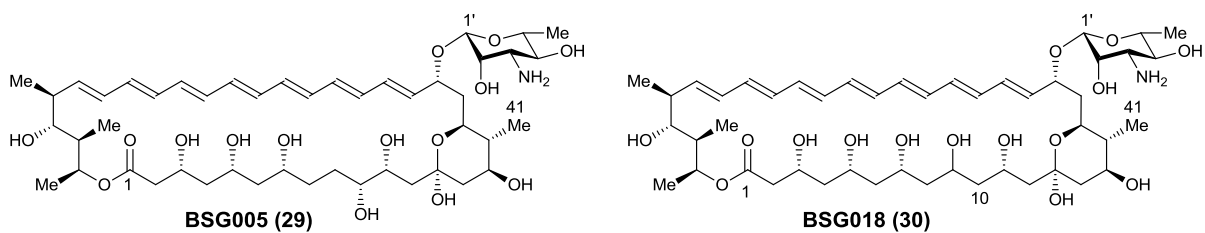


Figure 1.21 Structures of BSG005 (**29**) and BSG018 (**30**)

Tevyashova *et al.*, have shown that polyene macrolides in which the hydroxyl groups are in positions C-8 and C-9 or C-7 and C-10, as seen in **1**, **27** and **29**, have significantly higher antifungal activity than polyene macrolides with hydroxyl groups at both C-7 and C-9 as, seen in **28** and **30**.⁸³

Disruption of ER5 and NysL gave BSG022 (**31**) and disruption of ER5, NysN and NysL gave BSG019 (**32**).⁸² Removal of the C-10 hydroxyl group had little effect upon antifungal activity. It should be noted that **31** is a regioisomer of 8-deoxyamphotericin B (**33**) and **32** a regioisomer of **34**.

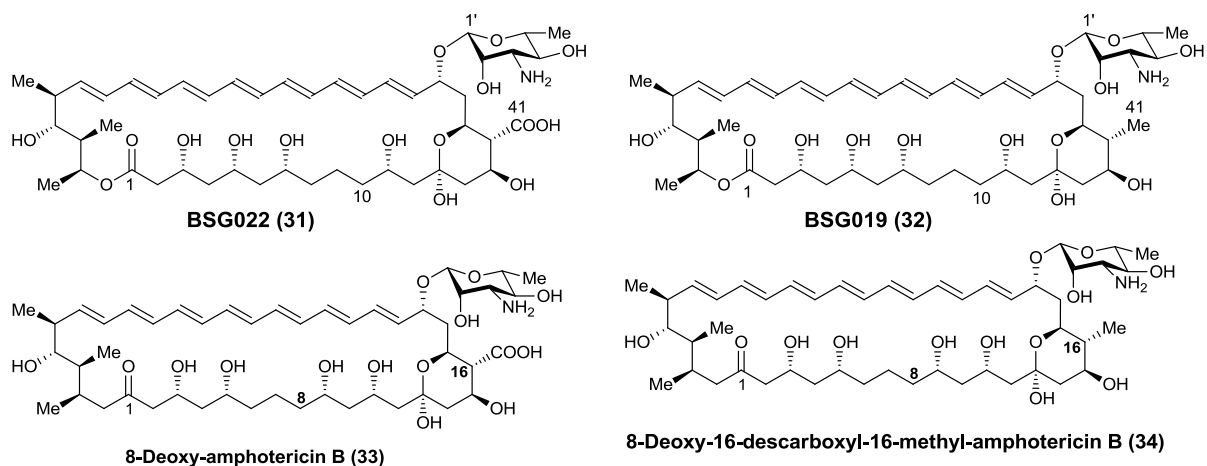
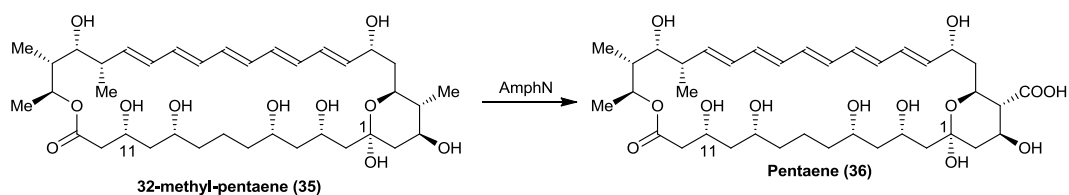


Figure 1.22 Structures of 8-deoxy-nystatin A1 (31), 8-deoxy-16-descarboxyl-16-methyl-nystatin A1 (32), 8-deoxy-amphotericin B (33) and 8-deoxy-16-descarboxyl-16-methyl-amphotericin B (34)

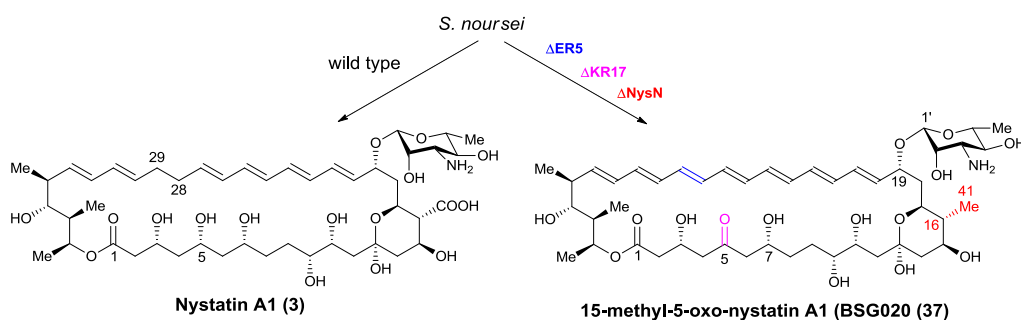
1.6.1 Genetic engineering of amphotericin biosynthesis genes

Recently, amphotericin analogues have been produced by manipulation of biosynthetic genes in *S. nodosus*. Using the KC515 vector, Caffrey has precisely deleted two modules in *amphC*.⁸⁴ AmphC normally assembles the heptaene portion of **1**.⁷³ The resulting disruptant produced a range of pentaenes, one of which was isolated as the methyl ester and partially characterised by MS and NMR which were consistent with **36**.⁸⁵ However, these compounds showed limited stability. Despite the considerable alteration in overall shape, it appears that AmphN has recognised and oxidised **35**, but AmphDI did not recognise the modified substrate.⁸⁵ MS indicated some additional oxidation, presumably by AmphL.



Scheme 1.3 Oxidation of 32-methyl-pentaene (**35**) to pentaene (**36**) by AmphN

There are reports of several naturally occurring polyenes with a carbonyl group or two, in the polyol chain. Brautaset and Zotchev have deleted KR17, along with NysN and ER5 to obtain the 5-oxo heptaene analogue of nystatin A1, 'BSG020' (**37**).⁸⁰

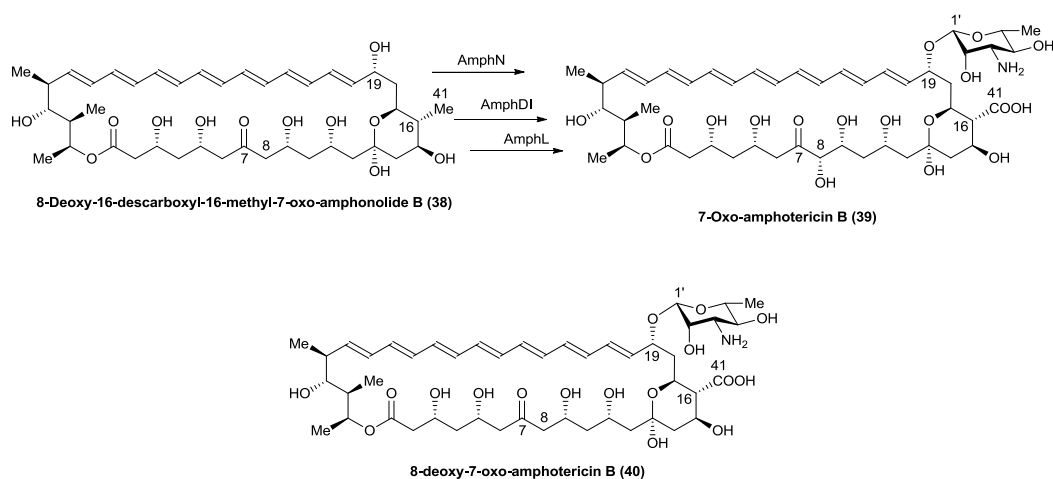


Scheme 1.4 Deletion of KR17 and ER5 to produce Nystatin A1 (**3**) and BSG020 (**37**) respectively

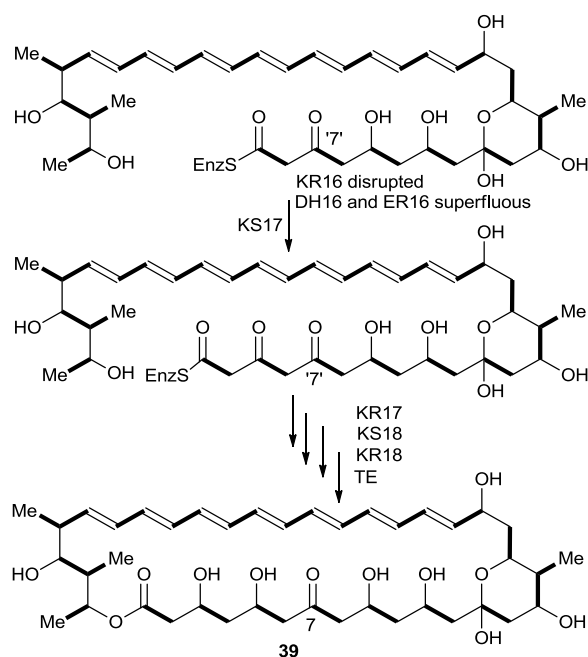
Following the precedent, Caffrey *et al.*, introduced an additional carbonyl group at C-7 in the polyol chain to increase serum solubility and reduce toxicity.⁸⁶ Caffrey inactivated the ketoreductase in module 16, responsible for the first step in the reduction of C-7 to a methylene unit. The strategy was to introduce as small a modification into the gene and enzyme as possible, so GCC-AAC-TAC sequence around the active site tyrosine was replaced with GCA-AGC-TTC converting Ala-Asp-Tyr with Ala-Ser-Phe.⁸⁶

The PKS is able to efficiently assemble the aglycone **37**, despite the presence of the extra oxo-group.

The disruptant produced the 7-oxo analogue (**39**) with and without hydroxylation at C-8, that whilst showing slightly reduced antifungal activity, showed considerable reduction in toxicity. Whilst AmphN and AmphDI recognise the 7-oxo substrates efficiently, AmphL is able to recognise and oxidise adjacent to the carbonyl, but only with reduced efficiency.



Scheme 1.5 The three post-PKS steps in the biosynthesis of 7-oxo-amphotericin B (**39**)

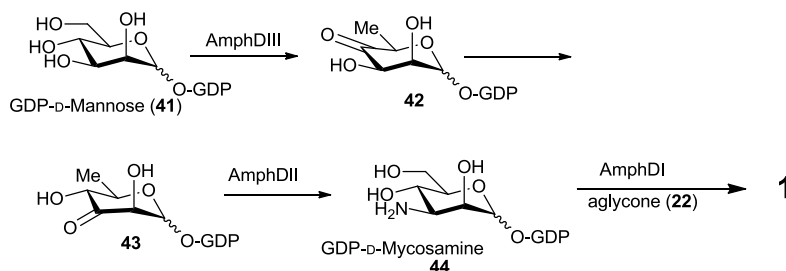


Scheme 1.6 The assembling of the PKS product in the biosynthesis of 7-oxo-amphotericin B (**39**)

The ketoreductase in module 17 (KR17) has to recognise a 3,5-dioxothioester substrate, that will have an enhanced level of enol present unless the substrate is held at an angled conformation to prevent tautomerisation. This would make the C-5 carbonyl less electrophilic and harder to reduce. In addition, the presence of the oxo group at C-7 in **1** converts an sp^3 carbon into an sp^2 carbon. The ring in amphotericin B (despite being so large) is strained, and this alteration in hybridisation may make ring closure by the thioesterase more difficult. The 7-oxo product has been shown to have reduced stability relative to **1**.⁸⁵

1.6.2 Genetic Engineering of Post PKS genes

The amino-sugar portion of **1** is assembled from GDP-D-mannose. AmphDIII (GDP-D-mannose-4,6-dehydratase) catalyses the dehydrogenation to **41**. This reaction involves the recycling of NADH/NAD⁺ to oxidise at C-4 and reduce at C-6. The next step is isomerisation, for which no enzyme activity has been identified. GDP-4-oxo-4,6-dideoxy-mannose (**42**) and GDP-3-oxo-3,6-dideoxy-mannose (**43**) may be in equilibrium, with AmphDII selecting **43**. However, Caffrey *et al.*, has suggested that an inactive cytochrome P450 may act as the isomerase.⁷³ AmphDII is a pyridoxal phosphate dependent transaminase. The resulting mycosamine is then attached to the aglycone (**23**) by the glycosyl transferase AmphDI.



Scheme 1.7 Biosynthesis of GDP-D-mycosamine (**44**)

Caffrey disrupted the *amphDIII* gene. Byrne *et al.*, showed that this mutant produced high levels of 8-deoxyamphoteronolide B (**43**) and A (**44**) isolated as the methyl esters.⁸⁷ This suggested that glycosylation by *amphDIII*, occurs subsequently to oxidation at C-16 by *amphN*, but prior to

oxidation at C-8 by *amphL*

AmphN.

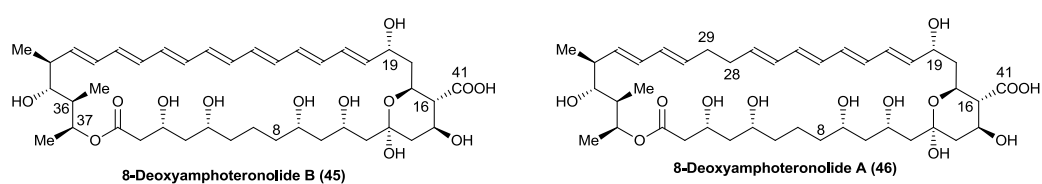
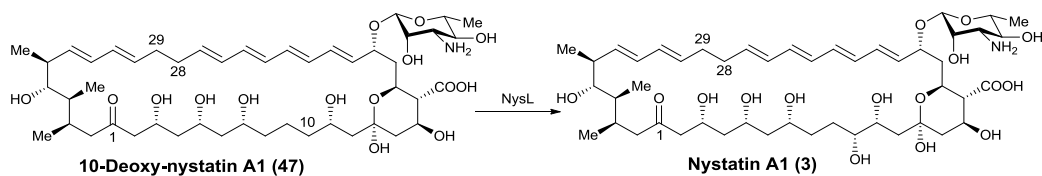


Figure 1.23 Structures of 8-deoxy-amphoteronolide B (**45**) and 8-deoxy-amphoteronolide A (**46**)

Significant quantities of an isomer of **45**, thought to be epimeric at either C-36 or C-37 were also isolated, suggesting that stereofidelity in these early PKS steps may be less than previously thought, with in wild-type the 'wrong' stereochemistry later 'edited' out or not isolated.⁸⁶

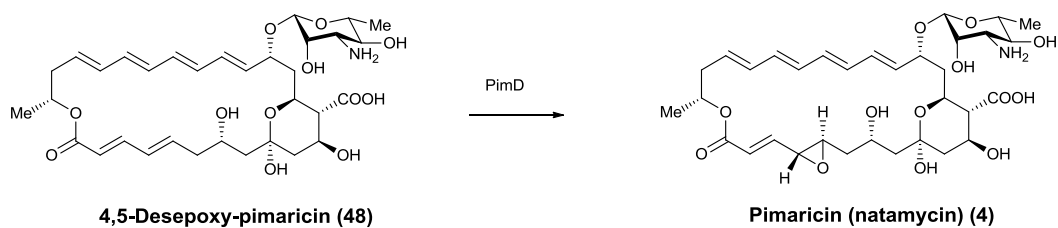
A series of targeted gene deletions and replacements has been carried out to assign the post-PKS genes and to obtain the resulting biosynthetic intermediates. Caffrey, *et al.*, has reviewed genetic engineering of polyene antibiotics.⁸⁸

The first attempt at targeted gene deletion in *S. nodosus* was the cytochrome P450 encoded by *amphL* that was thought to oxidise **22** at C-8. The corresponding gene in nystatin (**3**) biosynthesis (*nysL*) that hydroxylates at C-10 has now been located,⁸⁹ overexpressed and characterised.



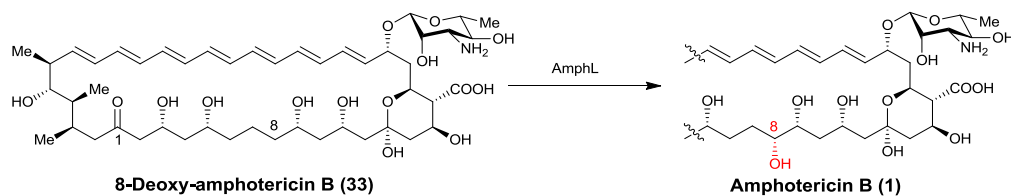
Scheme 1.8 Hydroxylation of 10-deoxy-nystatin A1 (**47**) by *nysL*.

The closely related gene in pimaricin (**3**) gene cluster is PimD, that epoxidises a double bond. Kells *et al.*, and Mendes *et al.* have determined its structure by X-ray diffraction and suggest the epoxidation occurs *via* a hydroperoxoferric intermediate.^{90,91}



Scheme 1.9 Epoxidation of 4,5-desepoxy-pimaricin (**48**) by PimD

The *amphL* gene was deleted by targeted integration of a phage KC515 vector. The resulting cultures contained 8-deoxy-amphotericin B (**33**) along with some **1** due to reversion which was due to precise excision of the phage. This observation confirmed that AmphL was the 8-hydroxylase, and indicated that AmphL can act as the final biosynthetic step.⁸⁵



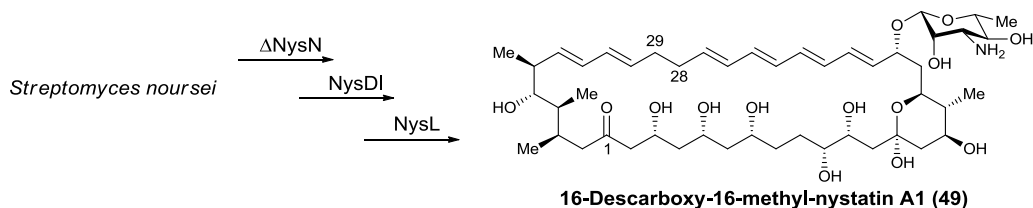
Scheme 1.10 Hydroxylation of 8-deoxy-amphotericin B (**33**) by AmphL

8-Deoxy-amphotericin B (**33**) was found to be extremely insoluble and required at least a dozen multilitre extractions of the mycelia with methanol to obtain.⁸⁵

Chaotropes (water structure breakers) have been shown to increase solubility of **1**.⁸⁵ Murphy *et al.* found that only two or three extractions of the mycelia with sodium thiocyanate saturated methanol was required to extract **33** from the mycelia,⁸⁵ an early indication that the actual 'state' (solvation, presence of impurities, conformation *etc*) of an analogue can dramatically affect its physical properties such as solubility. Unfortunately, the biological properties of **33** were not promising, presumably in part due to its low solubility. This low solubility made full purification and characterisation very difficult, some characterisation was performed instead on the more soluble *N*-acyl derivative.

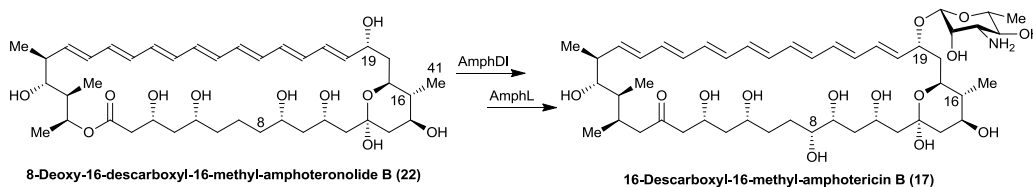
All subsequent experiments by Caffrey used gene replacement, to avoid the problem of reversion encountered with *amphL* mutant.

The other cytochrome P450 (*amphN*) is thought to oxidise the methyl group at C-16 to the carboxyl group in **1**. Zotchev *et al.*, has disrupted NysN and obtained 16-descarboxyl-16-methyl-nystatin (**49**) in low yield (6 mg/L) and found that it retained antifungal activity with reduced toxicity.⁸⁰ The low yield and otherwise normal growth suggested to Zotchev there may be feedback mechanism inhibiting the pathway.



Scheme 1.11 The post-PKS steps in the biosynthesis of 16-descarboxyl-16-methyl-nystatin A1 (**49**)

Caffrey has disrupted the gene encoding for the other cytochrome P450, amphN. In this early work, the gene coding the neighbouring ferredoxin was also disrupted, and the genes encoding perosamine (a regioisomer of mycosamine) biosynthetic genes inserted, to determine whether the AmphDI glycosyltransferase would recognise and add perosamine to the amphotericin aglycone. The first product to be isolated and characterised (in impure form) from this mutant was 16-descarboxyl-16-methyl-amphotericin B (**17**), showing that both AmphDI glycosylation and AmphL oxidation at C-8 can occur on ‘non-carboxylated’ substrates.⁹²



Scheme 1.12 Oxidation and glycosylation of 8-deoxy-16-descarboxyl-16-methyl-amphoterionolide B (**22**) by AmphL and AmphDI.

The product was found to have retained the antifungal activity of **1** (in a simple ‘lawn’ assay) with reduced toxicity (in a simple blood erythrocyte assay). Using elegant chemistry, Burke subsequently synthesised **17** and also reported superior therapeutic properties.⁸

Related mutants were subsequently analysed, and found to also produce high levels of the PKS product **22** as an extremely insoluble powder. This suggests that the post PKS genes are less efficient on the unoxidised 16-methyl substrate. As has been observed for all aglycones, **22** had no useful biological activity.

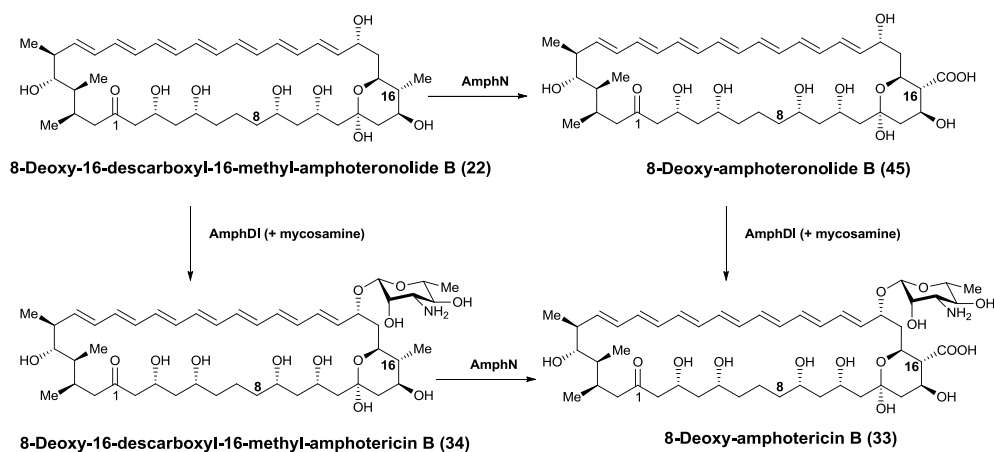
1.7 Aims of the project

Early work on impure 16-descarboxyl-16-methyl-amphotericin B (**17**) has indicated that it has a much improved therapeutic index over **1**.⁶³ The current extraction and purification procedures are difficult, inefficient and have yielded impure material with limited characterisation. Initial extractions contain a wide variety of polyenes such as aglycone, tetraenes and hexosylated material, an aromatic polyketide with similar polarity to the products, as well as polysaccharides and large amount of membrane debris. Analogues are frequently extracted at less than 1% w/w purity. Future mutants, with several disruptions would be expected to have further reduced yields, with even greater problems in purifying from the impurities, many of which have some affinity for the analogue, interfering with isolation. The primary aim of this project is to develop improved protocols for purification of **17**, and future mutants, so that they are readily available for biological assay and mode of action studies.

Chapter Two: Studies towards the efficient isolation and purification of 16-descarboxyl-16-methyl-amphoterionolide B from the “ Δ *amphNM+perDIDII*” mutant

2.1 Introduction

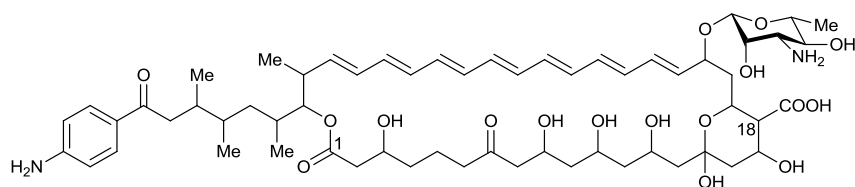
The *amphN* gene is thought to encode the cytochrome P450 responsible for the oxidation of the methyl group on C-16 to the carboxyl group in **1**¹² that is a common feature of most glycosylated polyenes. Caffrey has shown that this oxidation can occur before oxidation at C-8 by disrupting the *amphL* gene to give 8-deoxy-amphotericin B (**33**).⁹³ In a separate experiment, the mycosamine biosynthetic gene *amphDIII* was disrupted to obtain 8-deoxy-amphoterionolide B (**45**)⁸⁷ (as well as the corresponding 28, 29-dihydro analogue). This demonstrated that AmphN can act upon **22** as a substrate. However, it remained unclear whether AmphN always precedes AmphDI or whether the order is non-obligatory with **17** as an intermediate and possible substrate for AmphN.



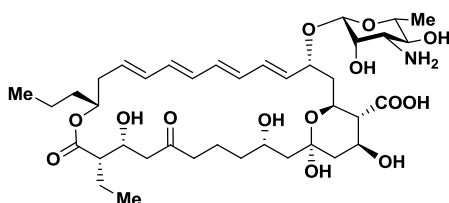
Scheme 2.1 Two possible post-PKS routes for the biosynthesis of 8-deoxy-amphotericin B

2.1.1 Closely related genes

The biosynthetic gene clusters for a number of polyenes related to amphotericin have now been investigated. These include amphotericin (1),⁷³ nystatin (3),⁷⁴ candicidin (50),⁹⁴ pimarinin (4)⁷⁹ and rimocidin (51).⁹⁵ All of these clusters contain cytochrome P450 genes homologous to *amphN*. As described in Chapter 1, Zotchev *et al.*, reported the disruption of the *NysN* gene in *S. noursei* and isolated 16-decarboxy-16-methyl-nystatin A1 (49).⁸⁰ This shows that the NysDI can act on the C-16 methyl precursor. Zotchev has inactivated *NysN* and obtained the nystatin analogue of 49 which also shows good antifungal activity and low toxicity in a mouse model of systemic mycosis.⁹⁶



FR-008-I (Candicidin) (50)



Rimocidin (51)

Figure 2.1 Structures of candicidin (**50**) and rimocidin (**51**)

AmphN and its close analogues NysN and FscP are unusual among the cytochrome P450s that modify macrolide antibiotics in that it appears to introduce two oxygen atoms into an unactivated methyl group.⁹² AmphN presumably binds to the hemiketal part of the amphotericin precursor (**22**) to oxidise the C-41 methyl group.⁷³ Modification of the exocyclic carboxyl group in amphotericin B can bring about a substantial reduction in its toxicity.⁶⁶

2.1.2 Disruption of the *amphN* gene

Caffrey, having sequenced the amphotericin gene cluster in *S. nodosus*, initially attempted to disrupt the *amphN* gene, to confirm its assignment as the cytochrome P450 that oxidises **22** to **45**.⁹² Targeted disruption of *amphN* was found to be problematic, with phage constructs failing to

integrate or giving unwanted chromosomal deletions that abolished polyene production.⁸⁵ The reasons for these failures were not understood but it was possible that the DNA sequence of the *amphN* might cause lethal accumulation of toxic polyene biosynthetic intermediates.

In 2005, Caffrey achieved the successful disruption of any of these genes when he reported disruption of *amphN* from the *S. nodosus* chromosome along with the neighbouring *amphM* ferredoxin gene resulting in production of low levels of 16-descarboxyl-16-methylamphotericin B (**17**) as determined by ESMS, and then NMR following *N*-acylation and partial purification.⁹²

This “ Δ *amphNM+perDIDII*” mutant was generated in early unsuccessful attempts to engineer the biosynthesis of 16-descarboxyl-16-methyl-19-(*O*)-perosaminyl amphoteronolides.⁹² Perosamine is a 4'-amino-3'-hydroxyl regioisomer of mycosamine.⁹⁷

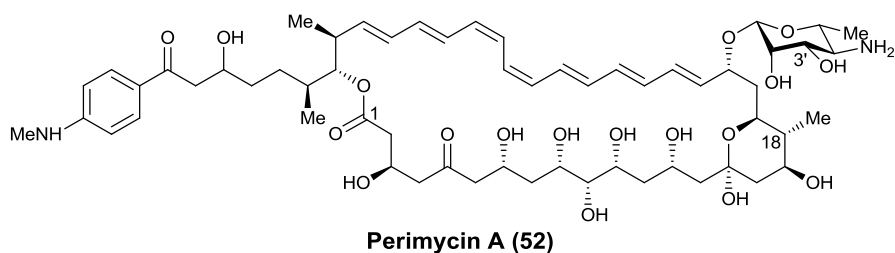
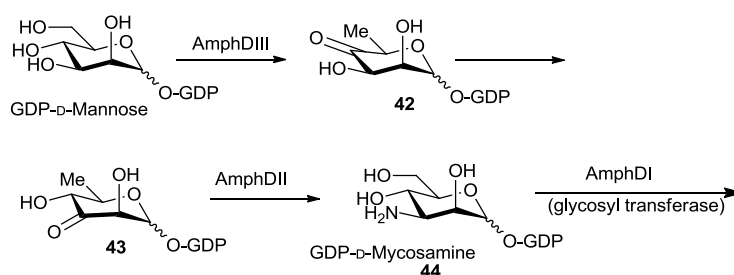


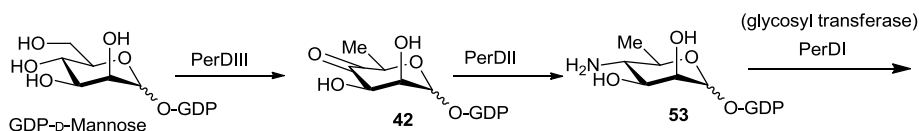
Figure 2.2 Structure of perimycin A (**52**)

The “ Δ *amphNM+perDIDII*” strain was constructed with *perDI* and *perDII* added adjacent to *amphDIDII*.⁹² The aglycone substrate for PerDI is

similar to the aglycone produced by AmphN, both having a methyl group at the equivalent position of amphotericin C-16. PerDI and PerDII are the analogues of AmphDI and AmphDII as in Scheme 2.2. Unusually amongst glycosylated polyenes, there is no isomerisation of 4-oxo (**42**) to 3-oxosugar (**43**) in *S. coelicolor* var. *aminophilus*,⁹⁷ resulting in the formation of, and attachment of perosamine instead of mycosamine.



Scheme 2.2 Biosynthesis of GDP-D-mycosamine (**44**)



Scheme 2.3 Biosynthesis of GDP-D-perosamine (**53**)

This strain, " $\Delta amphNM+perDIDI$ ", is presumed to be capable of synthesising both GDP-mycosamine and GDP-perosamine. Rawlings and Caffrey successfully isolated and partially characterised **17** from this strain.⁸⁵ However, no perosaminylated analogues were identified in production cultures, suggesting that the PerDI could not recognise the **22** as a substrate. The subsequent successful replacement of mycosamine with perosamine is discussed in Chapter 5. This strain, due to the high

level of recombination between directly repeated homologous *amphDI-DII* and *perDI-DII* sequences could readily lose all of these glycosylation genes, resulting in production of the aglycone (**22**).⁸⁵

2.1.3 Previous extraction protocols of polyenes from the “ Δ *amphNM+perDIDII*” mutant

In early work, Rawlings *et al.*, isolated **17** as the *N*-acetyl derivative.⁸⁷ In common with many of these analogues, **17** was isolated by methanolic extraction of the mycelia, resulting in small quantities of polyene in large amounts of membrane debris and saccharides etc, hindering purification. *N*-acylation of this crude extract, obtained by reaction with acetic anhydride and pyridine, enabled some purification from large amounts of impurities using flash chromatography⁸⁷ enabling provisional characterisation by NMR and MS on impure material confirming that the 16-methyl group was present.

In more recent work, Murphy *et al.*, grew the “ Δ *amphNM+perDIDII*” mutant in the presence of thiostrepton (20 mg/L).⁹³ Use of thiostrepton (20 mg/L) in preculture was found to reduce aglycone (**22**) production and maximise production of glycosylated NM (**17**). The sediment was extracted with methanol (1.13gH, 1.1gT), and the volatiles partially removed. The resulting crude precipitate containing mainly 8-hydroxy-16-descarboxyl-16-methyl amphotericin B (**17**) (600 mgH, 700 mgT in 6gW) was significantly

purified from tetraenes by water washes (400 mgH, 300 mgT in 1.6gWt), and then from membrane lipid by repeated selective dissolution with sonication in methanol and subsequent precipitation with EtOAc (110 mgH, 5mgT, in 466 mgWt) facilitating preparative HPLC purification. The resulting glycosylated heptaene product isolated was mainly **17** and not 8-deoxy-16-descarboxy-16-methyl-amphotericin B (**34**) showing that *amphL* was efficiently oxidising the 16-methyl heptaene intermediate (**22**), and also not requiring active AmphM ferredoxin. However, isolation of glycosylated tetraene C-16 methyl fractions showed largely 8-deoxy-16-descarboxyl-16-methyl amphotericin A (**54**).⁸⁵

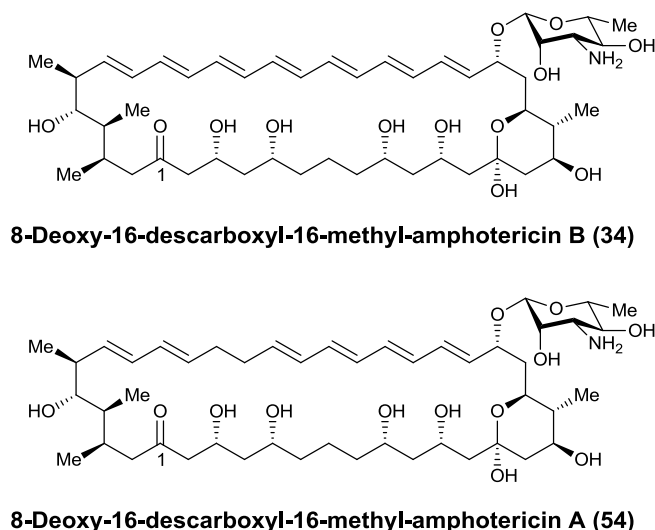


Figure 2.3 Structures of 8-deoxy-16-descarboxyl-16-methyl-amphotericin B (**34**) and 8-deoxy-16-descarboxyl-16-methyl-amphotericin A (**54**)

Kat Pugh was able to isolate the aglycone (**22**) from the same mutant as a very insoluble powder.⁸⁵ Methanolic extraction of sediment followed by partial removal of volatiles *in vacuo* gave a yellow precipitate of aglycone (>100 mgL⁻¹) containing less than 10% other polyenes and a relatively

small (<10% w/w) amount of lipid. Repeated washing with methanol improved purity, however, the final sample still contained lipids. Despite being extracted into methanol from mycelia, the purified aglycone was quite insoluble, illustrating how the properties can change with increasing purity (especially lipid removal). Despite the low solubility of **22**, many carbon and proton resonances could be assigned in the NMR spectra.

2.1.3.1 Sub-culturing

After inoculation of production culture, the remaining preculture was left on the lab bench. If the yield of **22** from the production culture was subsequently found to be high, then the remaining preculture was used to either make a new batch of production culture, or used to inoculate a fresh preculture, from which new glycerol deeps could be made. A sterile wire loop was used to aseptically transfer a vigorous single growth or small amount of growth from the surface of the liquid into new preculture medium.

2.2 Isolation, purification and derivatisation of 8-deoxy-16-descarboxyl-16-methylamphoterone B (**22**).

Kat Pugh in 2008 isolated the 'aglycone' (**22**), and despite lipid contamination and low solubility, assigned many of the resonances in the NMR spectra.⁸⁵ This Section describes my work in isolating and

derivatising **22** in order to improve the structural characterisation and attempt to obtain crystals for X-ray diffraction studies.

“*ΔampNM+perDIDI*” mutant (6 L) was grown routinely in preculture flasks (GYE medium) followed by production medium (24 x 250 mL) with XAD16 beads, as described in Chapter 6. The non-ionic absorbent beads are added as they had increased recovery yields on other mutants.⁸⁵ They may increase yields by removing some product from solution, avoiding degradation or by avoiding product feedback inhibition.

After five day growth, the contents of each flask are centrifuged, to remove the supernatant. In common with other mutants, the product appears to be retained within the cell or absorbed onto the outside of the cell or beads, with only small amounts released into the broth. This requirement to extract from the mycelia rather than broth resulted in isolation in large amounts of membrane debris, complicating any isolation procedure. The range of products and yields was found to be unpredictable with each growth.

The mycelia (from 6 L of culture) were then extracted with (non-reagent grade) methanol (5 x 2 L). The first extract (2 L) usually contained *ca.* 300 mg heptaene in a large amount of contaminants. Subsequent extracts contained less visible impurity.

The extracts were combined (1.13 gH) and reduced *in vacuo* using a rotary evaporator. The water bath temperature was kept below 40 °C as work with other mutants had resulted in loss of compound with higher temperatures. As the volume of the extract is reduced, the water content of the supernatant increased and methanol content decreased, until when only 300-500 mL supernatant remained, it appeared largely aqueous, and a yellow precipitate formed.

Storage at 4 °C overnight gave a yellow precipitate containing mixed heptaene (342mgH in 1500mgWt). The precipitate was found to be very insoluble, even in methanol. NMR analysis indicated low levels of other heptaene (<10%) and impurities (<10%w/w). The level of insolubility in methanol is an easier method of purification, such that, repeated washes with methanol selectively removed other polyenes and membrane debris that are much more soluble in methanol. The repeated methanol washes, however, were unable to remove all the lipids completely, presumably due to some lipid participating in oligomeric structures with the aglycone, and thus being tightly associated with the heptaene.

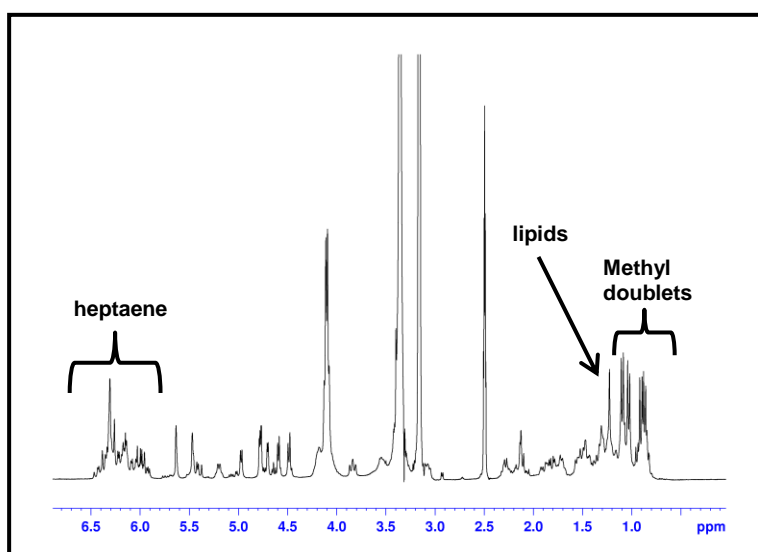


Figure 2.4 Proton NMR showing the presence of lipids in aglycone (**22**) after purification

2.3 Derivatisation of aglycone (**22**) with benzoyl chloride

The aim of this derivatisation was to derivatise the eight alcohol moieties as benzoyl derivatives to aid improved characterisation and obtain crystals suitable for an X-ray diffraction analysis. This derivative was produced because benzoylation is a quicker and easier reaction that was expected to produce crystalline products in a very short time. Also benzoylation was attempted because it was thought that esterifying all the polyols would provide enough bulk on the amphotericin molecule to obtain crystals. The presence of the benzoyl group was also expected to increase the solubility of the aglycone, hence enable better purification.

The aglycone, **22** (323 mgH in 500 mgWt) was suspended in dichloromethane and pyridine and reacted with benzoyl chloride (12 eq.) with DMAP as catalyst. The crude product obtained after 60 h had traces of the heptabenzoylated derivative. The octabenzoylated derivative (**45**) of aglycone (**22**) was obtained by separation from the heptabenzoylated derivative on a flash silica column (EtOAc-hexane). The presence of the desired product was confirmed by analytical Si-HPLC

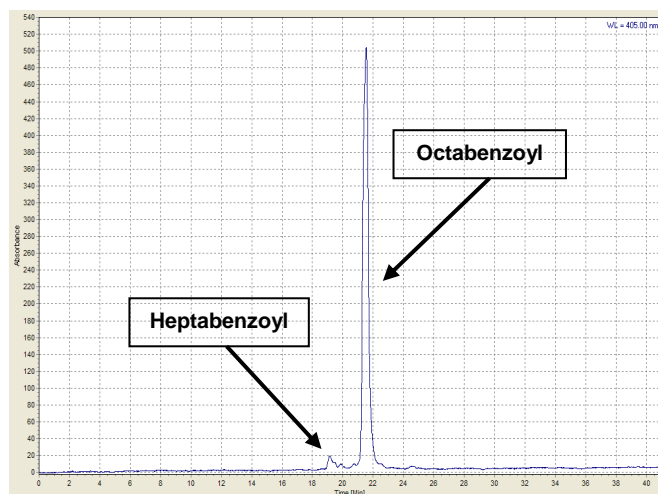


Figure 2.5 Si-HPLC of octabenzoyl amphoteronolide B showing traces of heptabenzoyl amphoteronolide B (flash column product)

Driver *et al.*, reported the formation of 13,14-anhydro derivatives of **1** while carrying out pertrimethylsilylation of **1**.⁵⁴ The 13,14-anhydro derivatives were confirmed by ¹³CNMR where a quarternary carbon resonance at 153.5 ppm was observed. If similar 13,14-anhydro derivatives had been formed during the benzoylation reaction, the expected partial structure would have been **55**.

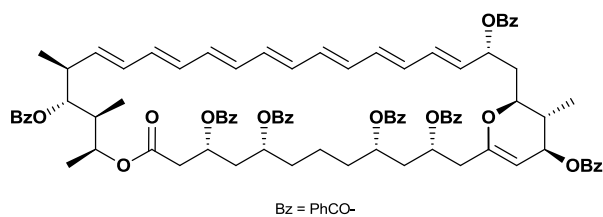


Figure 2.6 Structure of 13,14-anhydro derivative of octabenzoyl product (**55**)

Examination of product purified by flash column chromatography above by ^{13}C NMR spectroscopy showed no evidence of a quaternary signal at 153.5ppm (Figure 2.7). This confirms that no anhydro derivative such as **55** was present after purification. Any anhydro derivative that resulted from the reaction, if at all present, was most likely purified out. Also the molecular weight of **55** is 1442 Da, which is different from the value obtained by ESMS or FAB MS.

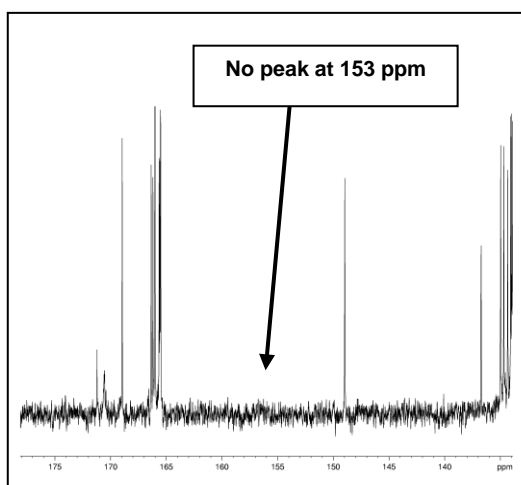


Figure 2.7 ^{13}C -NMR of octabenzoyl aglycone showing no resonance at 153.5ppm

Further purification of **57** was carried out by preparative HPLC (normal phase; EtOAc-hexane). The product obtained was then analysed by NMR to afford full characterisation. The spectra obtained were not as expected. ^{13}C NMR spectroscopic analysis showed a resonance characteristic of a ketone at 203 ppm, as shown in figure 2.8, indicating that the lactol had been trapped in the ring opened form as the benzoyl ester. Early work by MacPherson and Borowski had shown that reacting protected amphotericin B with hydroxylamine or *O*-methylhydroxylamine had trapped the lactol as the open ring oxime derivative.^{54,9}

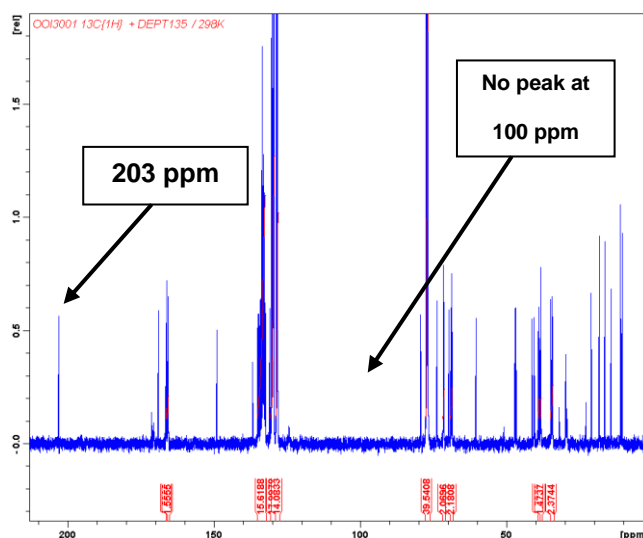
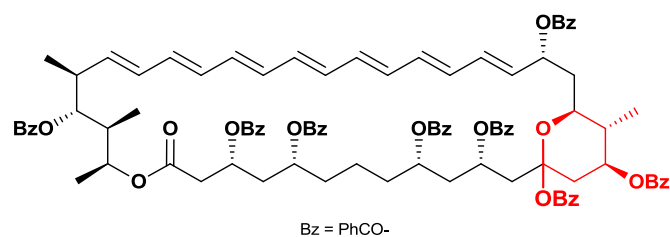
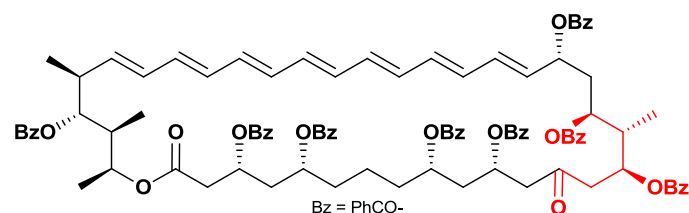


Figure 2.8 ^{13}C -NMR of **57** in CDCl_3 showing resonance at 203 ppm and no acetal peak at 100 ppm.

This implies that instead of obtaining **56**, the NMR confirms that **57** was obtained.



56



57

Figure 2.9 The possible conformation of the octabenzoyl derivative of **22**

The lactol is thought to be in equilibrium with the tautomeric open chain hydroxyl ketone. This hydroxyl ketone is then thought to be trapped as the benzoyl ester.

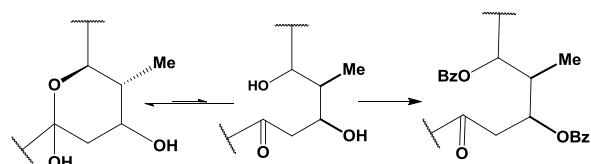


Figure 2.10 Suggested mechanism for the production of octabenzoyl lactol

The presence of four characteristic heptaene peaks by UV spectra confirmed that the heptaene chromophore had not decomposed as observed by previous workers while carrying out amphotericin derivatization.

The positive ESMS gave a peak at 1582.7 ($M + \text{water}$)⁺ and FAB mass spectra at 1564.67 (M^+) rather than the expected protonated analogues, it is not clear why this has occurred. The sample examined by FAB-MS contained some heptabenzoylated derivative, which was observed as the ($M - \text{water}$)⁺ peak, indicating that the final position to be benzoylated is 17-hydroxyl as the ring opened lactol.

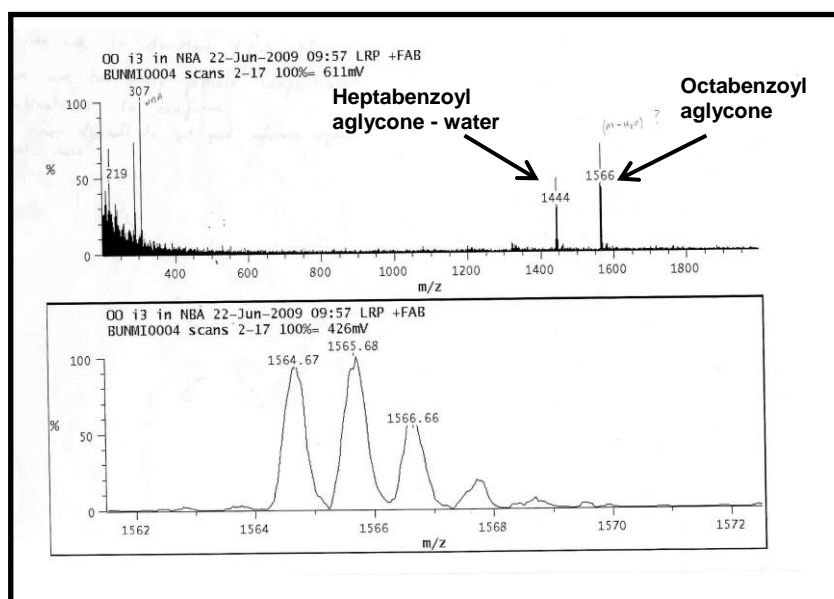


Figure 2.11 FAB-MS showing a mixture of heptabenzoyl and octabenzoyl amphoteronolide B

The presence of 14 protons in the proton NMR in the polyene region also confirms the presence of the heptaene. The combination of MS and ¹³C NMR indicates the structure of the octabenzoyl formed as follows:

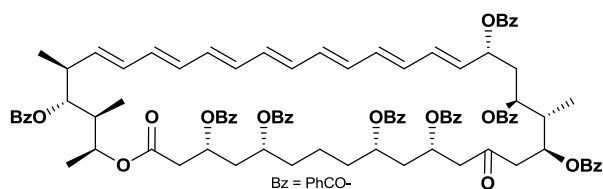


Figure 2.12 Octabenzoyl aglycone (**57**)

High resolution mass spec obtained for the octabenzoyl product isolated after HPLC prep is as shown below:

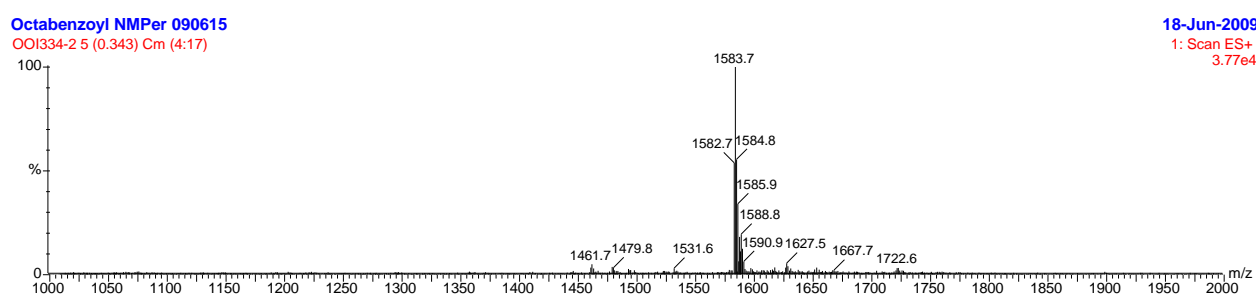


Figure 2.13 ESMS (+ve) showing presence of Octabenzoyl amphoteronolide B (**57**)

High resolution ESMS gave the molecular formula $C_{97}H_{99}O_{20}$ (calculated exact mass= 1583.6730; observed $[M+Na]^+$ = 1583.6671

Carbon NMR showed a lactone resonance at 169 ppm and eight benzoate ester carbonyls at 165.5-166.5 ppm with two carbons at 166 ppm. A ketone resonance (C-13) was observed at 203 ppm as discussed earlier.

Carbon resonance at 68-75 ppm shows eight methine carbons (C- 3, 5, 9, 11, 15, 17, 19, 35) and eight methylene carbon resonances between 34-47.5 ppm (C- 2, 4, 6, 8, 10, 12, 14, 18) and three methine carbon

resonances between 34-47.5 ppm (C- 16, 34, 36). 133-136 ppm show the polyenic methine resonances with three carbons at 133.45 ppm and two carbons at 133.26 ppm. 128-133 ppm show the methine resonance from 8 benzoyl rings with a total of twenty four carbons with two carbons each at 132.97 ppm, 129.5, 130.1, and 128.4 ppm. 10-22 ppm show four methyl resonances as expected, (C- 39, 41, 38, 40), and ^{13}C -DEPT show three methine resonances between 20-49 ppm.

2.4 Crystallisation procedure for octabenzoyl aglycone

The aim of the benzylation of **22** was to obtain crystals that will enable full structural characterisation and an understanding of the stereochemistry of **22**. Various attempts were made to further purify **57** by crystallisation. Initial crystallization of **57** was attempted by solvent diffusion. Crystals were formed by the slow evaporation of a solution of **57** (EtOAc-hexane solution (30% v/v). After six weeks, the presence of some crystalline material was observed. This crystal however, did not diffract.

Another attempt to grow crystals was by diffusion of hexane into an EtOAc solution of **57** in ethyl acetate. This method did not produce very good crystals.

Recrystallisation in hot methanol gave fine 'needle-like' yellow crystals. These crystals also did not diffract.

Unfortunately, after several attempts, no crystal of **57** of quality sufficient for X-ray diffraction could be grown. It is thought that the crystallisation using the solvent diffusion of a solution of **57** in EtOAc-hexane will potentially produce much better crystals if larger amounts of **57** were available.

2.5 Variation and optimisation of benzoylation method

2.5.1 Optimisation of duration of reaction

Initial reaction procedure was carried out by reacting benzoyl chloride (12 eq.) with crude product of **22** (105 mgH in 280 mgWt) for only 3 h. After organic extractions and purification by flash silica column, the heptaene eluted (25% EtOAc-hexane) produced a mixture of esters (99 mgH in 220 mgWt). Analysis by ESMS (+ve) showed 1374 (hexabenzoyl amphoteronolide B + H₂O)⁺, 1478 (heptabenzoyl amphoteronolide B + H₂O)⁺, while ESMS (-ve) showed 1252 (pentabenzoyl amphoteronolide B), and 1460 (heptabenzoyl amphoteronolide B).

The results obtained from this reaction showed that the reaction had not reached completion in spite of the large excess of benzoyl chloride used. This is thought to be due to differing steric hindrance of some hydroxyl groups on the molecule. For example, C-35 is a secondary alcohol with secondary carbons on either side.

Further optimisation involved leaving the reaction for 24 h. After the reaction, organic extractions, and purification by flash silica column, the heptaene eluted (25% EtOAc-hexane) produced predominantly heptabenzoyl amphoteronolide B with traces of the octabenzoyl derivative present. Analysis by ESMS (+ve) showed 1478 (heptabenzoyl amphoteronolide B + H₂O)⁺, 1479 (heptabenzoyl amphoteronolide B + H₂O + 1)⁺, 1583 (octabenzoyl amphoteronolide B + H₂O)⁺, 1584 (octabenzoyl amphoteronolide B + H₂O + 1)⁺, while ESMS (-ve) show 1460 (heptabenzoyl amphoteronolide B).

Increasing the duration of the reaction to 60 hours, however, afforded a product that was predominantly octabenzoylated.

2.5.2 Optimisation of purification of product

Reaction of crude **22** (132 mgH in 350 mgWt) with benzoyl chloride for 60 h at RT gave **57** which was extracted with water, sodium bicarbonate, copper sulphate and water to give **57** which was further purified by dry loading onto the flash silica column. This was because it was not possible to obtain about 2 mL (50% EtOAc-hexane) especially for reactions when crude product of **22** of >100 mg was used. After purification on the column, the desired product was about 41% pure.

In order to further improve the purification method, extraction of the product into 50% EtOAc-hexane after the organic extractions was carried out. The product was then wet loaded onto a flash silica column. The product obtained after purification on the flash silica column was 54% pure.

Even though, wet loaded flash columns gave 'purer' products, whenever the product obtained after reaction was >150 mg, it had to be dry loaded onto the flash silica column for purification due to its insolubility in about 2 mL of solution (50% EtOAc-hexane).

The level of purity obtained after the first column (54%) made further purification on another flash column necessary.

2.6 Conclusion

8-deoxy-16-descarboxyl-16-methyl-amphoterone B (**22**) was isolated and purified. In an attempt to obtain full characterisation and X-ray, an octabenzoyl derivative was synthesised, however, the crystals obtained did not diffract.

The "*ΔamphNM+perDIDI*" mutant was observed to also produce a glycosylated heptaene (**17**). There is a need to isolate, purify and characterise this analogue and this is discussed in the next chapter.

Chapter Three: Isolation, purification and characterisation of 16-descarboxyl-16-methy-amphotericin B and 8-deoxy-16-descarboxyl-16-methyl-amphotericin A

3.1 Introduction

In recent work, Caffrey has disrupted the *amphN* gene from the amphotericin B gene cluster in *S. nodosus* that is responsible for the oxidation of the C-16 methyl group to a carboxyl group.⁹² As discussed in Chapter Two, he simultaneously introduced the *perDIDII* genes (from *Streptomyces aminophilus*) alongside the *amphDIDII* genes in *S. nodosus* in an attempt to generate the perosaminylated amphotericin analogue. However, this “ Δ *amphNMper+DIDII*” disruptant instead generated predominantly the PKS product aglycone (**22**), as discussed in Chapter Two, along with variable levels of 16-descarboxyl-16-methyl-amphotericin B (**17**) with no evidence of the perosaminylated analogue. Addition of thiostrepton to the preculture medium and not the production medium increased production levels of **17** and reduced that of aglycone (**22**).

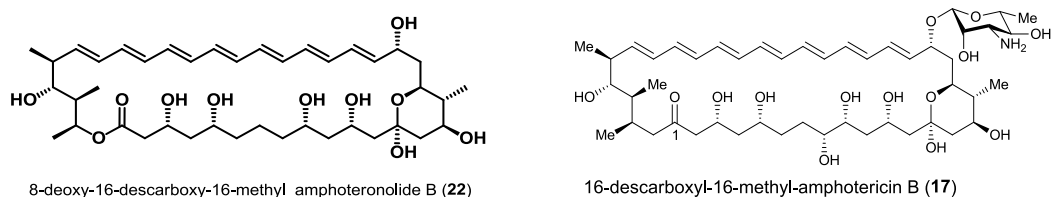


Figure 3.1 Structures of 8-deoxy-16-descarboxyl-16-methyl-amphoteronolide B (**22**) and 16-descarboxyl-16-methyl-amphotericin B (**17**)

Initial studies to isolate **17** were from this “ $\Delta amphNM+perDIDI$ ” disruptant. However, during the course of this work, Caffrey supplied an ‘*amphNM*’ mutant (without the addition of the *perDIDI* genes, and referred to as ‘*amphNM*’) with increased yields of **17** and reduced levels of aglycone (**22**). This chapter describes the isolation, purification and characterisation of **17** (along with the corresponding 28, 29-dihydro-tetraene) from these mutants.

3.2 Extraction and purification of 16-descarboxyl-16-methyl-amphotericin B from the “ $\Delta amphNM+perDIDI$ ” mutant

3.2.1 Cultures from the “ $\Delta amphNM+perDIDI$ ” mutant

3.2.1.1 Pre-cultures and production media inoculated with thiostrepton

GYE preculture media with thiostrepton (20 mg L⁻¹) added was inoculated with “ $\Delta amphNM+perDIDI$ ” mutant. The thiostrepton appeared to slow the growth, possibly due to its antibacterial activity, and after four days, aliquots (5-10 mL) were transferred to production (FD) media (28 x 250

mL; with thiostrepton (20 mg L^{-1}). These grew at a 'normal' rate, and mycelia along with the Amberlite XAD16 resin was harvested after five days. Methanolic extract (2 L, soaked overnight, 4x) of the sedimented mycelia and XAD16 from FD media was analysed by HPLC. The results obtained showed the presence of both **17** and **22** (3:8), with UV analysis indicating an overall heptaene (36 mg L^{-1}) and tetraene (33 mg L^{-1}) yield per litre of production broth. The heptaene yield was comparable to that reported by Murphy *et al.*,⁸⁵ The chromatogram obtained from HPLC was also similar to that reported by Murphy *et al.*, and indicated that in the crude extract *ca.* 25% of the heptaene was **17** ($t = 20 \text{ min}$), with a smaller peak (5-10%) thought to be 8-deoxy-16-descarboxyl-16-methyl-amphotericin B ($t = 23 \text{ min}$) and aglycone **22** ($t = 35 \text{ min}$).

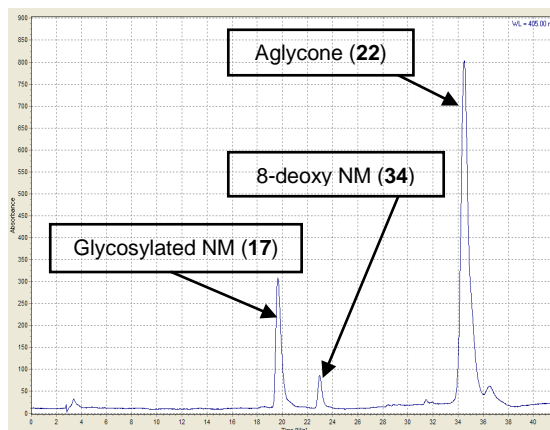


Figure 3.2 RP-HPLC (405 nm) of the crude methanolic extract of "*ΔamphNM+perDIDI*" grown with thiostrepton in the preculture and production media

3.2.1.2 Pre-cultures inoculated with thiostrepton and production media inoculated without thiostrepton

Aliquots of GYE preculture (with thiostrepton) inoculated with “*ΔamphNM+perDIDI*”, after four days growth, were transferred to production media (28 x 250 mL, without thiostrepton). These grew at a ‘normal’ rate, and the mycelia along with XAD16 resin was harvested after five days and soaked in methanol (2 L) overnight at 4 °C (4x extractions). UV analysis showed a comparable level of heptaene production (37 mgL⁻¹) to growth with thiostrepton in the production medium. However, analysis by HPLC showed almost double the amount of **17** present (ca 48%).

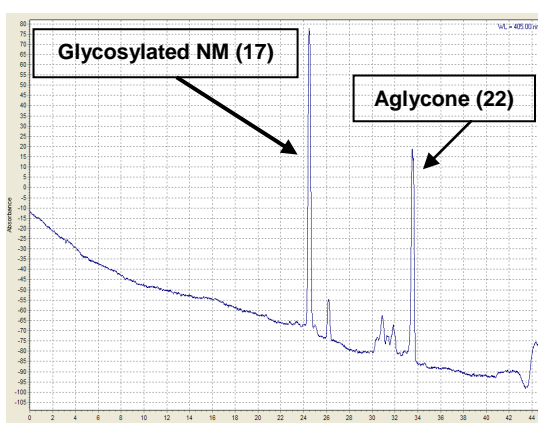


Figure 3.3 RP-HPLC (405 nm) of the crude methanolic extract of “*ΔamphNM+perDIDI*” grown with thiostrepton in the preculture but not in the production media

3.2.1.3 Pre-culture and production media without thiostrepton

GYE preculture inoculated with “*ΔamphNM+perDIDI*” mutant in the absence of thiostrepton was observed to grow at a ‘normal’ rate (2 days).

Aliquots (5-10 mL) were transferred to production media (28 x 250 mL, without thiostrepton). These grew at a 'normal' rate, and mycelia along with XAD16 resin was harvested after five days. Methanolic extracts (2 L, o/n, 4x extractions) of the sedimented mycelia and XAD16 from the FD media was analysed by HPLC. The results obtained showed the presence of **17** (ca 70% along with 8-deoxy ca 20%) with only traces (5-10%) of aglycone (**22**) present. The overall heptaene yield was relatively low (16 mg L⁻¹) relative to that obtained by Murphy *et al.*,. However, the estimated yield of **17** produced (11 mg L⁻¹) was better than that reported by Murphy *et al.*, (9 mg L⁻¹) in which thiostrepton was added to both GYE and FD media.

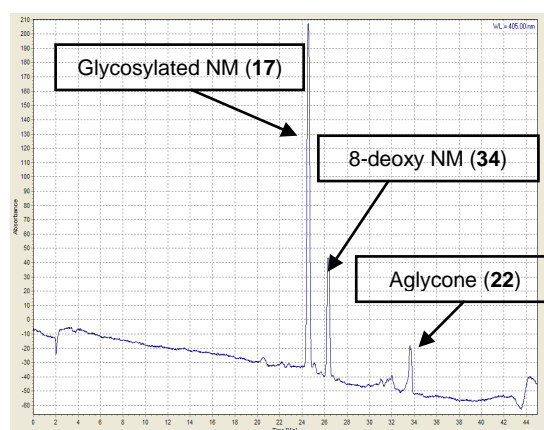


Figure 3.4 RP-HPLC (405 nm) of the crude methanolic extract of “*ΔamphNM+perDIDI*” grown without thiostrepton in both the preculture and production media

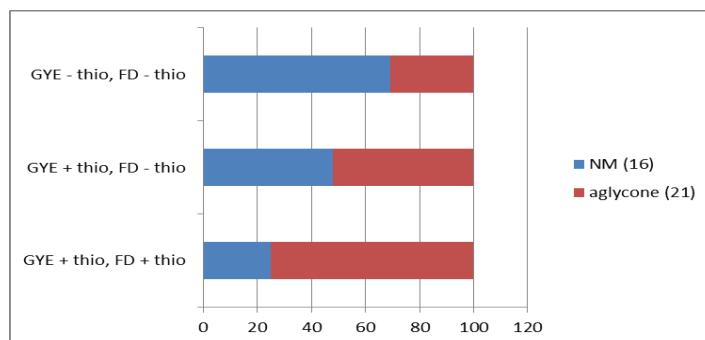


Figure 3.5 Comparison of the ratio of **17:22** isolated from “*ΔamphNM+perDIDI*” using different growth conditions

The results obtained showed that inoculating GYE media without thiostrepton, and subsequent inoculation of FD media, produced the best results. Therefore, subsequent growths of “*ΔamphNM+perDIDI*” media were carried out using this procedure.

The quicker growth of precultures without thiostrepton relative to precultures with thiostrepton further confirms the likelihood that the presence of thiostrepton in the GYE media is reducing the rate of the growth of the preculture with thiostrepton.

3.2.1.4 Duration of incubation

The effect of the duration of incubation of the “*ΔamphNM+perDIDI*” mutant was investigated. It was thought that increasing the duration of incubation may reduce the yield of the total heptaene due to their reported instability and sensitivity to various conditions such as broth at 30 °C.

The production media (derived from the same preculture flask) was incubated for five days or fourteen days and the resulting sediment extracted three times with methanol (2 L, o/n). After five days of incubation, the media was thick and looked 'healthy', and yielded total heptaene (36 mg L⁻¹ broth) comparable to previous experiment in Section 3.2.1.2 (36 mg L⁻¹). After fourteen days, the production broth appeared 'watery' possibly due to lysis. However, the total heptaene isolated was higher (46 mg L⁻¹). The XAD16 beads in the media may be absorbing polyenes as they are excreted, thus ensuring their stability, even after several days at 30 °C. The levels of total heptaene in each extraction (first to third) are presented in Figure 3.6.

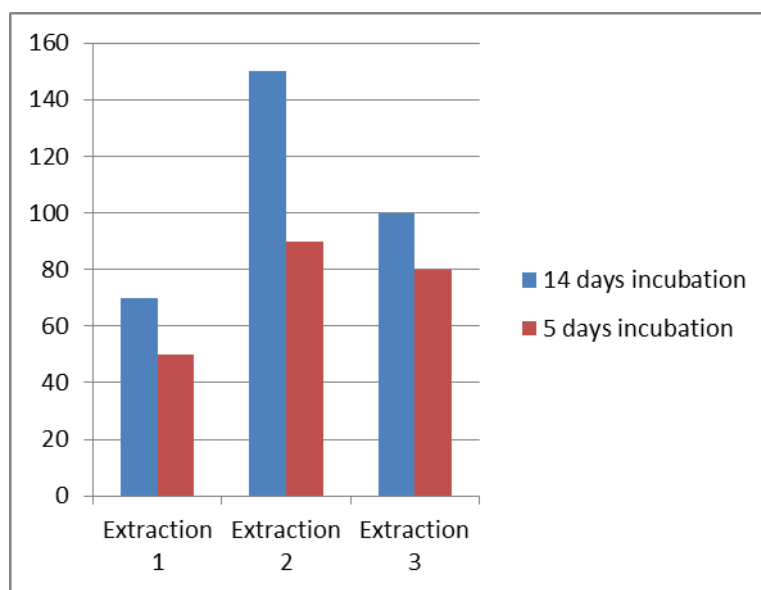


Figure 3.6 Comparison of the amount of total heptaene (in mg) isolated from “*ΔamphNM+perDIDI*” mutant under the same growth conditions but with varying duration of incubation

The results obtained showed a significant increase in the amount of total heptaene isolated after fourteen days of incubation. It was however,

important to investigate the effect of the duration of incubation on the actual amount of **17** produced.

RP-HPLC analysis showed that extracts from the five day incubation contained a lower **17:22** ratio relative to extracts from the fourteen days incubation. It is not clear why this occurs, but may be due to the level of expression of the post-PKS genes at this early time.

These results show that the media should be left growing for more than five days.

Considering that the yield of **17** per growth is not predictable or consistent, the incubation period should not necessarily be changed for other amphotericin analogues without a similar study.

The HPLC showed that there is no difference in the **17** isolated from the cells. The methanolic extracts (from five day and fourteen day incubation) were then combined for further purification.

3.2.2 Extraction of 16-descarboxyl-16-methyl-amphotericin B (17) from the “*ΔamphNM+perDIDI*” mutant

3.2.2.1 Variation in extract yields

The table below shows amounts of total heptaene per seven litre broth isolated from cultures (4 x 2 L), all derived from the same GYE preculture, inoculated under the same conditions, and incubated for the same duration, and extracted with methanol (2 L for each extraction). In these experiments, extraction 1 contained the highest amount of heptaene, unlike Section 3.2.1.3 above where extraction 2 contained the highest amount. The total amount was varied 600-900 mg.

Table 3.1 Typical amounts of total heptaene (mg/7 L broth) contained in each extract from the “*ΔamphNM+perDIDI*” mutant grown under identical conditions

	Total heptaene (mg/7 L broth)				
	Growth A	Growth B	Growth C	Growth D	Growth E
Extract					
1 st	370	350	220	250	270
2 nd	240	200	170	170	250
3 rd	190	130	100	140	170
4 th	100	100	90	120	110
Total	900	780	580	680	800

In another experiment, after completion of growth (14 days; 28 x 250 mL) of the "*ΔamphNM+perDIDI'*" disruptant, the extraction of **17** involved the separation of the mycelia and resin from the broth by centrifugation. UV assay of the broth (after dilution in methanol) indicated low levels of heptaenes and tetraenes, and the broth was discarded. However, the broth had been observed to show very high aromatic peaks at about 280 nm.

Methanol (2L; standard grade) was added to the sedimented material, with periodic swirling, for several hours. A large proportion of the methanol was removed by decanting, and fresh methanol added, and the procedure repeated four times. The first methanolic extracts usually contained relatively high levels of non-heptaene contaminants. It has also been reported that methanolic extracts of the sediment gives membrane lipids, aromatic compounds, dextrin derived oligosaccharides along with heptaenes and tetraenes.⁸⁵ The first extract also contained elevated tetraene levels. This is thought to be due to the relative solubility of the tetraenes in methanol, and that the tetraene is more soluble than the heptaene **17**, which in turn is much more soluble in methanol than the aglycone (**22**). Conversely, the fourth extract was relatively free of many contaminants but was shown by HPLC to have high level of aglycone, so the fifth extraction was not done. The methanolic extracts were combined and purified.

3.2.3 Purification of 16-descarboxyl-16-methyl amphotericin B (17) from “ Δ *amphNM+perDIDI*” mutant

The combined methanolic extracts (689 mgH, 653 mgT) derived from seven litres of culture broth were reduced in volume using a rotary evaporator with water bath set at below 40 °C to about 300 mL. At this stage, the remaining brown viscous supernatant appeared largely aqueous. Either immediately, or after leaving in the fridge overnight, a yellow precipitate (ca 11 gWt) formed, which can be isolated by centrifugation (603 mgH, 468 mgT).

3.2.3.1 Water-washes

The production of the tetraene as a co-metabolite during the biosynthesis of amphotericin is as expected as discussed in Chapter 1. Generally, tetraenes are more water soluble, so this aids separation from heptaenes. It has been suggested that the reduction of the C28-C29 double bond of the tetraene (**2**) causes a change in the conformation of the large ring sufficiently to significantly alter the distance between the carboxyl and amine group, thus, affecting the pH profile of the zwitterion formation, hence, enhancing the selective precipitation of **1** from its tetraene (**2**).

The yellow precipitate (603 mgH, 468 mgT) obtained from the brown viscous suspension stored overnight, was sonicated in and washed with de-ionised water several times. This was to afford further separation of **17**

from the oligosaccharides and other water soluble polyenes, especially, the tetraene.

After two waterwashes of the yellow precipitate from the "*ΔamphNM+perDIDI*" mutant, some tetraenes are still retained in the resulting yellow precipitate (462 mgH, 233 mgT in 3415 mgWt). This showed that repeated water washes, even though reduces the amount of tetraene present significantly, does not completely remove the tetraenes.

Further water washes could have been tried, but it has been observed that after two water washes a significant amount of heptaene is retained in the supernatant. More water washes could have also resulted in the retention of heptaene aglycone (**22**) while losing the more water soluble heptaene **17** in water wash. Two water washes is thus ideal, in order to maintain a good yield of heptaenes. The use of much less amount of water could have facilitated selective solubility of the tetraenes without dissolution of the heptaenes. This would have afforded better separation while maintaining a high yield of heptaene product.

Considering the varying ratio of heptaene to tetraene in different growths, it was difficult to establish the ideal volume of water that will afford good separation.

If large amounts of heptaene are present in the supernatant after water washing, it could be recovered by adding some XAD16 to this solution.

The beads are then isolated, and extracted with methanol. This procedure improves the recovery of the heptaene and could also be used in the future to obtain new analogues that are more water soluble.

The purification procedure was monitored by RP-HPLC to ensure that the desired product (**17**) was retained. UV analysis was used to assay the total heptaene (and tetraene) present in a sample, whilst RP-HPLC was used to detect how many heptaenes were present and in what ratio.

Generally, polyenes display considerable affinity for both lipid and oligosaccharide contaminants, thus hindering purification, and their solubility properties depend upon level of purification. Some oligosaccharides present in the crude extract of **17**, are removed during the water wash but most of the membrane lipids remain. The lipids constitute a major impurity accounting for about 80% of the weight of the yellow precipitate obtained after water wash.

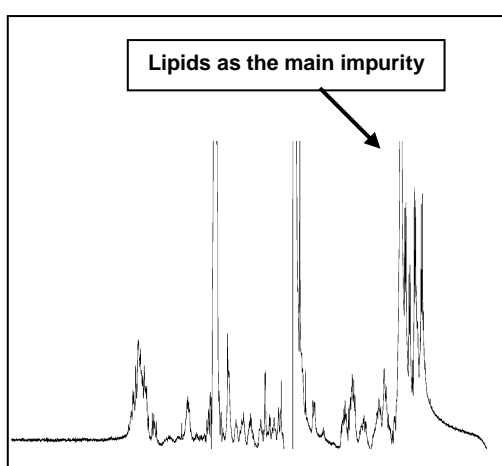


Figure 3.7 Proton NMR of **17** after water wash confirmed that the precipitate contains largely lipids.

3.2.4 Purification using ethyl acetate wash

A sample of the yellow precipitate obtained after water washes (126 mgH, 52 mgT in 890 mgWt) was dried and was suspended in methanol (20 mL), separated by centrifugation and the supernatant obtained slowly added dropwise to stirred ethyl acetate (200 mL). This was then stored at 4 °C overnight to afford precipitation of **17**. This procedure is as reported by Murphy *et al.*,⁸⁵ The precipitate obtained after about 18 hrs (99 mgH, 35 mgT in 463 mgWt) still contained some tetraene. Murphy *et al.*, reported improved separation was obtained by suspending the precipitate in much less methanol (5 mL) and making it up to a 10% solution in ethyl acetate.⁸⁵ Subsequent use of this purification method, however, did not improve the purity of **17** significantly. It was thus concluded that the procedure reported by Murphy *et al.*, was not consistent.

Other purification methods were considered in order to obtain a significant increase in the level of purity of **17**.

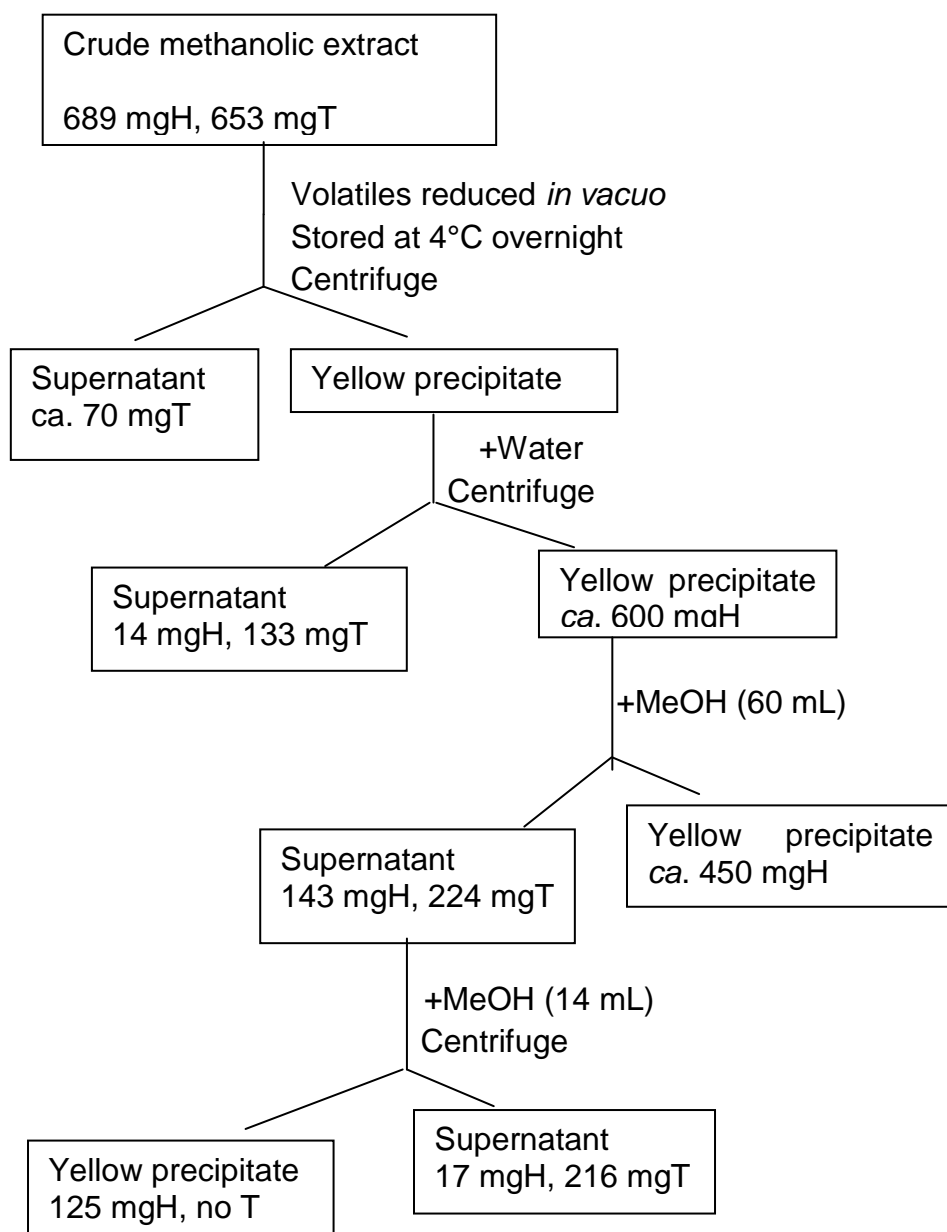
3.2.5 Purification using ether

In another batch of "*ΔamphNM+perDIDI*" grown, the methanolic extracts were concentrated *in vacuo* and the resulting yellow precipitate (613 mgH,

867 mgT in 7425 mgWt) was water washed twice to give a yellow precipitate (547 mgH, 502 mgT in 3518 mgWt). This precipitate was suspended in methanol (10 mL) and the resulting supernatant concentrated *in vacuo* and then suspended in diethyl ether (100 mL). The precipitate obtained after centrifugation (256 mgH, 100 mgT in 883 mgWt) was suspended in methanol. Results obtained (precipitate) showed a significant reduction in tetraene. The process should have been repeated to afford better separation of tetraene from **17**. The effect of this process on the level of lipid was not checked. This procedure shows promise and should be examined in future work.

3.2.6 Purification using methanol (differing solubility)

This method involved a slightly different procedure from that reported in earlier attempts to purify **17**. The procedure carried out is as shown in Scheme 3.1:



Scheme 3.1 Purification procedure for the isolation of **17** using partial dissolution in methanol

This method of purification is based on the different solubilities of heptaene and tetraene. The tetraene still present after water washing were found to be easily removed by repeated selective dissolution with sonication in minimal amount of methanol. At each step, optimisation of

the volume of methanol used may be required to achieve effective separation.

The significance of this method is that the tetraene was removed without using the ethyl acetate wash method as reported by Murphy *et al.*,⁸⁵ This method was used for the purification of subsequent batches.

RP-HPLC shows that the heptaene obtained from this method was only **17**. This was observed to be about 40% pure by weight. Proton NMR spectroscopy showed that the major impurity in this sample of **17** obtained was the 'lipids'. This shows that the partial dissolution of the yellow precipitate in methanol was effective at removing tetraenes; it was not effective at reducing the level of 'lipids' present in the sample.

3.2.7 Analysis of 16-descarboxyl-16-methyl-amphotericin B (**17**) from the "*ΔamphNM+perDIDI*" mutant

The 16-descarboxyl-16-methyl-amphotericin B (**17**) extracted from the sedimented material was contaminated with overwhelming amounts of membrane lipids, saccharides, aromatics and other polyene material. Despite considerable efforts, which included water washes, partial purification in methanol, and preparative RP-HPLC, it had not so far been possible at this stage to obtain the material pure enough for full structural

characterisation by NMR spectroscopy. None of the purification protocol discussed above could completely remove the membrane lipids.

Preliminary proton NMR analysis of **17** gave spectra consistent with those obtained by Murphy *et al.*,⁸⁵

FAB-MS and ESMS were carried out on the 'purified' sample from the " $\Delta amphNM+perDIDI$ " mutant. The results obtained were consistent with those reported by Murphy *et al.*,⁸⁵

Murphy *et al.*, reported positive ion peaks at 916.5 (M + Na)⁺, and 876.5 (MH- water)⁺, corresponding to the expected RMM of **17** (893.5Da).⁸⁵ The observed accurate mass was 894.51939, while the calculated mass for C₄₇H₇₆NO₁₅ was 894.51959.

3.3 Extraction and purification of 16-descarboxyl-16-methyl amphotericin B (**17**) from the '*amphNM*' disruptant

A strain of *S. nodosus* in which the *amphNM* genes are disrupted (without the insertion of the *perDIDI*) was provided by Caffrey (University College, Dublin) and in this work was referred to as '*amphNM*'. This disruptant was found to generate adequate quantities of both **17** and **22** without the addition of thiostrepton. The yields of the required **17** were increased (37mg L⁻¹) in comparison to **17** isolated from the " $\Delta amphNM+perDIDI$ "

strain (16 mg L^{-1}). The ratio of **17:22** isolated from the 'new' *amphNM* was largely increased in comparison to that obtained from " $\Delta\textit{amphNM}+\textit{perDIDI}$ " mutant.

3.3.1 Cultures from the '*amphNM*' mutant

During studies on this disruptant, efforts were made to increase titre levels. It was found that yield obtained were dependent on the preculture and its source. If a particular preculture subsequently gave a high yield, a spore or colony would be aseptically transferred using a wire loop to a fresh GYE medium.

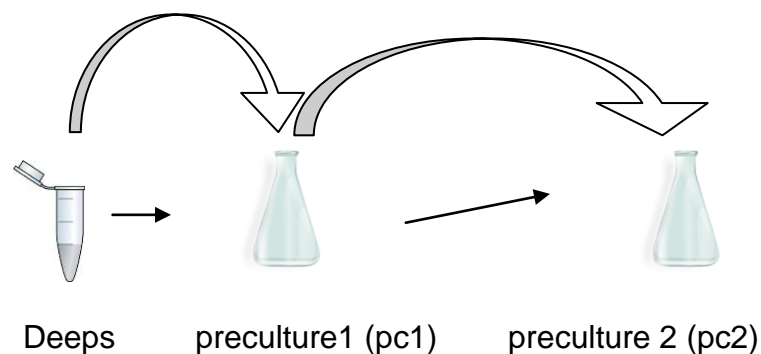


Figure 3.8 An illustration of the preparation of preculture 1 ('pc1') and preculture 2 ('pc2') of the *amphNM* mutant

It was observed that the ratio of **17:22** in the extracts from 'pc1' is significantly lower than that obtained from the extracts from 'pc2'. This is as shown in Figure 3.9.

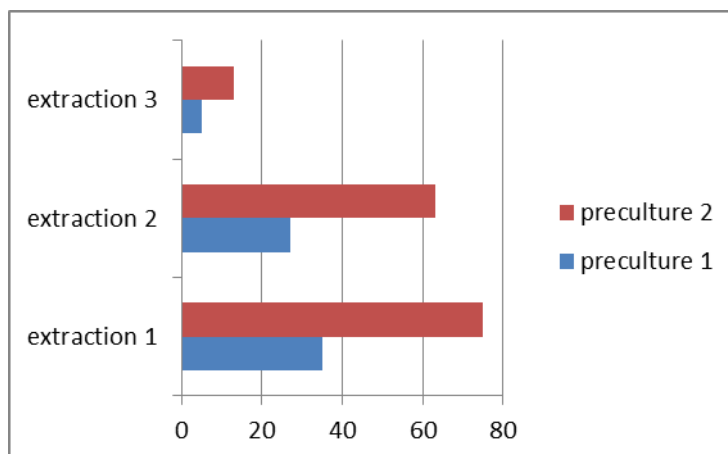


Figure 3.9 Comparison of yield of **17** (as a percentage of total heptaene) isolated from preculture 1 ('pc1') and preculture 2 ('pc2')

The variation observed between 'pc1' and 'pc2' is not fully understood. It could be due to the *amphDIDII* not recognising the aglycone or that the *amphDIDII* is acting a lot slower because of the change in the aglycone.

Murphy *et al.*, also reported formation of increased levels of aglycone in subsequent production cultures when he carried out repeated subculturing of the " $\Delta amphNM+perDIDII$ " mutant in thiostrepton-free GYE media.⁸⁵ Subsequent growths were therefore routinely made from a second preculture 'pc2'.

The cultures were routinely incubated for about fourteen days instead of five days due to the better yield observed with " $\Delta amphNM+perDIDII$ " mutant as discussed in Section 3.2.1.3.

As with the " $\Delta amphNMperDIDII$ " mutant, the amount of extract isolated from the *amphNM* disruptant varied significantly from batch to batch. The

reason for this is not fully understood but it is thought that it has to do with the method of inoculation. It is not possible to predict how viable spores in an aliquot of media inoculated will be.

Table 3.2 Variations in the amount of total heptaene (in mg) isolated from different growths of *amphNM* mutant using second preculture 'pc2'

Extractions	Growth	Growth	Growth	Growth
	A	B	C	D
1	120	90	120	230
2	60	130	70	210
3	60	100	60	100
4	40	80	40	90
Total	280	400	290	630

3.3.2 Extraction of 16-descarboxyl-16-methyl-amphotericin B (17)

3.3.2.1 Erlenmeyer flask

In a typical growth, media and XAD16 resin (28 x 250 mL) were each inoculated with preculture (10 mL) and shaken (120 rpm, 28 °C) for four days. After centrifugation, the sedimented mycelia was collected in a beaker (2 L) and crushed using a large spoon. Extraction with methanol was carried out in a 5 L Erlenmeyer flask (4 x 4 L over four days).

As with extracts from “*ΔamphNM+perDIDI*” mutant, the first methanolic extracts contained high levels of non-heptaene contaminants and elevated tetraene levels. It was also observed that the first extraction usually contained more **17** than **22**. While subsequent extractions contained higher proportion of **22**.

UV assay of the combined extracts indicated the presence of heptaenes (420 mg) and tetraenes (272 mg). HPLC analysis showed several heptaenes, a major heptaene peak at 20 min correlates to the expected **17**, a tetraene peak at 22 min, and a later heptaene peak at 35 min aglycone as shown in Figure 3.2.

3.3.2.2 Muslin Cloth

Extraction of sediment using muslin cloth has proved to be convenient and more time saving than using Erlenmeyer flask. The set up for extracting using muslin cloth and a vegetable colander (both readily available from shops e.g. Fenwicks, Leicester) is as shown in Fig 3.10:

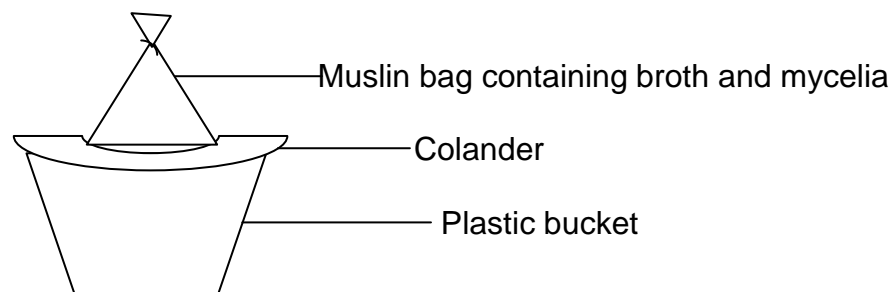


Figure 3.10 Set-up for separation of mycelia and beads from broth

The muslin cloth was allowed to drain and not squeezed because it was observed that cells escaped through the pores of the cloth if squeezed.

It was observed that methanolic extracts from muslin cloth had much less aglycone (18% of total heptaene) present than that observed when centrifugation (Erlenmeyer method) is used (31% of total heptaene). This is thought to be due to the relatively small volume of methanol (1 L) used for extraction in the muslin method. The volume used is just enough to dissolve predominantly **17** and not high levels of **22**. This aided subsequent purification steps.

3.3.3 Purification of 16-descarboxyl-16-methyl amphotericin B (**17**) from the '*amphNM*' mutant

The combined methanolic extracts (421 mgH, 600 mgT) were reduced *in vacuo* (ca. 300 mL) resulting in an aqueous supernatant and yellow precipitate that was collected by centrifugation and washed (with sonication) with water (2 x 100 mL). The resulting yellow precipitate was analysed by UV (262 mg H, 255 mg T) and HPLC.

HPLC and ESMS of the resulting yellow precipitate indicated that the major products present were 16-descarboxyl-16-methyl-amphotericin B (**17**), 8-deoxy-16-descarboxyl-16-methyl amphotericin A (**42**) and 8-deoxy-16-descarboxyl-16-methyl-amphoterionolide B (**22**).

The purification procedure used for the crude extract of **17** obtained from the new *amphNM* was the same as that used for crude extract of **17** from the " Δ *amphNM+perDIDI*" mutant. Waterwashes were carried out to remove significant amounts of tetraene and partial dissolution in methanol was carried out to fully separate the heptaene and tetraene.

Due to higher yields of **17** obtained from the *amphNM* disruptant when compared with **17** from " Δ *amphNM+perDIDI*", purification by partial dissolution was found to be much easier. The level of purity obtained for the **17** after partial dissolution (40%) is however, the same as that obtained from " Δ *amphNM+perDIDI*".

3.3.4 Analysis of 16-descarboxy-16-methylamphotericin B (**17**) from the '*amphNM*' mutant

The proton NMR obtained for **17** isolated from the *amphNM* disruptant is consistent with that obtained from " Δ *amphNMperDIDI*" mutant and that reported by Murphy *et al.*. ESMS data obtained was also consistent with that reported by Murphy *et al.*, as discussed in Section 3.2.7.

3.4 8-deoxy-16-descarboxy-16-methyl amphotericin A (**54**)

Initial studies of the tetraene produced by "*ΔamphNM+perDIDI1*" mutant has shown the presence of 8-deoxy-16-descarboxy-16-methylamphotericin A (**54**) instead of the expected 16-descarboxy-16-methylamphotericin A.⁸⁵

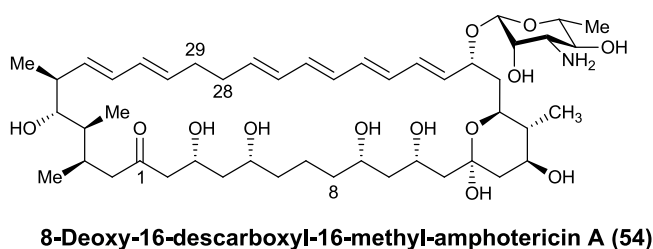


Figure 3.11 Structure of 8-deoxy-16-descarboxyl-16-methyl-amphotericin A (**54**)

In wild type amphotericin B (**1**), the tetraene isolated as the co-metabolite is amphotericin A (**2**), with a hydroxyl group at C-8. It is unclear why the *amphNM* mutant produces heptaene compound that is hydroxylated at C-8, whereas the tetraene compound is not. It is possible that the AmphM ferredoxin normally cooperates with both the AmphL and AmphN cytochrome P450s. In the *amphNM* disruptant, AmphL may recruit a different ferredoxin to form a complex that acts less efficiently on the tetraene. This could also be due to the shape of the tetraene resulting in a conformation not recognised by AmphL.

In the study of amphotericin and its analogues, little is known about the tetraenes produced. Attempts to extract, isolate and purify **42** are reported in this work.

3.5 Extraction of 8-deoxy-16-descarboxyl-16-methyl amphotericin A (**54**)

Crude extracts of **54** were obtained from the '*amphNM*' mutant. As mentioned in Section 3.3.3, water washes was used to remove significant amounts of tetraene. Initial studies involved the addition of XAD16 to the supernatant from the water wash, followed by partial dissolution of the beads in methanol, gave predominantly **54**. Removal of volatiles *in vacuo* from the methanolic solution resulted in a brown, sticky slurry. This is thought to be due to large amounts of sugars present in the sample.

When the water washes is used to remove tetraenes, sugars are also present in the supernatant after the wash. Also, the addition of XAD16 affords removal of tetraenes as well as sugars, from the aqueous mixture. Due to similar solubilities of sugars and tetraenes, their separation was cumbersome. A better means of obtaining the tetraene was therefore expedient.

During the purification of **17** by partial dissolution in methanol described in Section 3.2.6, it was observed that the tetraenes isolated had little or no sugars present. Therefore **54** was isolated from the supernatant of the

methanol suspension. Volatiles were removed *in vacuo* to afford a pale yellow precipitate (143 mgH, 224 mgT in 1195 mgWt).

Analysis by RP-HPLC with detection set at 318 nm, showed the presence of two very close peaks with elution at 20.5 min and 21.5 min.

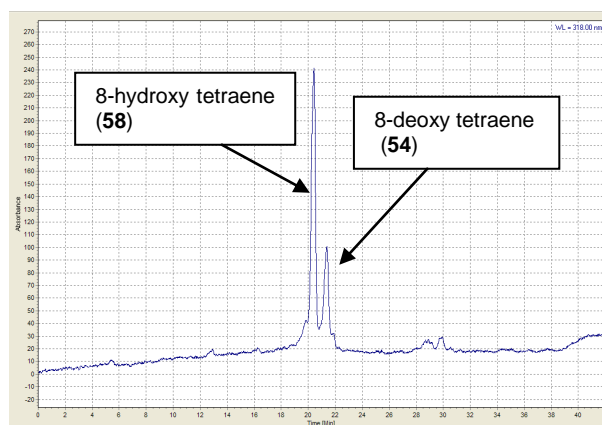


Figure 3.12 RP-HPLC showing the crude extract of tetraenes present in *amphNM* disruptant

One of these peaks is thought to be the tetraene fraction that is hydroxylated at C-8.

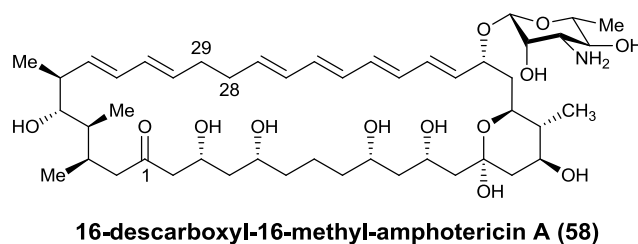


Figure 3.13 Structure of 16-descarboxyl-16-methyl-amphotericin A (58)

This hydroxylated analogue was however, not isolated. It is thought that due to its solubility, **58** was purified out. The second peak (at 21.5 min) is thought to be **54**.

3.6 Purification and analysis of 8-deoxy-16-descarboxyl-16-methyl amphotericin A (**54**)

The main impurities in the yellow precipitate were residual heptaenes (from the purification of **17**) and lipids. No attempts were made to further purify **54** obtained. This was mainly because of the solubility of **54** in most polar and organic solvents. It was thought that any purification required can be carried out when the Fmoc reaction had been carried out (See Section 4.5).

3.7 Conclusion

The efficient oxidation of C-16 methyl branch has been shown to occur even in the absence of the other two-post PKS modification.⁸⁷ The disruption of *amphNM* produces **17** with yields lower than that of **1**. The yield of **17** can be improved by inoculating the preculture and production media without thiostrepton. The purification of **17** involves waterwashes and partial dissolution in methanol to achieve a product of about 40% purity. The main impurity is lipids and various methods attempted could not remove the lipids completely. There is therefore a need to develop a

purification protocol that will improve the purity of the desired product, **17**, mainly by removing the lipids present.

Chapter Four: Fmoc derivatisation

4.1 Introduction

Protecting groups are usually used in multi-step organic synthesis. They are generally used to selectively protect certain functional groups whilst other functional groups in the molecule are selectively chemically modified. Subsequent removal (deprotection) generates a selectively modified molecule.

4.1.1 Protecting groups in amphotericin B 'chemistry'

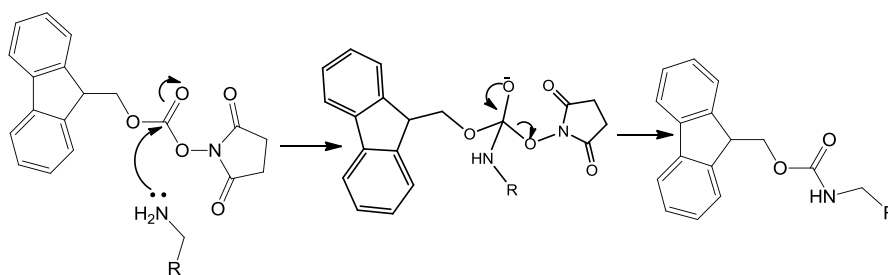
Derivatisation of amphotericin B (**1**) has been carried out using different protecting groups, some of which cannot be readily removed to generate the parent functionalities.⁵⁴ Nicolaou *et al.*, synthesised a mixture of *N*-acetylated bisacetonide intermediates during the total synthesis of **1**,⁹⁸ and also confirmed the stereochemical requirements of **1** by silylation but did not attempt to remove the protecting groups in order to generate the parent compound. The ester used for the derivatisation of **1** during the synthesis of amphotericin B methyl ester (AME)⁶² and similar derivatives^{62,99} also could not be removed to generate the parent compound.

Chemical manipulation of **1** has concentrated almost exclusively on both the 16-carboxylate functionality, which has been derivatised as esters, amides⁹ and a hydrazide,¹³ and on the mycosamine amino group, where a variety of modifications have been carried out including the preparation of *N*-alkyl⁹ and *N*-acyl⁶¹ analogues. Most of these analogues were reported to retain biological activity.

4.2 *N*-Fmoc derivatives of amphotericin analogues

Fluorenylmethoxycarbonyl (Fmoc) derivatisation is a method used in organic synthesis for the protection of free amines and is used widely as an amine protecting group in amino acid coupling in solid phase.¹⁰⁰ It is usually a method of choice due to its robustness in acidic and neutral solvents and its easy removal in mild alkali.¹⁰¹ Some of the most common methods used for introducing the Fmoc group as the Fmoc carbamate is through fluorenylmethoxycarbonyl chloride (Fmoc-Cl) and 9-fluorenylmethylcarbonyl succinimidyl carbamate (Fmoc-OSu).

The reaction mechanism for Fmoc-OSu amine derivatisation involves a nucleophilic attack of the amino group, followed by displacement of the hydroxysuccinimide leaving group to generate a protected amine.



Scheme 4.1 Reaction mechanism for protection of amines using Fmoc-Osu

Protection with Fmoc has been applied in both solid and liquid-phase synthesis. Fmoc is labile to mild base which is compatible with the polyene nucleus. Also, the hydrophobicity of the Fmoc group will increase the solubility of the polyene resulting in more easily manipulated derivatives.

Driver *et al.*, used Fmoc to protect the amino group in their bid to synthesise 16-descarboxy-16-hydroxymethylamphotericin B (**19**), as the first monofunctionalised derivative of **1** without the carbonyl containing substituent at C-16.⁵⁴ The synthesis was also carried out without prior acetonide protection which was the common procedure then. The procedure used by Driver *et al.*, involved the use of **1** in DMF-MeOH, Fmoc-Osu (1.6 eq.) and pyridine (1.3 eq.) left stirring for 4 hours at RT to give 83% yield. The product obtained was not purified before being used for subsequent reactions, thus; no final yield after purification was obtained.

Matsumori and co-workers examined the intermolecular interactions of **1** and sterols by NMR, and synthesized the first fluorinated derivative of **1**.⁶⁵

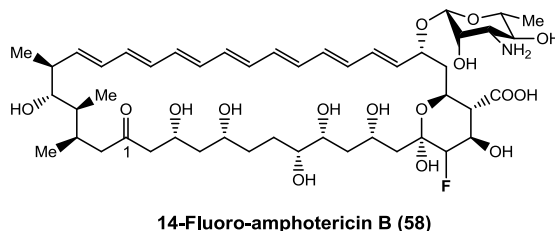
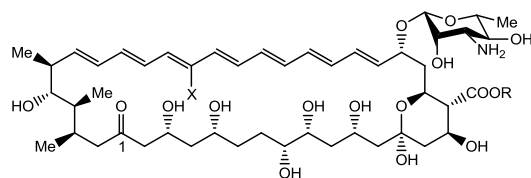


Figure 4.1 Structure of 14-fluoro-amphotericin B (**59**)

The first step in the multi-step synthesis involved the protection of the amino group on **1** using Fmoc-OSu in the presence of DMF and pyridine for 18 hours at RT. The N-Fmoc product was then used for subsequent reactions without purification. The deprotection of the N-Fmoc fluorinated macrolactone was carried out with piperidine in DMSO: MeOH (4:1) for an hour at RT to give 14-fluoro-amphotericin B (50% yield).

Tsuchikawa *et al.*, developed a practical and versatile method for synthesising a fluorinated amphotericin B derivative (28-¹⁹F-amphotericin B methyl ester '28-¹⁹F-AME' (**60**) by combining chemical synthesis and degradation of a natural product.⁹⁹ 28-¹⁹F-AME was synthesised to assist with the NMR-based investigations of the mechanism of the ion channel formation.



Amphotericin B (1): X = R = H
 Amphotericin B methyl ester (AME) (14): X = H, R = Me
 28-¹⁹F-amphotericin B methyl ester (59): X = F, R = Me

Figure 4.2 Structures of amphotericin B (**1**), amphotericin B methyl ester (**15**) and 28-¹⁹F-amphotericin B methyl ester (**60**)

Tsuchikawa and co-workers synthesised C-1 to C-21 by chemical degradation of the natural **1** and the ¹⁹F-labelled C-22 to C-37 by Stille coupling and Horner-Wadsworth-Emmons reactions.¹⁰²

The first step in the multistep synthesis of C-1 to C-21 involved the treatment of **1** with Fmoc-OSu followed by synthesis of the methyl ester using methyl iodide. After the formation of the fluorinated macrolactone, the Fmoc group was removed with piperidine (79% yield) before ketal hydrolysis.

Palacios *et al.*, in order to investigate whether the carboxylate at C-16 is required for the antifungal activity of **1** or not, synthesised various derivatives of **1** such as **17**.⁶³ This involved the use of Fmoc as a protecting group for the amino functionality of **1**. Palacios *et al.*, produced N-Fmoc methyl ketal intermediate to synthesise **17**. The procedure used involved the use of **1** (ca 55% pure) in DMF: MeOH (2:1), Fmoc-OSu (2.8 eq), pyridine (11.5 eq.) at 23 °C for 12 h. After the reaction, the reaction mixture was poured onto ether at 0 °C. After 30 min, the precipitate was

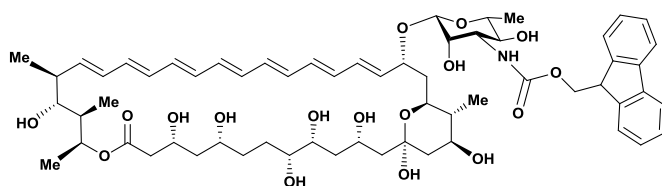
isolated by Büchner filtration. The deprotection step involved the use of CSA (0.55 eq.) in THF: MeOH (1:1) at 0 °C for 1 h to give the desired product (**17**), in 90% yield. The deprotected product was used for subsequent reactions without further purification.

The examples above serve as a precedent for the use of Fmoc as a convenient, stable, robust and quick intermediate during the synthesis of amphotericin derivatives. They also show that Fmoc derivative of **1** can be produced in good yield with a reaction carried out in relatively short time. The Fmoc derivatives are also UV active (at 254 nm) as well as non-polar enough for both TLC analysis and flash chromatography.

This chapter describes the investigation as to whether Fmoc protection can assist in the purification of **17** from crude extracts or partially purified samples. The aim was that Fmoc derivatisation would enable purification steps involving flash chromatography on large scale so that it is readily available in good purity for biological and mode of action studies elsewhere. In addition, this procedure might facilitate isolation and purification of other components such as the 28-29-dihydro tetraene (the tetraene analogue of **17**) analogues from the same extracts.

4.3 N-Fmoc derivative of 16-descarboxyl-16-methyl-amphotericin B (**17**)

Fmoc protection of the free amine on **17** generates a molecule rather less polar, making it possible to purify on a large scale by normal phase flash column chromatography.



16-Descarboxyl-N-fluorenylmethoxycarbonyl-16-methylamphotericin B (**61**)

Figure 4.3 Structure of 16-descarboxyl-N-fluorenylmethylcabonyl-16-methyl-amphotericin B (**61**)

In order to explore ways of better purification of **17**, there was a need to ascertain at what stage of the purification of **17**, the Fmoc protection should best be carried out. In this work, protection was investigated on

- The yellow precipitate after waterwashes, usually (*ca.* 20% w/w) heptaene (**17**), with reduced amounts of saccharides and membrane debris along with aglycone (**22**) and tetraene (**54**)
- The yellow precipitate after water-washes and initial purification by partial dissolution in methanol (*ca.* 35% w/w)
- Or after further purification by partial dissolution in methanol has been carried out on the extracts (*ca.* 41% w/w).

In order to achieve a maximum overall yield of pure product, there has to be consideration of loss of yield in each 'pre protection' purification step, versus the effect of high levels of impurity on the protection process along purification by flash chromatography.

4.3.1 Fmoc protection of water washed yellow precipitate

Most of the initial optimisation of the Fmoc protection method was carried out on extracts from the " $\Delta amphNM+perDIDII$ " mutant. More recent studies were, however, carried out on extracts from the '*amphNM*' mutant.

4.3.1.1 Fmoc protection of yellow precipitate after water washes

Initial studies were performed on yellow precipitate that had been water washed, as this process should reduce the level of saccharides that contain copious hydroxyl groups that may slowly compete for the Fmoc reagent, resulting in a more effective procedure.

The main impurities in the extracts of *amphNM* mutant, as discussed earlier, were membrane lipids, saccharides, aglycone (**22**), aromatics and the tetraene (**54**). The tetraene has much greater solubility than **17**. After two waterwashes of the yellow precipitate, the remaining tetraene present, even though much reduced (by about 30%) in comparison to the crude

extract, was difficult to separate from the heptaene by further water washes. In order to avoid loss of more heptaene material during purification, it was thought that due to the differing polarity of the heptaene and tetraene, N-Fmoc tetraene will be easily separated from the N-Fmoc heptaene using flash column chromatography.

Methanolic extraction → waterwashes → yellow precipitate → Fmoc protection
flash chromatography → separate N-Fmoc heptaene and N-Fmoc tetraene
deprotect → purified NM (17)

Scheme 4.2 Hypothesis for the Fmoc protection of water washed yellow precipitate

N-Fmoc reaction was carried out on a sample of waterwashed (x2) yellow precipitate from "*ΔamphNM+perDIDI*" mutant (180 mgH, 88 mgT in 930 mgWt (40% NM), using Fmoc-OSu (2 eq.) and pyridine (2 eq.) as previously used by Palacios *et al.*, when he carried out synthesis of amphotericin B derivatives.⁶³ The reaction was left stirring at room temperature for 16 h, in order to ensure that the reaction on the impure sample went on to completion.

The reaction mixture was added onto flash silica (3 g) and the volatiles removed *in vacuo*. Dry loading onto the silica column was carried out due to the insolubility of the sample (even in about 1-2 mL of 10% MeOH-EtOAc). It was thought that the contaminants in the reaction mixture contributed to its insolubility in small amount of required solvent. The first

column was mainly a filtration column with the aim of separating the desired product from large amounts of impurities present in the crude sample. After extensive washing (EtOAc), the product (70 mgH, 36 mgT in 340 mgWt) was eluted (10% MeOH-EtOAc). Proton NMR analysis of the eluted sample obtained from the first column showed that the main impurity was still membrane lipids. This showed that, even though washing with EtOAc reduced lipids levels, some remained. This may be due to strong non-covalent interactions between the polyenes and lipids. Thus, a second flash column was required to achieve high purity.

Analysis by UV and HPLC also showed that the product from the first column still contained a mixture of heptaene and tetraene. The TLC of the product from the first column was a smear with two spots from the heptaene and tetraene. The R_f for the *N*-Fmoc heptaene (**61**) and *N*-Fmoc tetraene (**63**) was 0.5 and 0.55, respectively. This suggested that ethyl acetate was not the ideal solvent for the separation of the heptaene and tetraene. The close R_f and subsequent lack of success in separating the *N*-Fmoc heptaene and *N*-Fmoc tetraene suggest that the polarity of both compounds was not much different.

Various solvent mixes were tested by TLC in order to find the ideal solvent mix that will enhance separation of the heptaene and tetraene. The best separation was obtained with methanol-dichloromethane (1:10) that gave an R_f of 0.4 and 0.55 for the heptaene and the tetraene, respectively,

showing that separation of heptaene and tetraene by flash column chromatography may be possible.

The product obtained after the first column was wet loaded onto a DCM column and after washing with DCM, the desired product (31 mgH in 45 mgWt) eluted with 7% MeOH-DCM. Even though the separation was obtained, the yield of the desired 'pure' heptaene was poor due to larger proportions of the eluent being a mixture (35 mgH, 20 mgT). Further attempts to obtain better separation using DCM as solvent proved futile.

It was thought that carrying out the Fmoc protection after reducing the amount of tetraene in the crude extract will enhance the efficiency of the procedure and further improve purity.

4.3.1.2 Fmoc reaction on yellow precipitate after water-washes and initial partial dissolution in methanol

Yellow precipitate obtained from growth of "*ΔamphNM+perDIDI*" was water washed (x2) (270 mgH, 81 mgT in 1315 mgW). The resulting precipitate was partially dissolved in methanol (3 mL). The remaining yellow precipitate (75 mgH, 21 mgT in 220 mgWt, 90% NM by HPLC), was reacted with Fmoc-OSu and pyridine for 17 h at RT. TLC of the reaction mixture at 17 h showed the presence of the product. The reaction mixture was concentrated *in vacuo* and extracted (x2) with MeOH-EtOAc (10%).

The supernatant (73 mgH, 20 mgT) obtained was reduced *in vacuo* and wet loaded onto a flash silica column. Washing with copious amount of EtOAc and MeOH-EtOAc gave the desired product (70 mgH, 11mgT in 159 mgWt) eluting with 5% MeOH-EtOAc. Proton NMR showed largely lipids and little aromatics as well as the desired product.

The product obtained after the first column was wet loaded onto a DCM column and the desired product (65 mgH, 7 mgT in 78 mgWt) eluted with 7% MeOH-DCM. Proton NMR showed the presence of some greatly reduced membrane lipids. Thus this procedure dramatically reduced the levels of membrane lipids in the samples, but failed to reduce the tetraene impurity (*ca.* 20%)

4.3.1.3 Fmoc reaction on *amphNM* extract free of tetraene

The next investigation was to perform Fmoc protection on samples with reduced tetraene levels obtained using methods outlined in Chapter 3.

A sample of yellow precipitate obtained from a growth of *amphNM* was water washed (x2). The precipitate was purified by repeated partial dissolution in MeOH to give a yellow precipitate (95 mgH in 230 mgWt, >92% NM) which, after drying, was reacted with Fmoc-OSu and pyridine for 17 h at RT. The reaction mixture was concentrated *in vacuo* and extracted (x2) with MeOH-EtOAc (10%). The supernatant (92 mgH)

obtained was reduced *in vacuo* and wet loaded onto a flash silica column. Purification on the first flash column (MeOH-EtOAc) gave the desired product (90 mgH in 163 mgWt) eluting with 5% MeOH-EtOAc. However, in order to further purify the desired product, a second column in MeOH-EtOAc was carried out which gave **61** (85 mgH in 93 mgWt). However, HNMR showed the presence of some remaining membrane lipids.

It was observed that separating the heptaene and tetraene before Fmoc reaction helped improve the yield (91%) of the **61** obtained. It also helped purification because there was only one main impurity left to purify out-lipids.

The product obtained was further purified by semi-preparative Si-HPLC and analysed by ESMS and NMR.

Analysis by positive ion ESMS showed peaks at 713.5 (indicating loss of Fmoc group, sugar and water) and 1138.6, corresponding to the sodium adduct of **61** (1115 Da).

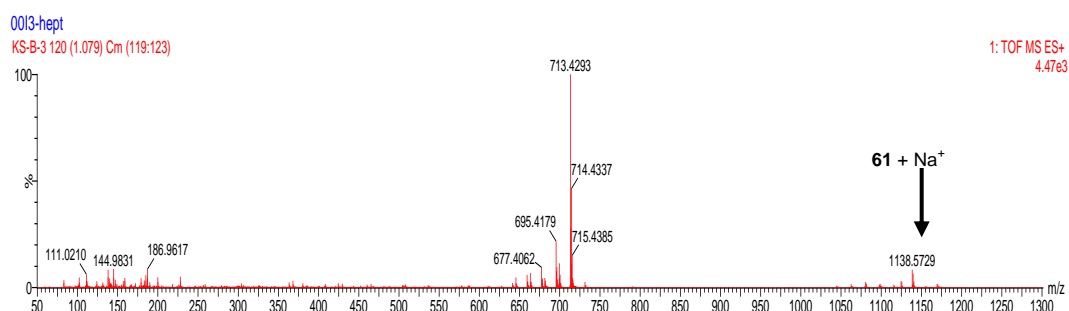
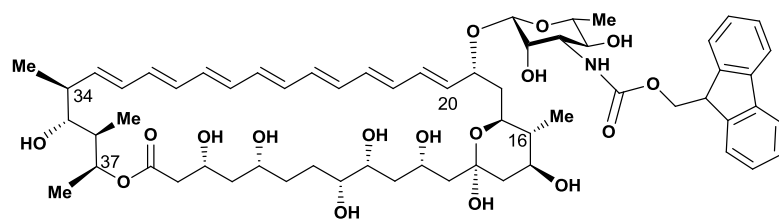


Figure 4.4 Positive ion ESMS showing the sodium adduct of **61**



16-Des-carboxyl-N-fluorenylmethoxycarbonyl-16-methylamphotericin B (61)
RMM: 1115Da

Table 4.1 Heterocorrelation (in DMSO-d₆) observed for N-Fmoc NM

(61)

δ_H	δ_C	Carbon atom number
0.99	12	41
1.05	18, 42	38
1.1	16	
1.2	17	6'
1.25	29	Lipid
1.5	47	
1.55	30	
1.75	39	
1.85	45	16
2.15	42	36
2.3	42	34
3.1	74, 77	
3.2	69, 73	
3.4	57, 68	
3.5	69	
3.6	69	

δ_H	δ_C	Carbon atom number
3.8	69	
4.1	66	
4.2	66, 68	
4.35	76	
4.5	98	1'
5.2	69	37
5.45	137	20
5.95	137	33
6.05	132	26
6.2-6.5	132-135	
6.8	113	
7.1	128	
7.35	127	3'', 6''
7.4	128	2'', 7''
7.8	125	1'', 8''
7.9	120-122	4'', 5''

Heterocorrelation NMR spectroscopy revealed carbon resonances has no cross peak at 21 ppm correlating to 1.7 and 1.0 ppm, which is indicative of the absence of an 8-deoxy compound.

Proton NMR revealed resonances at 1.25 ppm indicative of traces of glycerides and resonances at 6.8 to 7.15 ppm indicative of an unidentified aromatic metabolite.

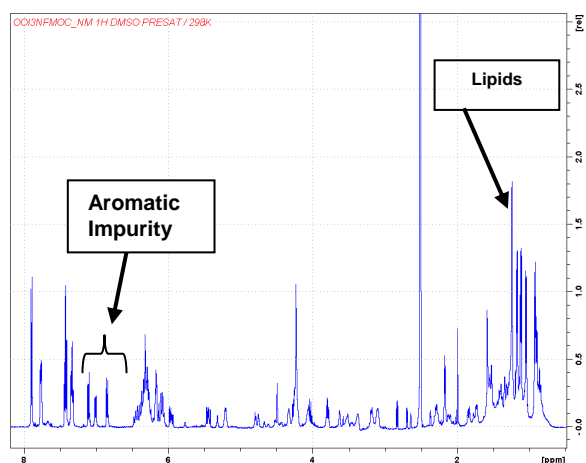


Figure 4.5 Proton NMR of **61** showing presence of lipids and aromatic impurity

HMBC experiment of **61** did not produce very good results presumably due to the quantity of the sample obtained and the low sensitivity of the HMBC.

4.4 Variation and optimisation of Fmoc protection method

4.4.1 Optimisation of the Fmoc reaction

4.4.1.1 Adding more Fmoc after 1 hour

Initial reaction procedure used involved the addition of more Fmoc-OSu after about an hour of reaction at RT. This was as carried out by Driver *et*

al., it was thought that this will enhance reaction completion by increasing the equivalents of Fmoc-OSu.⁵⁴

Yellow precipitate from a growth of "*ΔamphNM+perDIDI*" was waterwashed and partially purified with methanol. The resulting precipitate (39 mgH in 138 mgWt, ca 40% NM) was reacted with Fmoc-Osu (14 mg; 1.0 eq.) and pyridine (1.3 eq.) for an hour at RT after which more Fmoc-OSu (9 mg; 0.6 eq.) was added to the reaction mixture and left stirring at RT for 14 h. Yellow precipitate (23 mgH) was obtained after ether precipitation. Purification on two (MeOH-EtOAc followed by DCM) flash silica columns gave **61** (13 mgH in 19 mgWt).

4.4.1.2 Reaction without stepwise addition of Fmoc

The stepwise addition of the Fmoc-OSu was thought to be unnecessary because the duration of the reaction was increased, as described in Section 4.3.1.3, and this was expected to give the reaction plenty of time to reach completion. It was also observed that carrying out the reaction without step wise addition of Fmoc gave better yield (97%) than the yield obtained when step wise addition of Fmoc was used (83%). Subsequent reactions were therefore, carried out without stepwise addition of Fmoc-OSu.

4.4.2 Optimisation of the work up after reaction

4.4.2.1 Ether precipitation

Initial studies on the Fmoc protection of the derivatives of **17** involved obtaining a precipitate of **61** from the reaction mixture, after about 16 h of reaction, with ether to afford a yellow precipitate which was collected by centrifugation. This was as reported by Palacios *et al.*⁶³

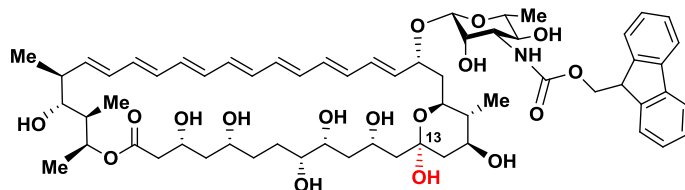
Precipitate from water washed sample of **17** was purified by repeated partial dissolution in methanol to give a yellow precipitate (146 mgH in 512 mgWt, ca 50% NM) which was reacted with Fmoc-OSu and pyridine for 16 h at RT. The supernatant from the reaction mixture was precipitated in cold ether (0 °C, 300 mL) to afford a supernatant (71 mgH) and precipitate (70 mgH). The precipitate obtained was purified on a flash silica column (DCM) to give **61** (68 mgH in 75 mgWt). Positive ion ESMS carried out after the second column showed 1138.8 (M+Na)⁺.

Precipitation in ether was carried out with cold diethyl ether (0 °C) in order slow down the precipitation of the desired product, thus, enhancing separation of **61** from other impurities. Ether was also added dropwise over about ten minutes.

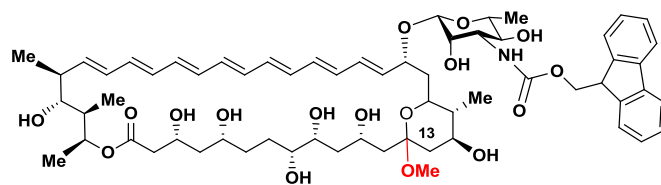
RP-HPLC showed supernatant from the ether precipitate contains mainly aglycone and hexoses while the precipitate from ether contains a mixture

of aglycone **22**, and some **61**. The presence of some aglycone in the precipitate shows that the amount of ether used was a large excess. It could also imply that the ether precipitation was not slow enough to enhance better separation.

NP-HPLC carried out on the precipitate from ether, showed the presence of two main products. This is as expected because Palacios *et al.*, reported the isolation of **61** (hydroxyl) and **62** (methyl ketal) from the precipitate obtained from ether after Fmoc reaction. Precipitating with ether is thought to create a very anhydrous condition for the formation of the acetal.



16-descarboxyl-*N*-fluorenylmethoxycarbonyl-16-methylamphotericin B (**61**)



16-descarboxyl-*N*-fluorenylmethoxycarbonyl-13-methoxy-16-methylamphotericin B (**62**)

Figure 4.6 Structures of *N*-Fmoc derivative of **17** (**61**) and 13-methoxy-*N*-Fmoc derivative of **17** (**62**)

This is also thought to be due to an equilibrium that exists between the two products when in acidic methanol. Si analytical HPLC carried out on the

products, immediately after precipitation with ether, showed the presence of **61** as the main product. However, when a sample of **61** was left at 4 °C overnight, **62** was observed.

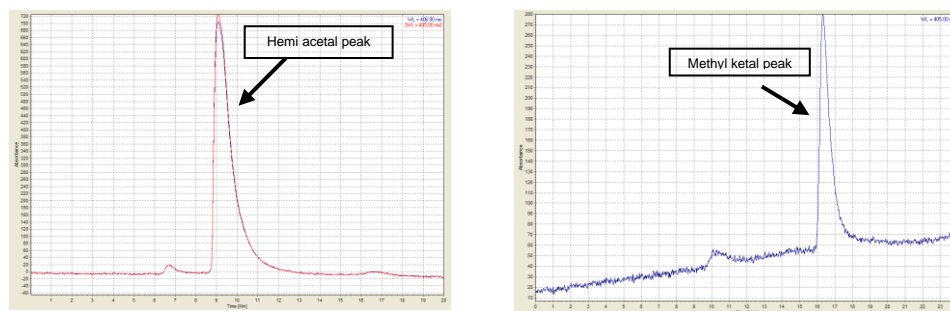


Figure 4.7 NP-HPLC showing the hemi acetal (left) and methyl ketal (right) isomers from the N-Fmoc derivative of **17**

Attempts to revert the ketal to the hemiacetal were not successful. One of such attempts involved adding water to an aliquot of a mixture of **61** and **62** and leaving it to stand overnight. Analysis by Si-HPLC showed no change in the ratio of **61:62**.

It was thought that reversion would be easier after deprotection and purification on a semi-preparative Si-HPLC using water and methanol (with 1% HCOOH). The results obtained are discussed later in this chapter.

Further purification of the N-Fmoc derivatives obtained was carried out by semi-preparative NP-HPLC. The two peaks were collected and analysed by ESMS, HPLC and NMR. Positive ion ESMS of **61** after HPLC prep

showed 1138.2 (M+Na)⁺. Positive ion ESMS of **62** after HPLC prep showed 1153.3 (M+Na)⁺

Attempts were made to optimise the method used and it was then proposed that the product, **61**, should not be precipitated with ether to prevent formation of the methyl ketal (**62**).

4.4.2.2 Reaction and purification without ether precipitation

The new modified method for the work up after the Fmoc reaction involved the separation of the suspension obtained after the reaction of Fmoc-OSu with **17** for about sixteen hours. The suspension was separated using a centrifuge. The supernatant obtained was then dried onto flash silica (3 g) *in vacuo* and further purified by flash column chromatography in MeOH-EtOAc.

This new method, as described in Sections 4.3.1.2 and 4.3.1.3, was optimised and it was observed that the product obtained was mainly **61** and it was stable without any reversion to **62**. This showed that precipitation without ether produced no methyl acetal. **61** obtained was further purified by semi preparative HPLC (Si) to afford characterisation by NMR.

In order to confirm the stability of **61** obtained using the new method, Si-HPLC was carried out after 6 days and after 1 year. No difference in number of peaks was observed. Also UV assay carried out showed no loss of heptaene activity. This implies that the product had not degraded, hence, it is robust enough to store at 4 °C for a long time.

4.4.3 Optimisation of purification procedure after reaction work up

4.4.3.1 Using chromatotron instead of second flash column

This experiment was to investigate the potential of using a chromatotron to replace the second flash column chromatography used previously.

The use of chromatotron has been successfully employed in the separation of various natural products.¹⁰³ Also, the ease of monitoring the process by UV-Vis, as well as the time and solvent saving separations, made investigating this technique very attractive.

Crude extracts obtained from the '*amphNM*' mutant (421 mgH, 600 mgT in 9248 mgWt) were reduced *in vacuo*, the resulting yellow precipitate water washed and then repeatedly partially dissolved in methanol to give a yellow precipitate (232 mgH, 33 mgT in 958 mgWt, *ca* 69% NM) which was reacted with Fmoc-OSu and pyridine to give **61** (202 mgH, 32 mgT).

The large amounts of impurities in the sample of **61** obtained, made it necessary to carry out a filtration column (MeOH-EtOAc) as before, prior to attempting further purification on the chromatotron. The product from the first column (152 mgH, 21 mgT in 435 mgWt) was loaded onto the chromatotron and two recycles gave **61** (148 mgH in 159 mgWt) which was eluted with 5% MeOH-DCM

The purification on the chromatotron was carried out in MeOH-DCM because the product from the first column was poorly soluble (in 2 mL MeOH-EtOAc) and also because DCM is the best solvent that can separate heptaene and tetraene. The high UV visibility of the Fmoc moiety on the amphotericin analogues also made monitoring the purification process straightforward. Monitoring of the separation was better carried out by TLC analysis of fractions collected from the chromatotron. Better purity could have been achieved by collecting the fractions from the chromatotron in much smaller volumes.

It was observed that **61** obtained from the chromatotron had better purity (93%) than that obtained from a second flash silica column (91%). This is thought to be due to the reduced level of lipids in **61** obtained from the chromatotron, as also observed by proton NMR.

A sample of **61** in MeOD from the chromatotron left in a NMR tube overnight at RT was observed to contain crystals. The crystals obtained were needle like and very tiny. Analysis by X-ray was unsuccessful

because the crystals did not diffract. However, proton NMR carried out gave interesting results.

The supernatant were carefully separated from the crystals. The crystals left in the NMR tube were dissolved in copious amounts of methanol, concentrated *in vacuo* and analysed. Unexpectedly, the proton NMR showed that this supernatant was predominantly of 'pure' N-Fmoc NM (**61**) free from lipids.

Proton NMR of the crystals showed the presence of lipids and **61**. This suggests that the lipids and **61** co-crystallised together.

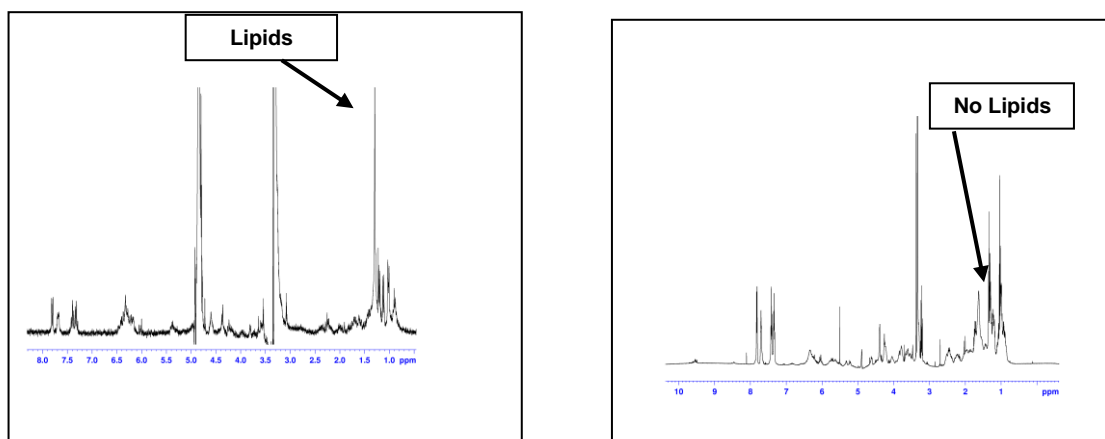


Figure 4.8 Proton NMR showing precipitate (left) and supernatant (right) from crystals of **61**

be predominantly tetraene (179 mgH, 309 mgT in 2128 mgWt). This was reduced *in vacuo* and reacted with Fmoc and pyridine for about 16 h to give a dark brown supernatant (113 mgH, 344 mgT). This was reduced *in vacuo* to give dark brown slurry which was wet loaded onto a flash silica column. Elution at 6% MeOH-EtOAc gave the desired product, **63** (39 mgH, 296 mgT in 601 mgWt). This product was loaded onto the chromatotron in 10%MeOH-DCM and elution at 6% MeOH-DCM gave **63** (10 mgH, 282 mgT in 304 mgWt).

The presence of a mixture (heptaene, tetraene and some lipids by proton NMR) in the final product from the chromatotron was quite disappointing. It was then thought that using a flash silica column to enhance purification should be attempted.

4.5.2 Purification using a second flash silica column

The tetraene used for this reaction was from the batch used in Section 4.3.1.3. As expected, the supernatant from the partial dissolution of the water washed precipitate was mainly tetraene, **54** (58 mgH, 250 mgT in 912 mgWt). This was reacted with Fmoc-OSu and pyridine for 16 h, as with the heptaene. After the reaction, the suspension observed was separated by centrifugation and the resulting supernatant (57 mgH, 248 mgT) was concentrated *in vacuo* and extracted with 10% MeOH-EtOAc (x2) to give a

light yellow solution (55 mgH, 247 mgT). The solution was reduced *in vacuo* (to 2 mL) and loaded onto a flash silica column.

The column was flushed with EtOAc (4x column volume) in an attempt to eliminate the lipids. The desired product eluted with 7%MeOH-EtOAc (25 mgH, 242 mgT in 664 mgWt). A second flash silica column (EtOAc) was used to further enhance purity of the desired product. Elution with 5% MeOH-EtOAc gave **62** as a mixture (9mgH, 240 mgT in 258 mgWt)

Further purification by semi preparative Si-HPLC afforded 50 mgT in 52 mgWt. This was used for analysis and characterisation of **63**.

Proton NMR showed the presence of aromatic peaks due to Fmoc moiety between 7.33-7.82 ppm and double bond chromophore due to the tetraene at 6.1-6.4 ppm.

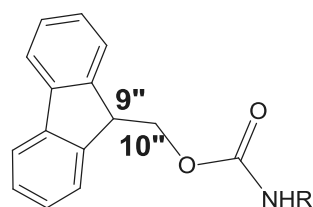


Figure 4.10 Fmoc region of **63** showing C-9'' and C-10''

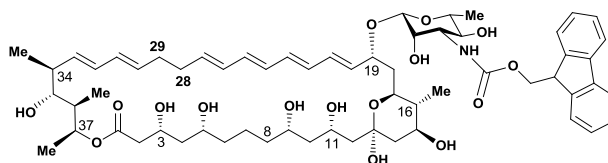
Methylene resonance on the Fmoc (10'') was at 4.38/4.40 ppm with the neighbouring methane proton (9'') at 4.26 ppm. Aromatic impurity was present between 6.5-7.0 ppm.

Proton-proton correlation showed coupling between 1.25 ppm (H-16) and 1.01 ppm (H-41) as expected. 1.24 (H-16) was coupled to 3.57 (H-15), 1.24 (H-16) was coupled to 3.73 (H-17), 3.73 (H-17) coupled to 1.83 (H-18b), and 3.29 (H-35) coupled to 2.36 ppm (H-34).

NMR analysis showed that there are a lot of cross peaks missing in the COSY due to small or large coupling constants.

Carbon NMR was carried out in DMSO due to the low solubility of **63** in methanol. Analysis of the carbon NMR showed a lactone resonance at 170.7 ppm (C-1) as expected and a carbonyl resonance at 158.82 ppm (C-11"). The 12 polyenic carbons at 131.73-135.9 ppm were observed as 13 peaks instead of 12. The methine C-1' (100.19 ppm) and C-13 (98.75 ppm) resonances were observed downfield due to neighbouring oxygen atoms as expected. The carbons on the fluorene were also observed to be diastereotopic.

DEPT experiment showed methine carbon resonances from the Fmoc aromatic protons were observed as 4 peaks with each of the peaks showing two carbons. Three methine carbon resonances between 41.98-44.72 (C-16, 34, 36) were observed as expected and eight methylene resonances were observed between 38-48.5 ppm (C- 2, 4, 6, 8, 10, 12, 14, 18) with C-18 shifted further downfield, supposedly, due to the presence of the Fmoc group.



8-Deoxy-16-Descarboxyl-*N*-fluorenylmethylloxycarbonyl-16-methylamphotericin A (**63**)

Table 4.2 Heterocorrelation NMR (in DMSO- d_6) observed for **63**

δ_H	δ_C	Carbon atom number	δ_H	δ_C	Carbon atom number
0.98	12.82	39	4.61	100.10	1'
1.07	17.48	40	5.22	72.82	37
1.21	17.37	38	5.57	132.53	30
1.24	44.72	16	5.72	135.52	27
1.30	18.24	6'	5.79	134.92	20
1.40	22.67	7b	6.14	132.66	26
1.65	23.76	7a	7.33	128.19	3'', 6''
3.59	58.32	4'	7.40	128.81	2'', 7''
4.22	68.62	3	7.70	126.26	4'', 5''
4.37	68.81	11	7.82	120.93	1'', 8''
4.46	79.33	19			

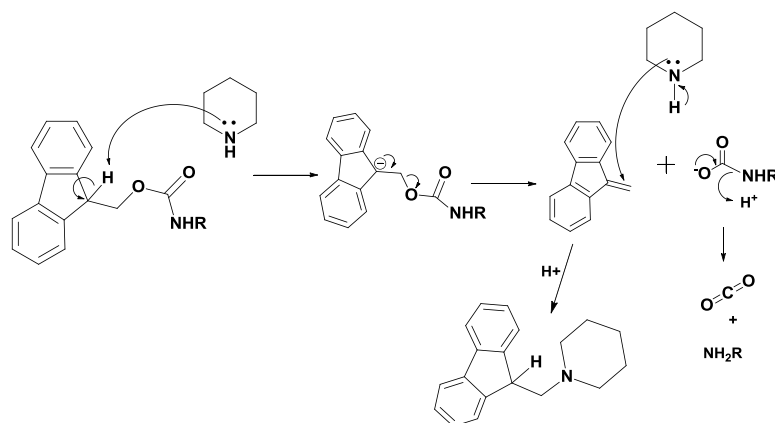
Heterocorrelation NMR spectroscopy revealed a carbon resonance at 22.67 ppm correlated with proton at 1.65 and 1.40 ppm, characteristic of an 8-deoxy analogue.

Analysis by positive ion ESMS gave peaks at 1101.6 (M)⁺, 1119.6 (M+H₂O)⁺ and 1124.6 (M+Na)⁺, or after loss of water 1084.6, corresponding to the expected mass of **63** (1101.6 Da).

Analysis of the elemental composition and accurate mass showed calculated mass for C₆₂H₈₅NO₁₇ to be 1116.5896 while the observed mass was 1116.6028 indicating a difference of 11 ppm.

4.6 Deprotection of 16-descarboxyl-*N*-fluorenylmethyloxycarbonyl-16-methyl amphotericin B (**61**)

The Fmoc group is removed typically with piperidine. The piperidine functions both as a base to fragment the Fmoc group and as a scavenger to trap the liberated dibenzofulvene (DBF) to form a fulvene-piperidine adduct via Michael type addition, thereby out-competing reaction with the amine.¹⁰⁴



Scheme 4.3 Reaction mechanism for the deprotection of the N-Fmoc protected compounds

Use of piperidine/DMF is better suited to Fmoc deprotection on solid phase than those in solution due to the low volatility of those solvents, the solvent-dependent reversible scavenging of DBF by piperidine and DBF polymerisation at high concentration.¹⁰⁴

4.6.1 Deprotection of 16-descarboxyl-*N*-fluorenylmethoxycarbonyl-16-methyl amphotericin B (**61**) containing some tetraenes

Initial studies involved deprotection of the mixture of heptaene and tetraene. It was thought that the tetraene would be isolated in the supernatant from ether after the deprotection reaction, leaving only the heptaene in the precipitate. In order to test this hypothesis, **61** (4 mgH, 2 mgT) from Section 4.3.1.1, was dissolved in DMSO (500 μ L) and reacted with piperidine (2 eq.) at RT for an hour. The reaction mixture was then

poured onto ether (18 mL) to afford a yellow precipitate (2 mgH, 1 mgT) and clear supernatant (1 mgH, 1 mgT). Deprotection was confirmed by HPLC, ESMS and TLC. However, there was no separation of the heptaene and tetraene as expected. It is thought that better separation could have been obtained if less ether had been used.

This showed that there was a need to further optimise the method for deprotection, but it was later decided that it would be easier to obtain the separation of the heptaene and tetraene before deprotection was carried out.

4.6.2 Deprotection of mixture of hemi-acetal (**61**) and methyl ketal (**62**)

N-Fmoc NM (**61**) obtained from Section 4.4.2.1 produced a mixture of isomers. One of the attempts to revert the acetal to the hemi acetal was to carry out deprotection on the mixture and hydroxylate the acetal during the work up of the reaction mixture. It was also thought that not precipitating the product with ether after the deprotection reaction would enhance reversion of **62** to **61**.

In order to test this hypothesis, a mixture of **61** and **62** (13 mgH) from Section 4.4.2.1 was dissolved in methanol (1 mL) and reacted with piperidine at RT for an hour. The reaction was stopped by adding some

water (2 mL). The resulting solution had a pH of 8. The pH was adjusted to 6 with 5% HCOOH/H₂O (1 mL). XAD16 amberlite was added to the resulting solution and the methanol removed *in vacuo*. The XAD16 in aqueous medium was left to stand for an hour and the desired product (10 mgH) was extracted (x2) with methanol. RP-HPLC of the methanolic extract showed deprotection but no reversion was observed. Proton NMR showed the presence of piperidinium peaks. These results were not expected because the presence of the product in aqueous medium was expected to hydroxylate the acetal (**62**). The result obtained is thought to be due to the stability of the acetal **62**.

In an attempt to optimise the deprotection method, another sample of **61** and **62** (20 mgH), from Section 4.4.2.1, was dissolved in methanol (1 mL) and reacted with piperidine (2 eq.) at RT for an hour. The work up after the reaction is as described in the preceding paragraph. However, the methanolic extract (18 mgH) from the XAD16 was concentrated *in vacuo* and the piperidinium extracted with DCM. The resulting precipitate (17 mgH in 19 mgWt) was dried *in vacuo* and analysed. RP-HPLC showed that deprotection was successful; however, reversion of **62** to **61** was not observed. Proton NMR also showed much reduced piperidinium peaks.

The product obtained was purified further by semi preparative HPLC to afford isolation of both isomers and allow characterisation.

4.6.3 Deprotection of 16-descarboxyl-*N*-fluorenylmethyloxycarbonyl-16-methyl amphotericin B (**61**) without tetraenes

The reaction was carried out as reported by Zumbuehl *et al.*,¹⁰⁵ **61** (16 mgH in 18 mgWt), from Section 4.3.1.3, was dissolved in DMSO (1 mL) and reacted with piperidine (2 eq.) for an hour at RT. The reaction mixture was poured very slowly onto ether (35 mL) to give a yellow precipitate (15 mgH). RP-HPLC showed 100% deprotection of product. ESMS also confirms the presence of **17** after deprotection. ESMS (+ve) showed 713 (aglycone-H₂O) and 917 (M+Na)⁺. Proton NMR obtained showed the absence of Fmoc related aromatic peaks but very large piperidinium peaks at 2.0 ppm and 1.4 ppm. These peaks could also be due to piperidine-fulvene adducts.

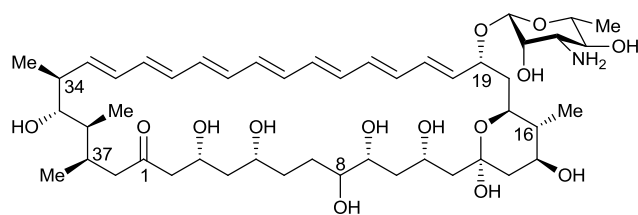
The product was recovered, concentrated *in vacuo* and dried further under high vacuum line overnight. ¹H NMR obtained showed a quintet at 3.3 ppm, and very large DMSO peak (2.6 ppm). The product was recovered again and the DMSO was extracted with water (20 mL, stepwise). The resulting precipitate was dissolved in methanol, concentrated *in vacuo* and dried under the high vacuum line to give **17** (12 mgH in 13 mgWt).

Further analysis of the precipitate by ¹H NMR showed the presence of aromatics as the main impurities left in the sample.

In an attempt to further optimise the deprotection method, the work up of the reaction was changed. Instead of pouring the reaction mixture onto ether, it was thought that better isolation of **17** would be achieved by adding ether slowly to the reaction mixture. This is a deviation from the procedure used by Zumbuehl *et al.*,¹⁰⁵ However, the sample used for the deprotection by Zumbuehl and co-workers was in larger quantities (1.1 g) and much higher purity (95% pure). The presence of more impurities in **61** to be deprotected makes further optimisation of the procedure expedient.

N-Fmoc NM, **61** (10 mgH in 11 mgWt), from Section 4.3.1.3, was dissolved in DMSO and reacted with piperidine for an hour at RT. Ether (10 mL) was added slowly to the reaction mixture. The yellow oily layer was separated from the clear supernatant. More ether (10 mL) was added to the yellow oil and the supernatant separated. The yellow layer was observed to be less oily and stuck to the flask. Methanol (3 mL) was added and the resulting solution was concentrated *in vacuo* and dried under high vacuum line to give a fine yellow precipitate (9 mgH in 9.5 mgWt). Proton NMR showed the absence of Fmoc moiety, lipids and much reduced aromatics.

The product obtained was purified further by semi preparative HPLC to afford isolation and characterisation.



16-descarboxyl-16-methyl-amphotericin B (17)

Table 4.3 Heterocorrelation NMR (in methanol- d_6) observed for **17** after deprotection

δ_H	δ_C	Carbon atom number
1.0	12	39, 41
1.15	18	40
1.2	44	38
1.3	18	6'
1.4	32, 36	18
1.5	36	36
1.85	42	36
2.2	42	29
2.3	42	
2.4	44	34
3.1	58	8
3.2	75, 80	35
3.3	74	5'

δ_H	δ_C	Carbon atom number
3.35	50	4'
3.4	70	9
3.55	70	15
3.6	76	17
3.7	72, 74	37
4.0	70	15
4.2	70	
4.4	70	
4.45	80	19 or 35
4.65	100	1'
4.85	98	13
5.4	137	33, 37
6.1	132, 137	20
6.15-6.6	130-136	21-32

Analysis by heterocorrelation NMR showed no carbon resonance was observed at 21 ppm and therefore no crosspeak at 21 ppm to 1.7 ppm and 1.00 ppm. This suggests that **17** obtained is hydroxylated at C-8.

Positive ion ESMS showed peaks at 713.4 (M-sugar-water)⁺, 876.5 (M-water)⁺, and 916.5 (M+Na)⁺ which corresponds to the expected mass of **17** (893.5 Da). Investigation into the accurate mass showed the calculated mass for C₄₇H₇₆NO₁₅ as 894.5212 whilst the observed mass was 894.5193 showing a difference of about 1.9 ppm.

4.7 Deprotection of 8-deoxy-16-descarboxyl-N-fluorenylmethyloxycarbonyl-16-methyl amphotericin A (**63**)

Deprotection of **63** was carried out on a mixture of heptaene and tetraene. This was due to the difficulty encountered in the various attempts to separate N-Fmoc NM heptaene (**61**) and N-Fmoc NM tetraene (**63**). It was thought that isolation could be carried out on a semi-preparative HPLC after the reaction.

The sample of **63** used was from the product obtained from the chromatotron as described in Section 4.6. N-Fmoc NM tetraene, **63** (9 mgH, 50 mgT in 64 mgWt) was dissolved in DMSO (1 mL) and reacted with piperidine (2 eq.) for an hour at RT. Ether (10 mL, x2) was added very slowly to the reaction mix to afford a light yellow precipitate (8 mgH, 44

mgT). The yellow precipitate was dissolved in MeOH (10 mL), concentrated *in vacuo* and the DMSO extracted with water (10 mL, x2). The resulting precipitate (7 mgH, 25 mgT) was dissolved in MeOH and concentrated *in vacuo*. Proton NMR confirmed deprotection.

The product obtained was purified further by semi preparative RP-HPLC to afford isolation and characterisation of the desired tetraene (**54**).

ESMS (+ve) showed 699.45 (M-sugar-H₂O)⁺, 862.54 (M-H₂O)⁺, 880.55 (M)⁺. Elemental composition/accurate mass analysis showed the calculated mass as 862.5317 while the observed mass was 862.5367 for C₄₇H₇₆NO₁₃.

Proton NMR obtained was similar to that reported in Section 4.5.2 without the aromatic peaks of the Fmoc moiety.

4.8 Conclusion

Purification of the crude extracts of amphotericin B analogues from “*ΔamphNM+perDIDI*” and ‘*amphNM*’ disruptant using an Fmoc intermediate was carried out. The optimum protocol for the Fmoc derivatisation of **17** and its deprotection were obtained. This protocol was also used for the purification of **61**. The results obtained showed that this novel purification method is convenient. However, optimisation of the method will be required from mutant to mutant. The amount of ‘purified’

analogues isolated using this Fmoc method can be further increased by scaling up the method described.

Chapter Five: Isolation, purification and characterisation of 16-descarboxyl-16-methyl-19-(O)-perosaminyl amphoteronolide B

5.1 Introduction

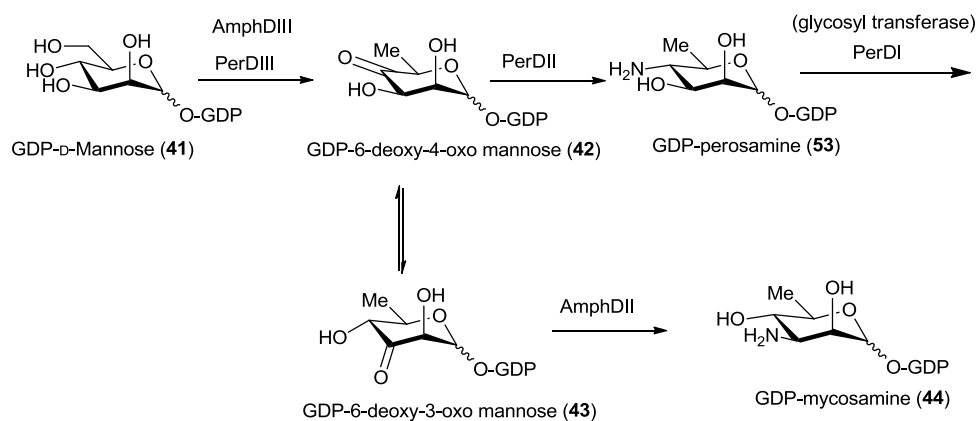
5.1.1 Glycosylation

Glycosylation is one of the most common and important reactions in biological systems.⁷⁸ A significant number of glycosylated small molecule natural products are clinically useful for the treatment of bacterial and fungal infections, cancer, and other human diseases.¹⁰⁶ Changes in the structure of the sugar moieties of glycosylated molecules can have profound effects on their activities, selectivity and pharmacokinetic properties.¹⁰⁷ Therefore, altering the glycosylation pattern of the parent structures has the potential to significantly modify or improve the properties of the parent system.⁷⁸ The sugar can be altered by *in vitro* biotransformation, or *in vivo* by mutagenesis.¹⁰⁸ Recently, the use of hybrid GTs has been employed.⁹³ Glycosylation engineering is a developing technology that is being applied to other natural products.¹⁰⁹ Altering sugar residues has enhanced the properties of doxorubicin, glycopeptide antibiotics and several other bioactive compounds.¹⁰⁶

5.1.2 Glycosylation in polyenes

Most polyene macrolides, such as amphotericin B (**1**), nystatin (**3**), candicidin (**50**) and pimaricin (**4**), are glycosylated with mycosamine (3, 6-dideoxy-3-amino-D-mannose). Previous studies have indicated that polyene glycosyltransferases show limited tolerance toward alternative substrates.¹¹⁰ Zhang *et al.*, have shown that AmphDI and NysDI have narrow sugar substrate specificity recognising only GDP-D-mannose (**41**) and GDP-L-gulose.¹¹¹ However, a regioisomer of mycosamine, GDP-D-perosamine (4, 6-dideoxy-4-amino-D-mannose), (**53**), which is used in the biosynthesis of perimycin in *S. aminophilus*, was not investigated in this study.

Perimycin is an aromatic heptaene that is unusual in that it is glycosylated with perosamine.⁹⁷ The biosynthesis of GDP-mycosamine (**44**) and GDP-perosamine (**53**) are closely related (Scheme 5.1). The first step (by AmphDIII or PerDIII) is common, the 4,6-dehydration of GDP-mannose (**41**) to GDP-4,6-dideoxy-4-oxo-mannose (**42**) (which may be in equilibrium via the enediol with the isomeric GDP-3,6-dideoxy-3-oxo-mannose (**43**)). No gene or enzyme has been located that promotes or mediates this equilibrium process. Pyridoxal phosphate mediated transamination (by PerDII) of **42** gives **53**. Alternatively, AmphDII selects the isomeric **43** and transaminates it to **44**. There is also a high degree of sequence identity between AmphDIII/PerDIII (76-81%), and AmphDII/PerDII (73-77%).⁹³



Scheme 5.1 Biosynthetic pathways to GDP-D-perosamine and GDP-D-mycosamine in *S. aminophilus* and *S. nodosus*

5.1.3 Glycosylation engineering in amphotericin

Caffrey *et al.*, has disrupted several genes responsible for the post-PKS modifications of the amphotericin B aglycone (**22**) to probe gene function, substrate flexibility of these enzymes, and biological activity of the affected functionalities.^{87,93} For example, the previous chapter describes disruption of the *amphNM* genes resulting in 16-descarboxyl-16-methyl analogues that show therapeutic potential. Another such disruptant involved the inactivation of the *amphDIII* gene which resulted in the production of 8-deoxy-amphoterolide A (**46**), as a major product in good yield.⁸⁷ The success of the disruption of the *amphDIII* gene was the first indication that glycosylation engineering experiments aimed at altering the sugar residue of **1**, might be possible. The analogue of *amphDIII*, *perDIII* (from perimycin biosynthesis in *S. aminophilus*) was cloned into pIAGO (an expression vector) and transformed into *S. nodosus* Δ *amphDIII*. This resulted in the production of a mixture of aglycone (**22**), **1** and tetraene (**2**).⁸⁷ This showed

that PerDIII can efficiently substitute for AmphDIII in the mycosamine biosynthetic pathway.

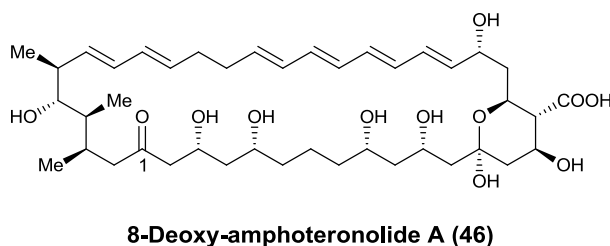


Figure 5.1 Structure of 8-deoxy-amphoteronolide A (**46**)

The insertion of *perDII* into the amphotericin gene cluster in *S. nodosus* might be expected to lead to the PerDII mediated transamination of **42** (generated by AmphDIII) into GDP-perosamine (**53**) (Scheme 5.1). The additional insertion of *perDI* might lead to the PerDI mediated glycosylation of the amphoteronolide aglycone (**22**) with perosamine, depending on the ability of PerDI to recognise **22**.

The *perDIDII* genes were inserted into the *S. nodosus* Δ *amphNM* genome close to the *amphDIDII* genes.⁸⁷ The " Δ *amphNM+perDIDII*" mutant (still containing the *amphDIDII* genes) instead produced aglycone (**22**) as the major product along with *amphNM* (**17**), as discussed in Chapter Two. This showed that PerDI does not recognise aglycone-Me, even though aglycone (**22**) resembles the glycosylation region of the perimycin aglycone (**65**) intermediate in perimycin production by *S. aminophilus* that PerDI normally glycosylates.

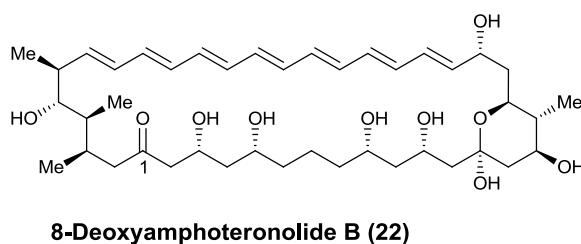
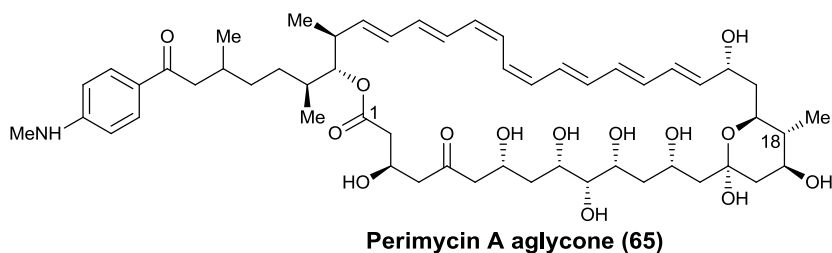
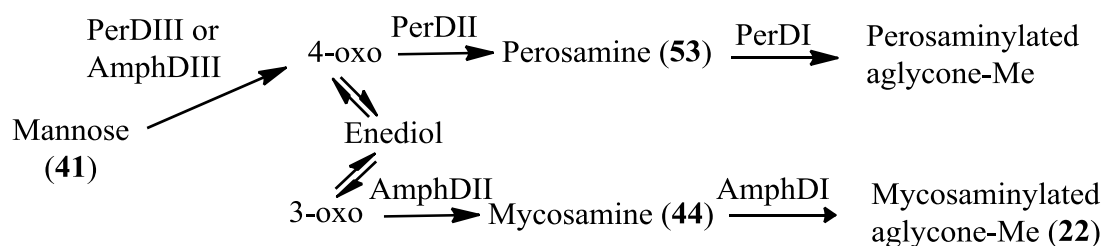


Figure 5.2 Structures of perimycin A aglycone (**65**) and 8-deoxyamphoteronolide B (**22**) showing similar glycosylation sites

From these observations, either PerDII cannot compete with AmphDII for the 3-oxo (**43**) and 4-oxo (**42**) equilibrium products from AmphDIII or PerDI cannot recognise **22** leading to an accumulation of D-perosamine (**53**). This latter explanation would account for the enhanced production of aglycone (**22**) due to the resulting shortage of **44**.

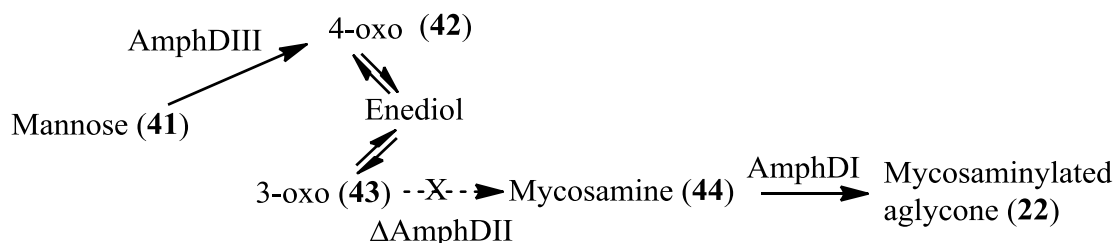


Scheme 5.2 Transformations possible in *S. nodosus* " $\Delta amphNM+PerDIDI$ "

Further attempts to carry out glycosylation engineering to form an amphotericin analogue involved the cloning of *perDII* (from *S.*

aminophilus) into pLAGO and introduced into *S. nodosus* $\Delta amphDII$ to form the $\Delta NM+PerDII$ disruptant.⁹³

S. nodosus $\Delta amphDII$ produces a mixture of amphoteronolides and deoxyhexosylated amphoteronolides. The extracts had no detectable antifungal activity, indicating the absence of any polyene glycosylated with an aminosugar, and also the absence of any adventitious enzyme substituting for AmphDII. *S. nodosus* $\Delta amphNMDII$ produced the corresponding 16-descarboxyl-16-methyl analogues, again without detectable antifungal activity. Reintroduction of *amphDII* on the pLAGO plasmid restored antifungal activity in both *S. nodosus* $\Delta amphDII$ and $\Delta amphNMDII$.⁹³ Hence, AmphDI does not attach GDP-perosamine onto the amphoteronolides (either as 16-methyl or 16-carboxyl forms).



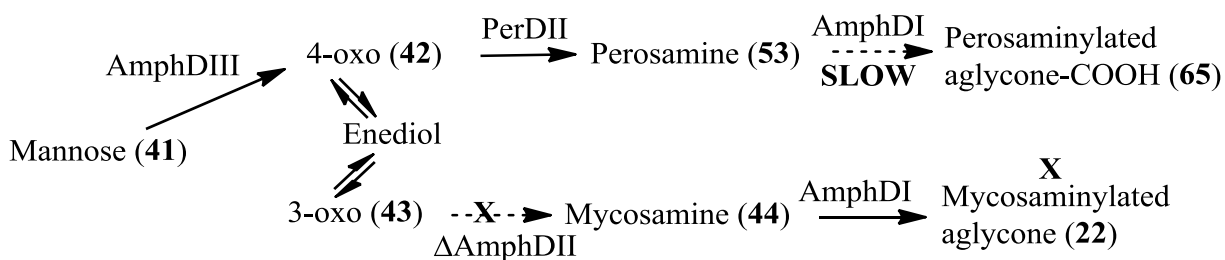
Scheme 5.3 Strategy for AmphDI attaching mycosamine onto the aglycone instead of perosamine

Replacement of *amphDII* in *S. nodosus* $\Delta amphNM$ with chromosomal *perDII* resulted in the production of low levels of aglycones, but no antifungal activity,⁹³ indicating that PerDI does not recognise

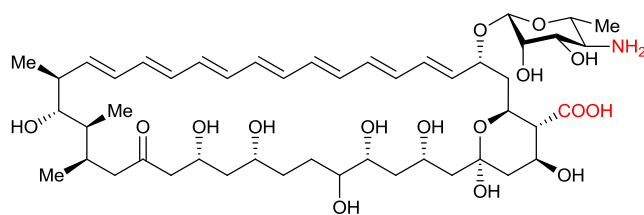
amphoteronolides lacking exocyclic carbonyl groups, despite its natural substrate also lacking a similar exocyclic carboxyl group.

5.1.4 19-(O)-Perosaminyl amphoteronolide B (66)

Addition of plasmid (pIAGO) borne *perDII* into *S. nodosus* Δ *amphDII* gave extracts with low levels of antifungal activity. HPLC showed low levels (2%) of a new polyene, whose mass was identical to that for **1**, suggesting production of low levels of 19-(O)-perosaminyl-amphoteronolide B and that AmphDI was able to inefficiently recognise and attach GDP-perosamine to 16-carboxyl-amphoteronolides. However, the extracts contained much higher levels of deoxyhexosylated analogues by HPLC and LCMS, indicating that either AmphDI prefers GDP-deoxyhexoses over GDP-perosamine, or at these low levels of production, adventitious glycosyltransferases are adding deoxyhexoses to the aglycone (not necessarily at C-19).⁹³



Scheme 5.4 Successful glycosylation of aglycone with perosamine



19-(O)-perosaminyl-amphoteronolide B (66)

Figure 5.3 Structure of 19-(O)-perosaminyl-amphoteronolide B (66)

In summary, Caffrey and co-workers have been able to establish that PerDI will not transfer perosamine onto amphotericin B aglycone (**22**), but AmphDI will, albeit inefficiently (and in the absence of GDP-mycosamine (**44**)).

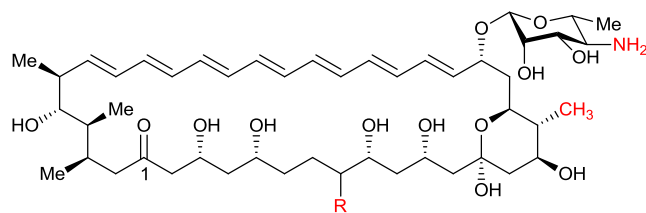
5.1.5 Hybrid glycosyltransferases

Sugar and aglycone substrate specificities have been altered by mutagenesis^{112,108} or by construction of hybrid GT enzymes^{113,93}. Examples include erythromycin,¹¹⁴ mithramycin,⁷⁸ tylosin,¹¹⁵ aminocoumarin¹¹⁶ and urdamycin A^{108,117}.

Glycosyltransferases (GT) are responsible for glycoside bond formation in natural products using sugar donors containing a substituted phosphate.¹⁰⁷ The acceptor substrate used is most commonly other sugars. In his work, Caffrey and co-workers used glycosyltransferases which typically have N-terminal (acceptor) and C-terminal (NDP-sugar donor substrate) domains.^{87,93}

Caffrey has observed that PerDI does not recognise the amphotericin aglycone (**22**) at all, and AmphDI only extremely inefficiently recognises perosamine, to produce 19-(*O*)-perosaminyl amphoteronolide B (**66**).⁹³ In order to obtain **66** in good yield, attempts were made to design a GT that will efficiently modify the amphotericin analogue with perosamine. One of such attempts involved the construction of a hybrid GT (linked to *perDII*). The DNA coding for the 8-deoxyamphoteronolide binding N-terminal domain of AmphDI was fused to the DNA coding for the perosamine C-terminal domain of the PerDI and PerDII (inserted into the pIAGO plasmid 'Hap2'). The desired product, **66**, was produced at about 25% of the total polyene along with aglycone and hexosylated material by HPLC. Murphy *et al.*, isolated and characterised several milligrams of **66**, which displayed comparable antifungal activity to **1**, with reduced toxicity.⁹³ The repositioning of the amino group to C-4' may enhance water solubility, along with reducing self-oligomerisation and binding to free lipid, whilst not affecting any binding to ergosterol and consequent pore formation.

The plasmid (pIAGO) based 'Hap2' (containing DNA for the hybrid GT along with *perDII*) was then introduced into *S. nodosus* Δ *amphNMDII*. Preliminary analysis of the crude extracts by HPLC showed low levels of a new heptaene product. Examination by LC-MS was consistent with the formation of 16-descarboxyl-16-methyl-19-(*O*)-perosaminyl amphoteronolide B (**67**). This would indicate that the hybrid glycosyltransferase is able to bind to GDP-perosamine and attach it onto the 16-descarboxyl-16-methyl aglycone (**22**).



R= OH 16-Descarboxyl-16-methyl-19-(O)-perosaminyl-amphoteronolide B (67)

R= H 8-Deoxy-16-descarboxyl-16-methyl-19-(O)-perosaminyl-amphoteronolide B (68)

Figure 5.4 Structures of 16-descarboxyl-16-methyl-19-(O)-perosaminyl-amphoteronolide B (**67**) and 8-deoxy-16-descarboxyl-16-methyl-19-(O)-perosaminyl-amphoteronolide B (**68**)

There is no C-8 hydroxy stereoisomer indicated in the above diagram. It can be assumed that this is the same as for **1**.

The aim of the work reported in this chapter is to develop an efficient protocol to extract, isolate, purify and characterise the new minor polyene product produced by this *pLAGO-hap2 amphNMDII* mutant. During this work, N-Fmoc derivatisation was investigated to improve the purification of **67** from the extracts.

5.2 Extraction and purification of 16-descarboxyl-16-methyl-19-(O)-perosaminyl-amphoteronolide B (**67**)

5.2.1 Growth of cultures

GYE media with thiostrepton (20 mg L⁻¹, freshly dissolved in DMSO) was inoculated with a *pHap2* 'deep'. After four days, aliquots (5-10 mL) were transferred into production (FD) media (24 x 250 mL; FD with thiostrepton

20 mg L⁻¹). The mycelia and beads (XAD16) were harvested after 7-10 days.

5.2.1.1 Yield variation based on culture used

It was observed that the yield of **67** varied based on the preculture batch used for inoculating the GYE media. The use of preculture made from deeps ('pc1'), as described in Chapter 3, was observed to produce less **67** (2 mg L⁻¹) when compared with extracts from growth from a second generation preculture ('pc2') (3 mg L⁻¹).

Analysis of the crude extracts by HPLC showed that extracts from 'pc1' also produces less **67** (<10% of the total heptaene) than that obtained from extracts from 'pc2' (ca 20% of the total heptaene). Analysis by HPLC also showed the significant presence of hexosylated polyenes in 'pc1' and not in 'pc2'.

5.2.1.2 Duration of incubation

Experiments were carried out to investigate if a variation in the duration of incubation of the cultures in the FD media will have an effect on the yield of **67**. Unlike the extracts from the *amphNM* mutant, no significant effect on the yield was observed when the duration of incubation was changed.

Mycelia and resin were collected by centrifugation, from growths incubated from the same deep and under identical conditions, apart from the time of incubation.

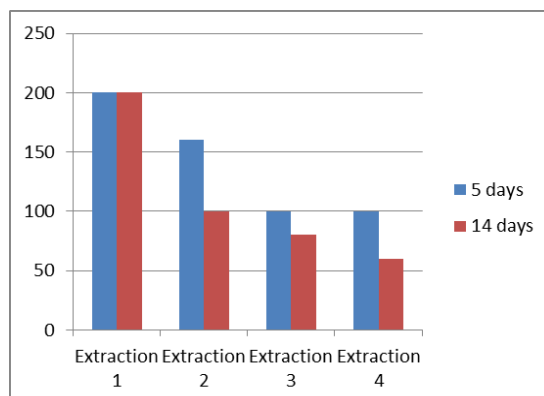


Figure 5.5 The effect of a change in the duration of incubation on the yield of **67**

The results obtained suggest that **67** can be grown in FD for 5 days to obtain the optimum yield of the desired analogue. This saves time and cost. The results obtained for the cultures incubated for 14 days also show no significant decline in the yield of the **67**. This suggests that **67** produced is stable in the culture (with XAD16), even when no more is being produced.

5.2.2 Harvest of mycelia

Two methods were used to separate mycelia and resin from the broth. Centrifuge followed by soaking of sediment in an Erlenmeyer flask; and 'muslin cloth', filtration by gravity to collect 'sediment', followed by soaking muslin cloth in a bowl.

5.2.2.1 Centrifuge

After 7-10 days, the mycelia and beads (XAD16) were harvested by centrifugation. The sedimented residue was finely dispersed in methanol (5 L) and left to soak overnight in a large Erlenmeyer flask. The supernatant (methanolic extract) was decanted and the sedimented mycelia and beads were re-extracted (4 x 2 L) with methanol.

5.2.2.2 Muslin cloth

After growth, the culture was decanted into a muslin cloth on a colander and left to drain into a bucket. The supernatant from the culture was collected in a bucket. It was observed that allowing the culture to drain overnight helped remove more aqueous material. However, the mycelial residue left on the cloth was still quite wet. This was then sedimented by centrifugation and placed back into the cloth. The cloth was tied loosely at the ends and whilst suspended, soaked in methanol (1 L). The methanolic extract was decanted after about 3 h and the mycelia and beads were re-extracted (2x) with fresh methanol. It was observed that only three extractions were required to deplete the sedimented mycelia of **67**.

Table 5.1 The total heptaene obtained from the methanolic extracts of **67** using centrifuge and muslin method

	Centrifuge (mg)	Muslin cloth (mg)
Extraction 1	120	55
Extraction 2	110	50
Extraction 3	90	50
Extraction 4	70	40
Extraction 5	45	N/A

The muslin method was observed to be a quicker method of recovering the sedimented mycelia from the production culture. The fewer extractions required from the muslin cloth method also make it a less expensive and more convenient method.

HPLC analysis of the extracts obtained from each method show that more **67** was recovered by muslin method relative to the Erlenmeyer method (20% more). This is thought to be due to the volume of methanol used for extraction. Considering that **67** is much more soluble than **22**, when less methanol is used for extraction more **67** will dissolve in preference to **22**. This was as expected. The relative amount of **67:22** in the combined methanolic extracts is as shown below:

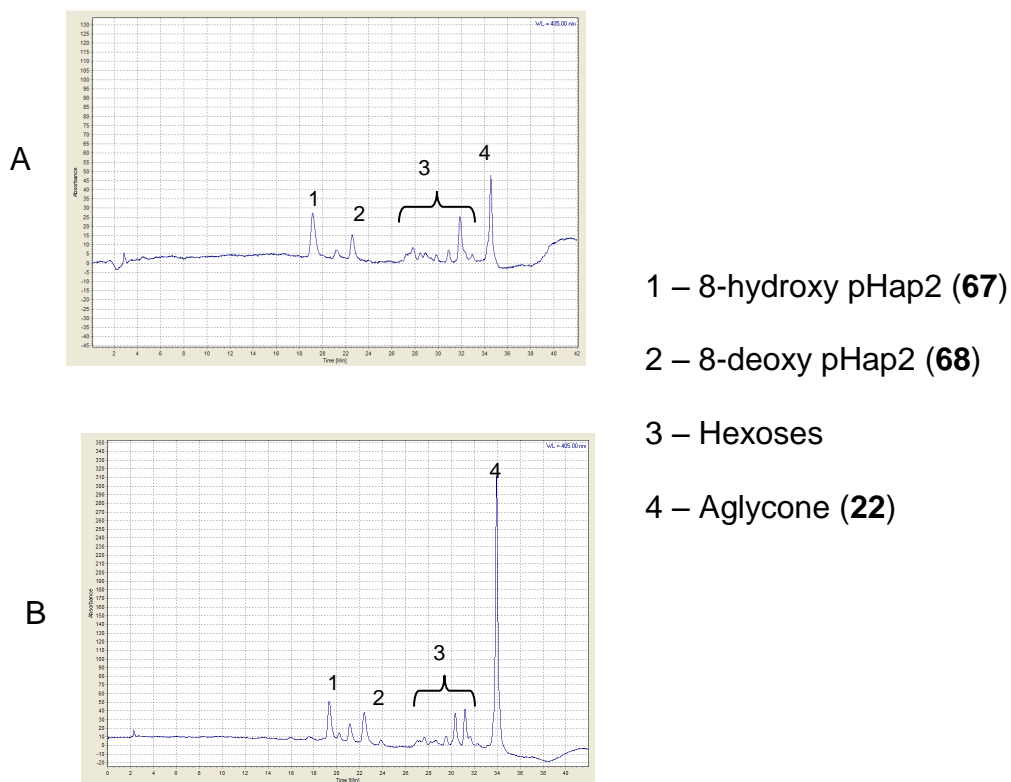


Figure 5.6 RP-HPLC showing combined methanolic extracts of **67** from muslin cloth (A) and Erlenmeyer method (B)

5.2.3 Variation of amounts in extracts

Unlike extracts from the *amphNM* mutant, the yield of **67** from the extracts was consistent from growth to growth.

Even though the actual amounts of total heptaene in cultures grown under the same conditions varied, the amount of **67** in the extracts, as observed by HPLC, was fairly consistent (15% of total heptaene). This was not as

expected because the *amphNM* produced varied amounts of **17** in extracts.

HPLC of each extract showed that the fourth extraction from the Erlenmeyer flask method contained mainly aglycone (>95%) and the third extract of muslin contained mainly aglycone (>90%). This is reminiscent of the later extractions (fifth) from the *amphNM* mutant, and confirms the greater solubility of the glycosylated material relative to the aglycone.

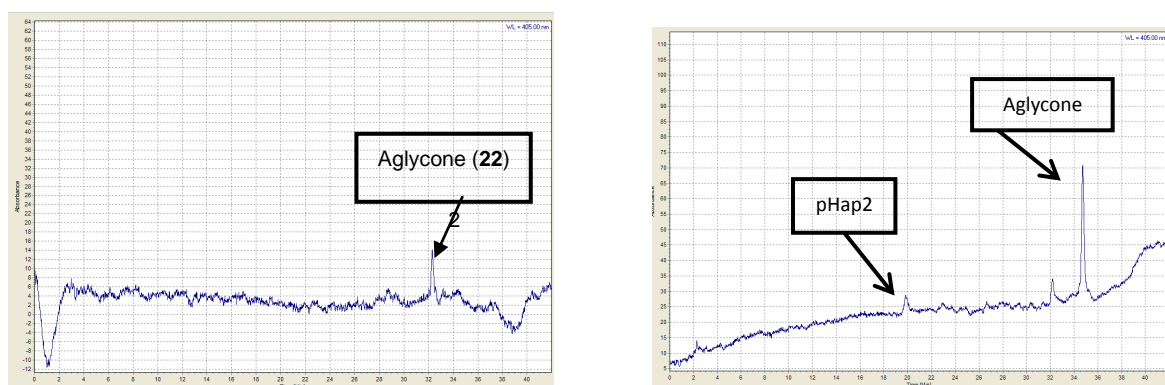
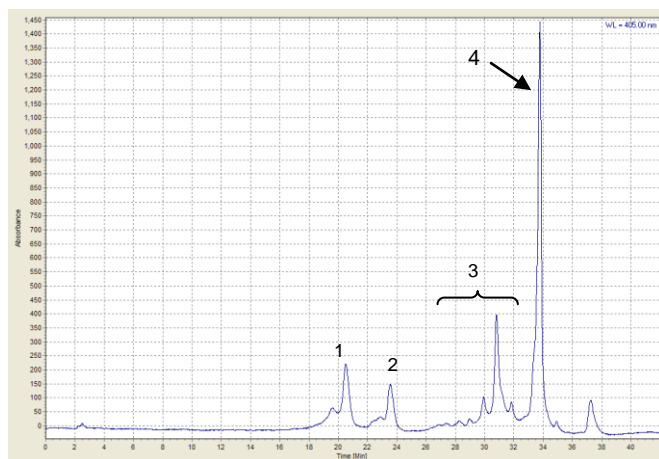


Figure 5.7 RP-HPLC showing fourth extraction from the Erlenmeyer flask method (left) and third extraction from the muslin cloth method (right)

5.2.4 Comparison of methanolic extracts from *amphNM* (**17**) and *amphNMpHap2* (**67**) disruptants

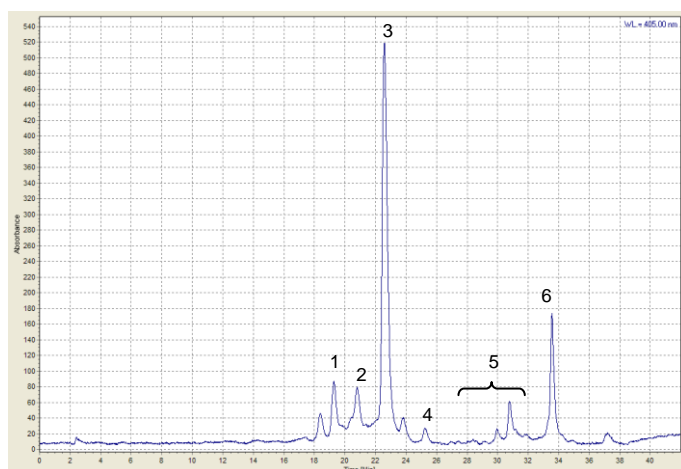
The RP-HPLC analysis of the methanolic extracts of *amphNMpHap2* showed the presence of a new minor heptaene peak thought to be **67**. A solution containing the *amphNM* product **17** was added to this sample,

and the HPLC analysis repeated to confirm that the *amphNMpHap2* product was not **17**.



- 1 – 8-hydroxy pHap2 (**67**)
- 2 – 8-deoxy pHap2 (**68**)
- 3 – Hexoses
- 4 – Aglycone (**22**)

Figure 5.8 RP-HPLC showing crude extract from the pHap2 mutant



- 1 – 8-hydroxy pHap2 (**67**)
- 2 – 8-deoxy pHap2 (**68**)
- 3 – 8-hydroxy NM (**17**)
- 4 – 8-deoxy NM (**54**)
- 5 - Hexoses
- 6 – Aglycone (**22**)

Figure 5.9 RP-HPLC showing a sample of the crude extract of the pHap2 mutant spiked with the crude extract from the *amphNM* mutant

The results obtained showed that the new heptaene peak is not **17**.

The new minor peak (thought to be **67**) was purified by semi-preparative HPLC. Positive ion ESMS gave peaks at 916 (M+Na)⁺, or after loss of water and sugar, at 713, corresponding to the expected mass of **67** (893.5 Da).

There was then a need to further purify the methanolic extracts obtained from **67** in order to isolate and characterise it to show that it is indeed the compound expected.

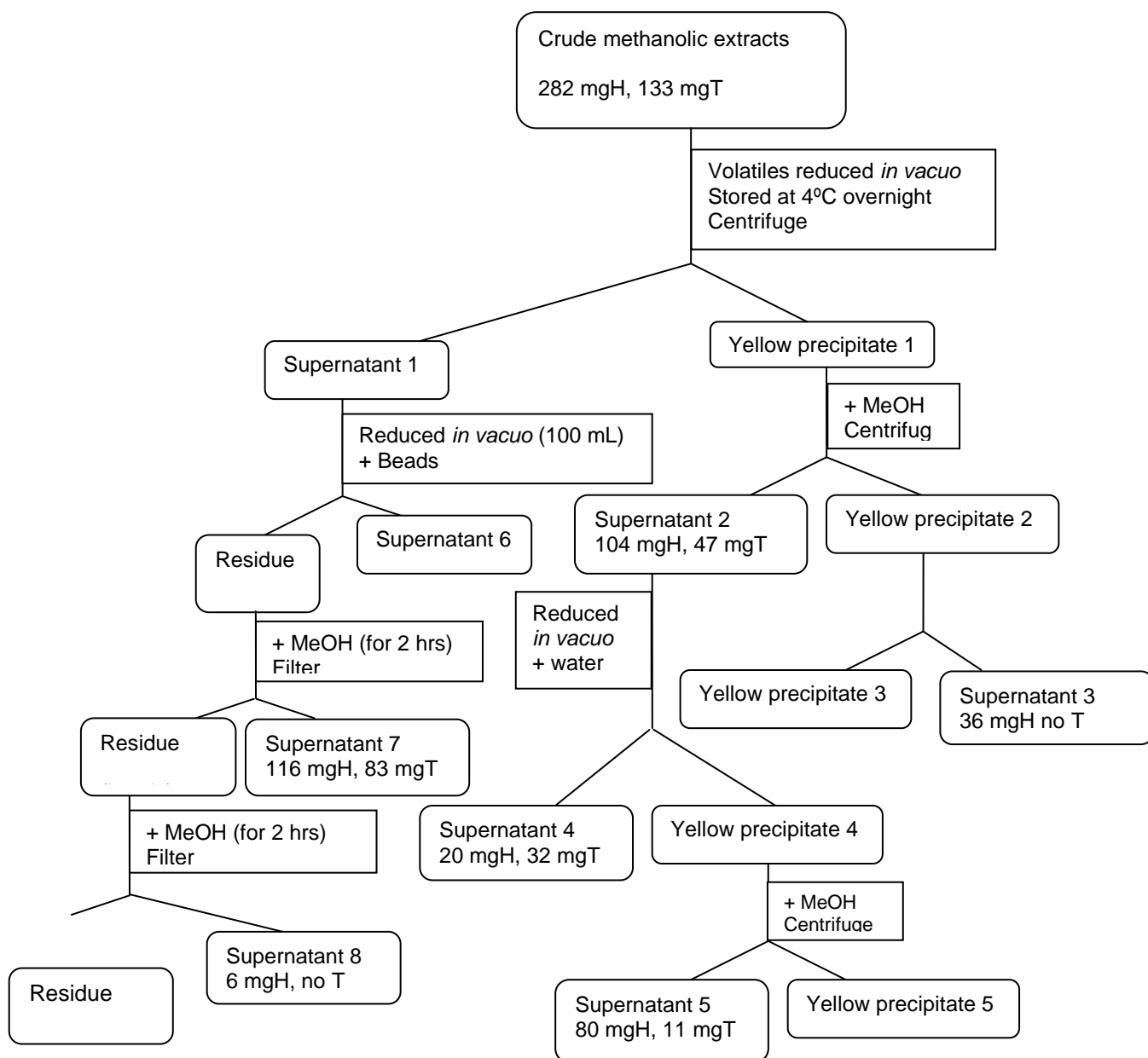
5.2.5 Purification of 16-descarboxyl-16-methyl-19-(O)-perosaminyl amphoteronolide B (**67**)

The combined methanolic extracts were concentrated *in vacuo* (below 40°C) until a yellow precipitate formed and placed overnight in the fridge. On examination by RP-HPLC and LCMS, the crude extract was shown to contain: pHap2 (**67**), deoxyhexosylated polyenes and aglycone (**22**).

The methanolic extracts of **67** were contaminated with overwhelming amounts of membrane lipids, other polyenic material, saccharides and aromatic impurities, analysis by proton NMR indicated less than 1% heptaene present.

5.2.5.1 Purification using partial dissolution in methanol

The yellow precipitate obtained after concentrating the combined methanolic extracts was recovered by centrifugation. Analysis by HPLC showed that the heptaene contained in this precipitate was largely (>90%) aglycone **22**. The precipitate was washed with water and purified further as shown in Scheme 5.5



Scheme 5.5 Purification protocol for the isolation of pHap2 using partial dissolution in methanol

The yellow precipitate separated from supernatant 1 (Scheme 5.5) contained largely aglycone (**22**), **67** and some soluble tetraenes, by HPLC. The significant difference between the amounts of heptaene present in the crude extract relative to that present in supernatant 2 (Scheme 5.5)

showed that most of the total heptaene was left in the precipitate as insoluble aglycone.

The yellow precipitate (ca. 2 g Wt) separated from supernatant 3 was like 'brick dust' and would have required copious amounts of methanol to dissolve. This is consistent with aglycone (**22**). The precipitate was thus set aside while further purification was carried out on the fractions containing **67**.

Unlike methanolic extracts from *amphNM* sediment, supernatant 1 from *amphNMpHap2* extract contained a significant amount of heptaene. Analysis by HPLC showed the presence of **67**.

After removal of all the volatiles from this supernatant, partial dissolution of the residue in methanol was used to separate **67** from **22**. This method of separation made a significant difference in the purification of **67** due to the large amount of aglycone present in the crude extract. However, the partial dissolution method could not be used to separate **67** from the corresponding tetraene, as used for the purification of **17**, due to the relative solubility of both **67** and tetraenes in methanol.

Analysis of **67** obtained from supernatant 7 and 8 (Scheme 5.5) by ¹HNMR, showed that it contained large amounts of sugars. Using small amounts of XAD16 beads could have enhanced separation of the sugars from the polyenes due to the greater affinity of the beads for polyenes.

RP-HPLC of supernatant 2 showed the presence of **67** and **22** whilst RP-HPLC of supernatant 3 showed the presence of only **22** and no **67**.

In order to obtain preliminary characterisation of **67**, a small sample was obtained using a semi-preparative RP-HPLC. This gave a product that is about 50% pure. However, the presence of high levels of lipids made any larger scale purification impractical, as only very light loading onto the column was possible.

The two main heptaene peaks were collected by semi-preparative RP-HPLC and analysed by NMR, and ESMS. The first peak was confirmed as **67** by ESMS. Positive ion ESMS for the first peak gave 713.4 (M-sugar-water)⁺, 892.5 (M-H)⁺.

Proton NMR of the first peak collected is shown in figure 5.10

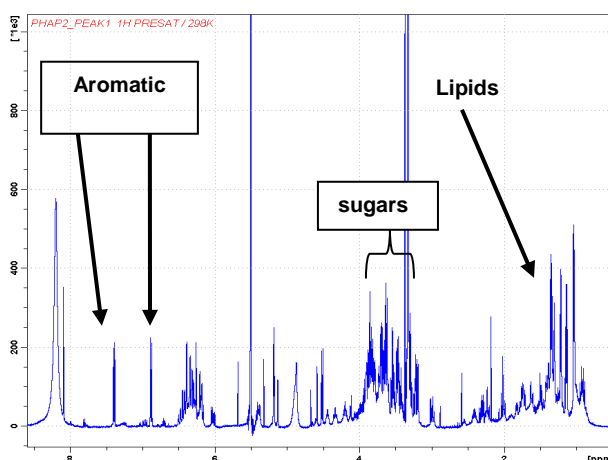


Figure 5.10 Proton NMR showing **67** after semi preparative HPLC

The presence of sugars, aromatics and lipids present in the NMR sample is indicative of the need for further purification of **67**.

Analysis by UV-Vis showed an absorbance for **67** at 402-404 nm (figure 5.11) and not 405 nm as with **1** or **17**. This may be due to impurities binding to and affecting the chromophore.

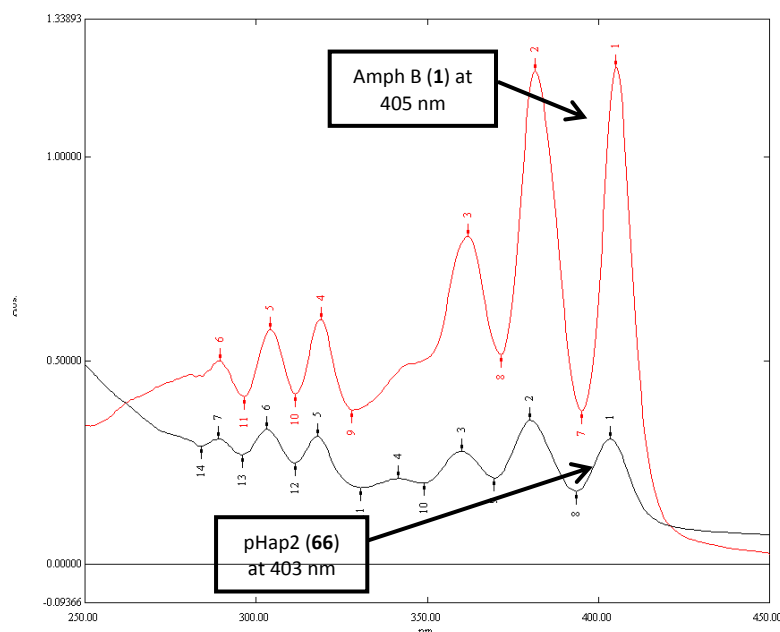


Figure 5.11 UV spectra showing the wavelength of **67** at 403 nm and not 405 nm

The second peak collected from the semi preparative HPLC was analysed by ESMS. ESMS (+ve) showed 697.42 (M-sugar-2H₂O)⁺, 713.42 (M-sugar-water)⁺, 876.49 (M-H)⁺. This shows that the second peak is the 8-deoxy-16-descarboxyl-16-methyl-19-(O)-perosaminyll amphoteronolide B (**56**) (877.5 Da).

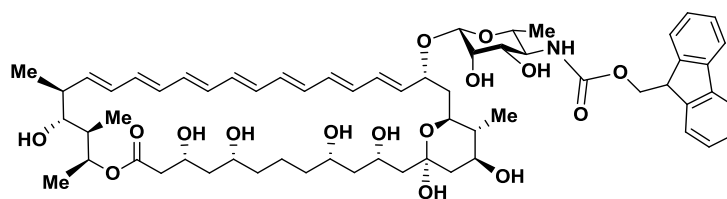


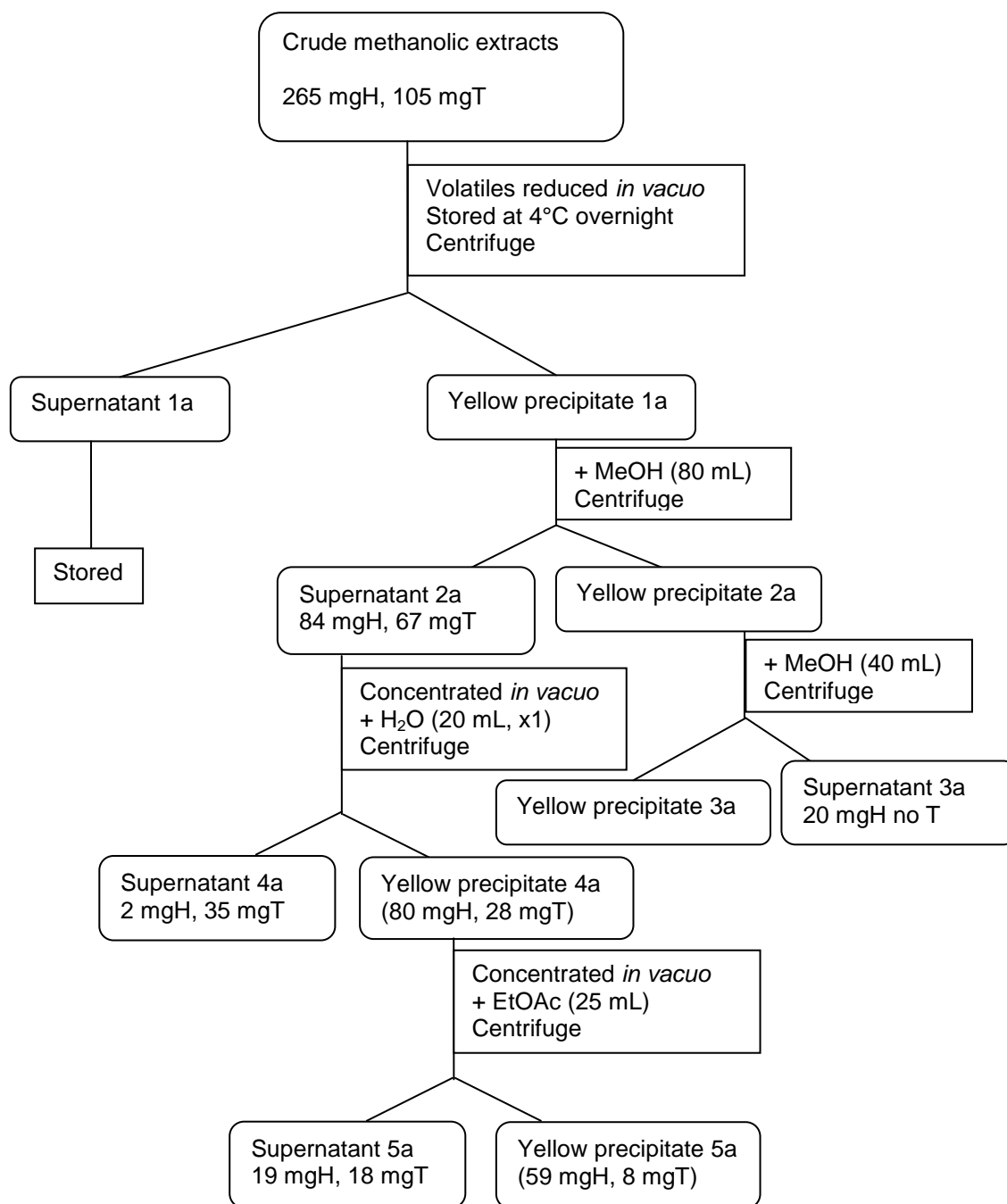
Figure 5.12 Structure of 8-deoxy-16-descarboxyl-16-methyl-19-(O)-perosaminyl-amphoteronolide B (**68**)

Small amounts and very low purity (50%) made further characterisation of the isolated compounds difficult. There was therefore, a need to further optimise the purification procedure.

5.2.5.2 Purification using water-washes and extraction in ethyl acetate

Due to the large amounts of sugars and lipids present in **67** isolated in Section 5.2.5.1, an attempt was made to purify the methanolic extracts obtained using water-washes and ethyl acetate extraction. It was expected that water will be used to remove the sugars, and ethyl acetate will be used extract the lipids.

In order to investigate this hypothesis, a new batch of **67** was grown and harvested after 5 days. The purification procedure is as shown in Scheme 5.6:



Scheme 5.6 Purification protocol for the isolation of **67** using water washes and extraction in ethyl acetate

The amount of heptaene present in the crude extract (265 mgH/ 7 L broth) was observed to significantly reduce when compared to that obtained in supernatant 2a (84 mgH). This is due to the high content of **22** in the crude extract. This is as expected because **22** is relatively less soluble in

methanol compared to the **67**. A single water wash (30 mL) was carried out to remove some sugars and tetraenes present in the sample. This is similar to the protocol discussed in Chapter 3 with **17**, however, only a single water wash with a small volume of water was carried out as **67** has greater water solubility than **17**.

The yield of the heptaene obtained after waterwash (95%) indicated that minimal heptaene activity was lost during this water wash. Proton NMR carried out on 'precipitate 4a' (Scheme 5.6) showed the presence of mainly lipids and about 3% polyenes. This indicates the very low level of purity of the sample at this stage.

Precipitate 4a was then thoroughly washed with ethyl acetate to remove lipid. Proton NMR analysis of precipitate 5a (Scheme 5.6) showed significantly reduced levels of lipids. However, the tenacity of the remaining lipid suggests strong complex formation with the polyene.

This can be explained using the 'barrel stave' idea discussed in Chapter 1 where there is a binding of the amphotericin molecule to the sterol molecule. The hydrophobic interaction of the heptaene of the amphotericin molecule and the alkenes in the glycerides is strong enough to allow for the intermolecular interaction of the lipophilic part of the glyceride molecule.

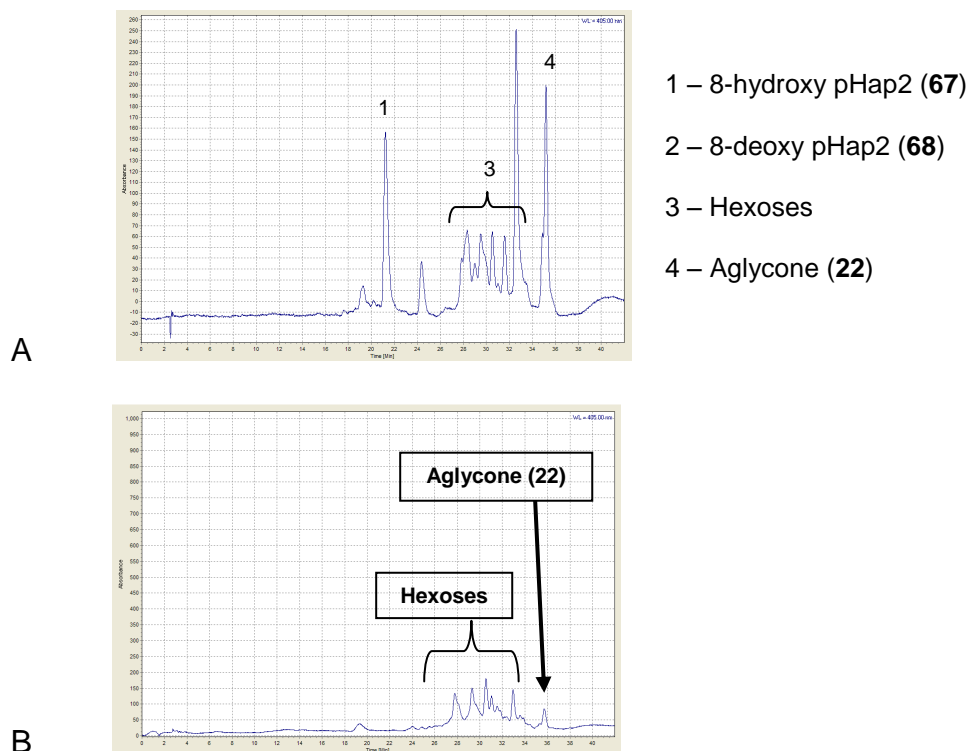
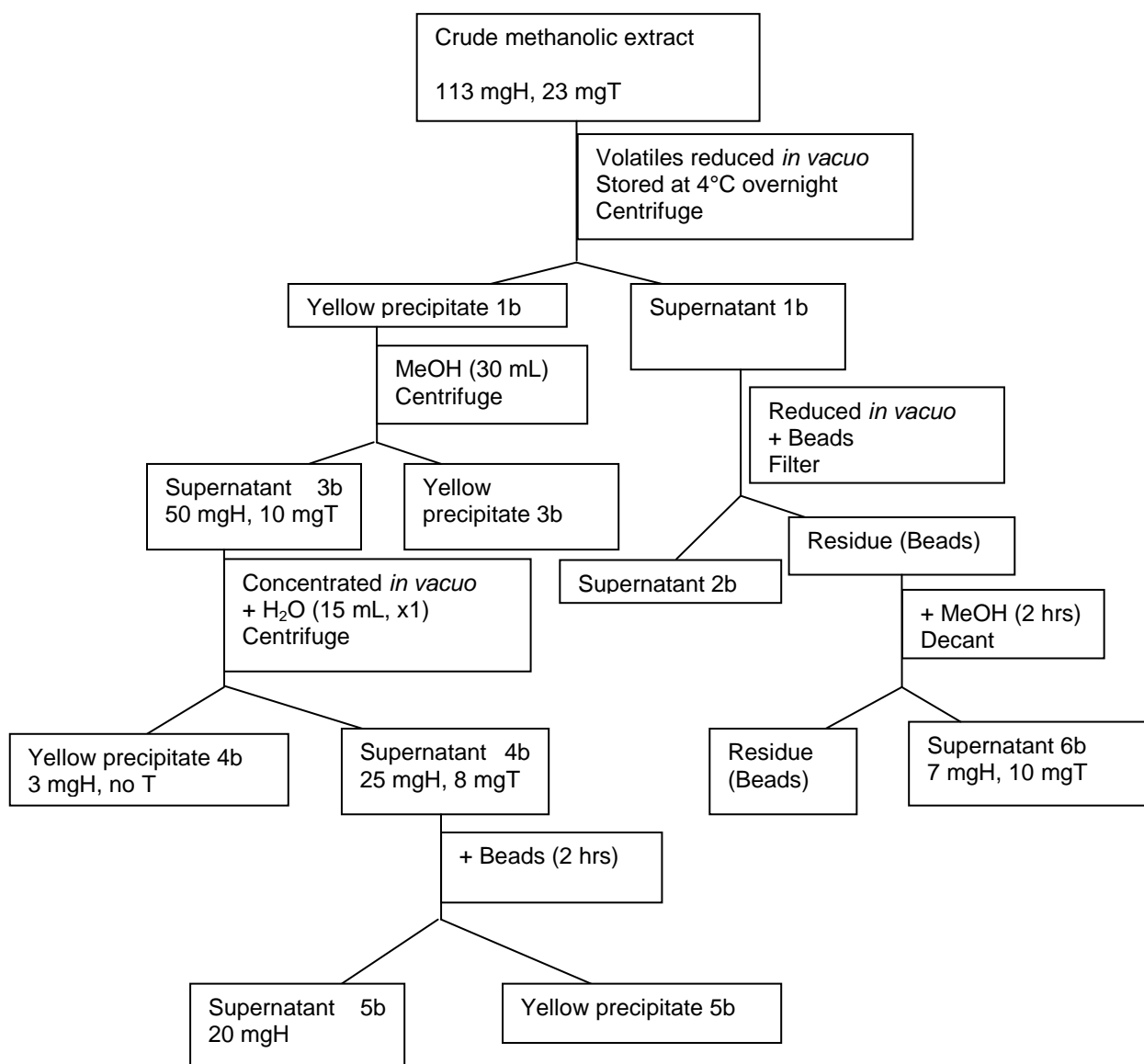


Figure 5.13 RP-HPLC showing precipitate (A) and supernatant (B) after ethyl acetate extraction of **67**

The result obtained by the analysis of the precipitate from the ethyl acetate extraction was consistent with those obtained in Section 5.2.5.2.

5.2.5.3 Purification using extraction in water

In another batch of **67** grown, the solubility of the **67** in water was exploited in the purification process.

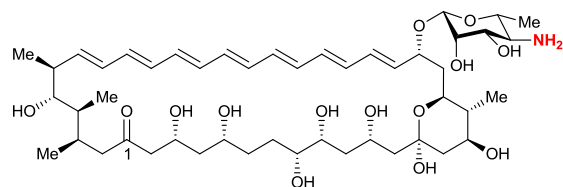


Scheme 5.7 Purification protocol for the isolation of pHap2 (**67**) using extraction in water

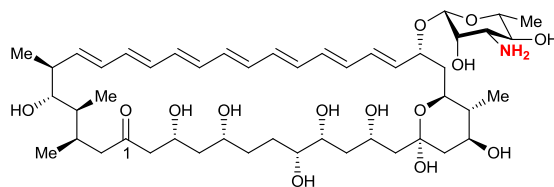
The batch used for this purification procedure had a very poor yield. The amount of heptaene obtained from supernatant 3b (Scheme 5.7) is as expected due to the large amount of **22** in the crude methanolic extract. When supernatant 3b was concentrated *in vacuo*, it was observed to be very 'syrupy'- brown and viscous liquid. This is thought to be due to the high amount of sugars present in the sample.

Water added to the viscous liquid was in a relatively larger volume than would be normally used. This is to afford extraction of the sugars and **67**. The amount of beads added to supernatant 4b (Scheme 5.7) was a relatively small amount (about 1g). This was to ensure that **67** is selectively separated from the mixture in the supernatant. The amount of **67** recovered from this purification method is 11% of the crude extract. This suggests that about 99% of all the expected **67** was recovered. This justifies this method as an effective and efficient method for the isolation of **67**.

The successful isolation of **67** from water showed that **67** is a lot more water-soluble in comparison to **17**. The solubility of **67** could be due to the lack of carboxyl group at C-16 and the position of the amino group on the sugar moiety of the molecule. The insolubility of **1** has been attributed to its amphoteric property due to the presence of a carboxyl and an amino group, both of which are charged at neutral pH. The absence of the carboxyl group in **67** will reduce the amphoteric nature of the molecule, hence, its solubility.



16-DESCARBOXYL-16-METHYL-19-(O)-AMPHOTERONOLIDE B (67)



16-DESCARBOXYL-16-METHYL-AMPHOTERICIN B (17)

Figure 5.14 Comparison of the position of the amino group in pHap2 (**67**) and *amphNM* (**17**)

The predicted equatorial position of the amino group will allow intermolecular interaction with water more readily. The solubility could also be due to lack of any steric hinderance around the amino group in the predicted structure of **67**.

Supernatant 5b (Scheme 5.7) was analysed by UV-Vis, NMR and ESMS. The results obtained were consistent with those obtained in Section 5.2.5.2. Proton NMR still showed the presence of lipids.

The relatively small amounts of **67** isolated and the low level of purity (< 30%) made full characterisation impossible. There was therefore, a need to attempt purification using the Fmoc intermediate as used in Chapter 4.

5.3 Fmoc derivatisation

Protection of the amino group using Fmoc-OSu was the method of choice as an intermediate during the purification of **67** due to the success of the same method in the purification and isolation of **17** and **54** as discussed in Chapter 4.

The main impurities in **67**, as discussed earlier, were membrane lipids, saccharides, aglycone (**22**), aromatics and the tetraene (**54**). The Fmoc protection reaction was carried out on:

- a) Yellow precipitate obtained from partial dissolution in methanol (Scheme 5.5)
- b) Yellow precipitate obtained from the extraction in water (Scheme 5.7)

5.3.1 Fmoc protection of yellow precipitate obtained from partial dissolution in methanol

After two waterwashes of the yellow precipitate from Section 5.3.5.1, the resulting precipitate had traces of tetraene present (<5%). The tetraene was difficult to separate from the heptaene by further water washes. In order to avoid loss of more heptaene material during purification, it was thought that the N-Fmoc tetraene (**63**) could be separated from the N-Fmoc heptaene by flash chromatography.

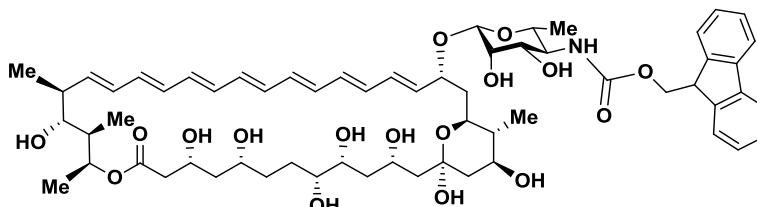
The yellow precipitate used for this reaction was obtained from supernatant 5 (Scheme 5.5) as described in Section 5.3.5.1. The supernatant (80 mgH, 11 mgT in 420 mgWt) was concentrated *in vacuo* and reacted with Fmoc-OSu (2 eq.) and pyridine (2 eq.) for about 16 hrs at RT. The reaction mixture was concentrated *in vacuo* and extracted (x2) with 10% MeOH-EtOAc. The supernatant (53 mgH, 9 mgT) obtained was reduced *in vacuo* and dry loaded onto a flash silica column, elution (5% MeOH in EtOAc) gave crude **69** (26 mgH, 5 mgT in 73 mgWt).

A second flash column gave (23 mgH, 3 mgT in 38 mgWt). However, after two columns, lipids were still present as indicated by proton NMR.

5.3.2 Fmoc protection of yellow precipitate from the supernatant during water wash

The yellow precipitate used for this reaction was obtained from supernatant 5b (Scheme 5.7) in Section 5.3.5.3. The precipitate obtained (20 mgH in 57 mgWt) was reacted with Fmoc-OSu and pyridine for 17 h at RT. The reaction mixture was concentrated *in vacuo* and extracted (x2) with MeOH-EtOAc (10%). The supernatant (18 mgH) obtained was reduced *in vacuo* and wet loaded onto a flash silica column. Purification on the first column (MeOH-EtOAc) gave **69** (17 mgH in 33 mgWt) eluting with 5%MeOH-EtOAc. In order to further purify **69**, a second column in MeOH-EtOAc was carried out to give **69** (15 mgH in 20 mgWt). However, ¹HNMR

showed the presence of some remaining membrane lipids. Positive ion ESMS also showed 1140 (M+Na)⁺, and 1155 (M+Na+water)⁺ which corresponds to the expected mass of **69** (1115 Da).



16-descarboxyl- *N*-fluorenylmethyloxycarbonyl-16-methyl-19-(*O*)-perosaminyl-amphoteronolide B (**69**)
RMM: 1115Da

Table 5.1 COSY showing proton to proton correlation of **69**

δ_H	δ_H	Proton atom number
0.99	1.2	39/38
1.0	1.4	41/16
1.15	1.8	
1.10	2.40	40/34
1.20	5.40	38/37
1.4	1.65	
1.4	3.6	16/15

δ_H	δ_H	Proton atom number
1.6	2.3, 2.35	4/2
1.6	4.2	4/3
3.8	4.3	9/11
3.9	4.2	5/3
6.0	6.2	20/21
7.35	7.70	3",6"/4",5"
7.45	7.80	2",7"/1",8"

The results obtained from the COSY showed a cross peak between H-41 (1.0 ppm) and H-16 (1.4 ppm) which confirms the presence of a methyl

group on C-16. The aromatic peaks at 6.85 and 7.10 ppm were observed to couple to each other.

The methyl doublet expected for H-6' at 1.3 ppm was not identified due to the large lipid peak at 1.25-1.40 ppm.

5.4 Variation/Optimisation of method used

The purification procedure after reaction work up was optimised to further improve the purity and yield of the desired product.

5.4.1 Purification using a third flash column

After the N-Fmoc reaction, purification was carried out on two flash columns. It was however, observed that the products from these columns still had lipids and aromatics as the main impurities. It was thought that purifying further on another flash column would further enhance purity.

Crude methanolic extracts (252 mgH, 105 mgT) obtained from a batch of **67** grown, was purified as described in Section 5.2.5.1, to give a yellow precipitate (78 mgH in 320 mgWt). The yellow precipitate was reacted with Fmoc-OSu and pyridine for about 17 h at RT. The reaction mixture was

extracted with MeOH-EtOAc (10%, x2) to give a yellow supernatant (72 mgH in 201 mgWt).

The resulting precipitate was shown by RP-HPLC and ESMS to contain mainly aglycone and hexoses.

The supernatant from the extraction in MeOH-EtOAc was wet loaded onto the flash silica column and the desired product eluted with 5%MeOHEtOAc (66 mgH in 133 mgWt). Proton NMR confirmed the desired product but showed the presence of lots of lipids, sugars and aromatics. ESMS (+ve) showed masses 757, and 1139 (M+Na)⁺ as expected .

The eluent was concentrated *in vacuo* and wet loaded onto another flash silica column. The desired product, **69**, eluted in 5% MeOH-EtOAc (60 mgH in 87 mgWt). Proton NMR obtained still showed the presence of aromatics, lipids and sugars.

TLC was carried out in order to detect the best solvent system that will enhance separation of lipids, aromatics and product. EtOAc was found to afford the best separation, though, the TLC was smearish.

The eluent was then loaded onto a third column and flushed with six times the column volume in EtOAc. The product (49 mgH in 52 mgWt) was

eluted in 3% MeOH-EtOAc. Proton NMR of eluent showed much reduced lipids and aromatics.

5.5 Deprotection of 16-descarboxyl-*N*-fluorenyl-16-methyl-19-(*O*)-perosaminyl amphoteronolide B (**69**)

As discussed in Chapter 4, an efficient method of deprotection of Fmoc protected amino group uses piperidine.

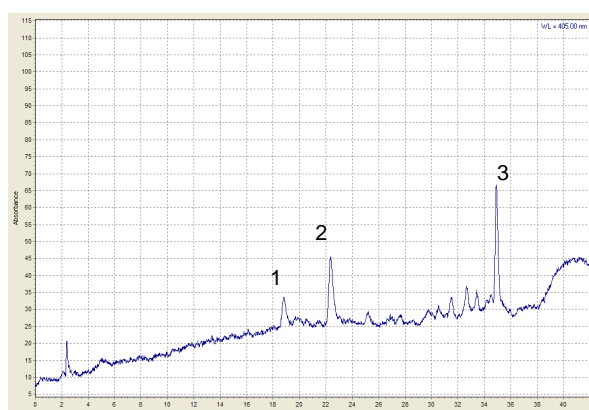
N-Fmoc pHap2 (**69**) (15 mgH in 20 mgWt), from Section 5.3.2, was reacted with piperidine (2 eq.) in DMSO (1 mL) for an hour at RT. Ether (10 mL) was added slowly to the reaction mixture. The yellow oily layer was separated from the clear supernatant. More ether (10 mL) was added to the yellow oil and the supernatant separated. The yellow layer was observed to be less oily and stuck to the side of the flask. Methanol (3 mL) was added and the resulting solution was concentrated *in vacuo* to give a fine yellow precipitate (12 mgH in 17 mgWt).

Proton NMR analysis of this yellow precipitate showed the absence of the Fmoc moiety, some heptaene, lipids, much reduced aromatics and very large DMSO peak (2.6 ppm). The product was resuspended in methanol, concentrated *in vacuo* and the DMSO was extracted with water (2 mL, x2, stepwise). The resulting precipitate was dissolved in methanol and

concentrated *in vacuo* to give **67** (11 mgH in 14 mgWt). Proton NMR showed much reduced DMSO peaks, some aromatics and heptaene peak.

Considering the water solubility of **67**, the supernatant from the water extraction was analysed by ^1H NMR to ensure no product was lost. This showed no heptaene present.

The precipitate from the water extraction was further analysed by RP-HPLC. This showed a glycosylated peak at 19 min as expected. Also, a peak at 35 min was observed corresponding to aglycone **22**.



1 – 8-hydroxy pHap2 (**67**)

2 – 8-deoxy pHap2 (**68**)

3 – Aglycone (**22**)

Figure 5.15 RP-HPLC showing deprotected **69** with traces of aglycone present

This suggests the presence of **22**. This is thought to be due to some of the **67** decomposing during the deprotection reaction and/or work up. A peak was observed at 22.5 min (385 nm). This suggests the aromatic moiety in the sample. Another peak at 30 min (319 nm) also suggests traces of tetraene.

The product obtained was purified further by semi preparative HPLC, however, no **67** was isolated. This is thought to be due to the very small amount of **67** present (5 mgH) before semi-preparative HPLC was carried out.

5.6 Conclusion/ Future work

The efficient production of mutants from the engineering of the biosynthesis of perosaminyl-amphoteronolide B in *S. nodosus* required a hybrid glycoyltransferase containing an N-terminal region of AmphDI and C-terminal region of PerDI.⁹³ The isolation of **67** showed that the Hap2 GT can transfer perosaminyl residues to amphoteronolides without the exocyclic carboxyl groups. An improved yield of **67** was obtained by inoculating the production media from 'old preculture' and not deeps. However, full characterisation of **67** was not obtained due to insufficient amounts of purified samples, even after use of Fmoc intermediacy to enhance purification. Removal of the main impurity, lipids, proved a lot more cumbersome than expected.

Chapter Six: EXPERIMENTAL

6.1 General Conditions

6.1.1 Instrumentation

UV assays of polyenes were run (in methanol) on a Shimadzu UV-2401PC spectrophotometer. For heptaenes, an absorbance of $1.7 \times 10^5 \text{ M}^{-1} \text{ cm}^{-1}$ at 405 nm was used, based upon the value reported for monomeric amphotericin in methanol, and for tetraenes an absorbance of $0.78 \times 10^5 \text{ M}^{-1} \text{ cm}^{-1}$ at 318 nm was used.¹¹⁸ Routine semi-quantitative UV assays are quoted using an RMM of 923 g mol^{-1} in the calculation for all analogues.

HPLC analysis was performed on a Varian Prostar diode array with Galaxie workstation and software. Analytical HPLC were run using 4.6 mm x 25 cm Supelco silica or C-18 silica (5 μm) with 1 mL min^{-1} flow rate. Semi-preparative HPLC using C-8 and C-18 reverse phase columns (25 cm x 21.2 mm) at 14.8 mL min^{-1} flow rate using silica, C-8 or C-18 columns. In general, every passage through semipreparative HPLC significantly reduced yield. Reverse phase HPLC used deionised water (solvent A) and standard (not HPLC) grade methanol containing (0.1% v/v) formic acid. Normal phase HPLC on silica columns was routinely run in methanol and ethyl acetate.

Typical programs for RP-HPLC were routinely run at 50% to 95% methanol (+ 0.1% v/v HCOOH) from 5 to 30 min.

Typical programs for Si-HPLC were run at 15% to 80% methanol in ethyl acetate from 2 to 31 min.

NMR spectroscopy was performed on a Bruker AV500 MHz AvanceIII, or Bruker AM300 MHz spectrometer. Chemical shifts are quoted in ppm from TMS. Coupling constants quoted in near-first order systems are 'observed' values. Proton resonances are (1 H, m) unless otherwise indicated. Attached proton test (APT) or 'DEPT135' were used in ^{13}C NMR spectroscopy. Spectra were analysed using Bruker's 'Topspin' or 'Spinworks'.

Electrospray mass spectrometry (ESMS) was performed on a triple quadrupole Micromass Quattro LC machine. FAB MS used 3-nitrobenzyl alcohol as matrix on Kratos Concept 1H double focussing high resolution spectrometer. LCMS Quadrupole time of flight mass spectrometry (QTOFMS) was run on a XEVO instrument with Waters Accuity UP-LC, with LC solvents: water (+ 0.1% HCOOH) and acetonitrile, gradient from 5% to 100%, with UV detector set at 405 nm or 319 nm.

IR spectra in Nujol were recorded on an IR Shimadzu Prestige-21, Fourier transform infrared spectrometer. ATR infra-red spectroscopy was run on a Perkin Elmer 'Spectrum One' instrument.

Sterilisation of all media and other materials were carried out in a Priorclave, tatecrol 2 front loading autoclave, with sterilisation at 121 °C for 20 min.

Centrifugation was performed using a Sorvall RC5B centrifuge with a GSA (13,000 rpm) or SS34 rotor (20,000 rpm) using polypropylene centrifuge tubes. Smaller scale centrifugation was performed using a MSE centaur 2 (benchtop) and MSE micro centaur.

Incubation of cultures was carried out in environmentally controlled shakers using New Brunswick Series 25 with 25 mm gyrotary and Sanyo Gallenkamp 'Orbisafe' with 32 mm gyrotary.

6.1.2 General Chemical Conditions

Commercially available materials were purchased from Sigma Aldrich (UK) or Fischer and used without further purification unless noted otherwise.

Due to the light and air sensitivity of heptaenes, all reactions were carried out under low light conditions and compounds were routinely stored at 4 °C. Reactions were monitored by UV-Vis spectroscopy and analytical thin layer chromatography performed using the indicated solvent on E. Merck silica gel 60 F254 plates (0.25 mm, Merck, Germany). The sorbent was

silica gel 60 (63-200 μm , Merck, Germany). Derivatised compounds were visualized using a UV ($\lambda_{254\text{nm}}$) lamp and stained by a solution of phosphomolybdic acid.

Compounds were dry loaded onto flash silica for purification by flash column chromatography unless otherwise stated. Flash silica was added to a solution of the compound, all volatiles removed *in vacuo* and the resulting powder added to the top of a flash silica column, followed by elution as normal.

Radial chromatographic separations were carried out on a Chromatotron silica gel plates of 1mm thickness with compounds visualised using an attached UV ($\lambda_{254\text{nm}}$) lamp.

'Reduced in volume *in vacuo*' refers to the use of a Büchi rotary evaporator with a water pump or Vacuubrand PC 3000 series and either dry-ice or water cooling with a water bath at less than 40 °C. The phrase 'and dried' refers to a sample left overnight on a high vacuum oil pump (<1 mmHg).

6.1.3 General Biological Procedures

6.1.3.1 Media

GYE media: Glucose (10 g L^{-1}), yeast extract (10 g L^{-1}) and deionised water (100 mL) adjusted to pH 7 with sodium hydroxide (2 M) in a tri-grooved Erlenmeyer flask (250 mL, previously washed with deionised water) and autoclaved at $121 \text{ }^{\circ}\text{C}$ for 20 min.

Production media (FD): (a typical growth involved 28 x 2 L tri-grooved flasks each containing 250 mL broth). All flasks are thoroughly rinsed with deionised water at the end of the previous washing up process in readiness for the next culture growth. Media components were obtained from Sigma-Aldrich. The production media (FD) contains fructose (20 g L^{-1} broth), Dextrin (corn, Type II, 15% soluble; 60 g L^{-1}), Soybean flour (Type I; roasted; 30 g L^{-1}), CaCO_3 (10 g L^{-1}) and Amberlite[®] XAD16 resin (50 g L^{-1}) and the flask necks plugged with a sponge before autoclaving at $121 \text{ }^{\circ}\text{C}$ for 20 min.

For mutants containing a thiostrepton marker, a recently prepared solution of thiostrepton in DMSO (20 mg L^{-1}) was added to the GYE and production media (after autoclaving) to give the working concentration of $5 \text{ } \mu\text{g L}^{-1}$.

6.1.3.2 Glycerol deeps

All cultures are maintained at -80 °C as glycerol 'deeps'. These are previously prepared either from frozen cell deeps (obtained as spore suspensions or deeps from P. Caffrey, Dublin) or prepared from a 'good' (high producing) growth.

Samples (deeps or spore suspensions) obtained from Caffrey were gently thawed and added to GYE media (100 mL) then incubated for 48 h (or until 'well grown'). Aliquots (0.5 mL) of the broth are then mixed with an equal volume of sterile glycerol in an Eppendorf tube, briefly vortexed and stored at -80 °C.

When a good yield is obtained from a production broth, the original preculture flask is left on the bench at RT and allowed to sporulate. An isolated colony is picked from the sporulated culture using a sterile loop and directly transferred into fresh GYE media and incubated for 48 h. Deeps are then prepared as described earlier to make fresh stock solutions for storage (-80 °C). When a particular mutant is required, the stock is revived by inoculating a deep in GYE media and incubating for 48 h.

6.1.3.3 Growth

The defrosted contents of a glycerol deep (1.5 mL) were added to GYE media and incubated (28 °C; 200 rpm) for 48 h. Aliquots (10 mL) are then used to inoculate production media (250 mL) and incubated at 28 °C for 4-5 d, to give a distinctive earthy odour and copious mycelia that when shaken slid slowly down the sides of the Erlenmeyer flask. Any flasks containing obvious signs of contamination (e.g. a 'yeasty smell' or a sickly milky cloudiness) were discarded after treatment with bleach.

6.2 Extraction of metabolites

6.2.1 Isolation of sediment (mycelia and XAD16 resin)

The whole broth (7 L) was either centrifuged (GSA, 12 000 rpm, 10 min) or filtered through a muslin cloth (Fenwick store, Leicester) on a metal colander to afford sediment (mycelia and XAD16). The supernatant was assayed (typically $< 10 \text{ mgH L}^{-1}$) and discarded.

6.2.2 Extraction of the heptaenes from the sedimented material

6.2.2.1 Erlenmeyer flask method

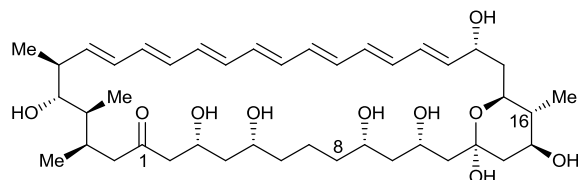
The sediment obtained was typically placed in an Erlenmeyer (5 L) flask and methanol (2 L) added, with frequent swirling. After a few hours, the

methanol could be decanted and fresh methanol added. This procedure was repeated until UV assay and/or HPLC analysis showed insignificant levels of heptaene product in the extract.

6.2.2.2 Using muslin cloth

The mycelia and XAD16 resin (from 7 L culture broth) was placed in muslin bag which was then repeatedly soaked in methanol (4 x 1 L). After a few hours, the muslin bag was raised above the methanol, allowed to drain (not squeezed out) and then placed in fresh methanol.

6.3 8-Deoxy-16-descarboxyl-16-methyl-amphoteronolide B (21)



Crude methanolic extracts (1.13 gH) were obtained as described in Section 6.2.1 and 6.2.3. Reduction in volume *in vacuo* (to ca. 300 mL) followed by storage at 4 °C gave a yellow precipitate (342 mgH in 1500 mgWt) which was collected by centrifugation. Analysis by HPLC indicated presence of 16-descarboxyl-16-methyl amphotericin B (**17**), 8-deoxy-16-descarboxyl-16-methyl amphotericin A (**54**) and aglycone (**22**). The dried precipitate was partially resuspended in methanol (500 mL) vigorously

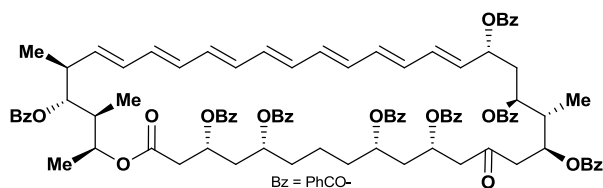
shaken with sonication, and the remaining yellow powder collected by Büchner filtration. This process was repeated until washings were clear, to give a yellow powder (285 mgH). The NMR data obtained was consistent with those previously reported.⁸⁵

δ_{H} (500 MHz; d^6 -DMSO) 0.85 (3 H, d, 41-H), 0.90 (3H, d, 39-H), 1.00 (3 H, d, 40-H), 1.10 (3 H, d, 38-H), 1.30-1.50 (m, 4-H,6-H,12-H), 1.70 (36-H), 2.10 (1 H, 2-H), 2.30 (34-H), 2.90 (35-H), 3.57 (9-H), 3.85 (1 H, 17-H), 4.61 (1 H, d, 5-OH), 4.71 (1 H, d, 19-OH), 4.79 (1 H, 35-OH), 4.99 (1 H, d, 9-OH), 5.21 (1 H, 37-H), 5.41 (1H, dd, 33-H), 5.50 (1H, br s, 11-OH), 5.65 (1 H, br s, 13-OH), 5.96 (1 H, dd, 20-H), 6.00 to 6.50 (m, 21-H to 33-H).

m/z (+ve ES) 755.5 (M+Na)⁺

m/z (-ve ES) 731.3 (M-H)

6.4 (3*R*,5*R*,9*S*,11*S*,15*R*,17*S*,19*S*,35*S*)-Octabenzoyloxy-13-oxo-(16*S*,34*S*,36*S*)-trimethyl (20*E*,22*E*,24*E*,26*E*,28*E*,30*E*,32*E*)-octatriacontaheptaeno-(37*S*)-lactone (**57**)



6.4.1 Reaction product obtained after 3 h

Crude **22** (105 mgH in 280 mgWt; 0.014 mmol) was suspended in DCM (25 mL) and pyridine was added (8 mL, 0.1 mmol). Benzoyl chloride (4

mL, 0.03 mmol) was added dropwise and then DMAP (3 mg, 0.03 mmol) was added with stirring at RT. The reaction was followed by TLC (40% EtOAc-hexane). The reaction mixture was stirred for 3 h at RT, diluted with DCM (20 mL), washed with water (30 mL), sodium hydrogen carbonate (30 mL; saturated), copper(II) sulfate (30 mL; saturated) and water (30 mL). After removal of volatiles *in vacuo*, the residue was dry loaded onto a flash column which was flushed (hexane) and then heptaene eluted (25% EtOAc-hexane) to give a mixture of penta, hexa and hepta-benzoylated aglycones (99 mgH in 220 mgWt).

m/z (+ve ES) 1374 (hexabenzoyl aglycone + water)⁺, 1478 (heptabenzoyl aglycone + water)⁺

m/z (-ES) 1252 (pentabenzoyl aglycone), 1460 (heptabenzoyl aglycone)

6.4.2 Reaction product obtained after 24 h

The reaction was carried out as described in Section 6.4.1 using **22** (211 mgH in 530 mgWt; 0.29 mmol) for 24 h at RT. After organic extractions and washes as in Section 6.4.1, the product was dry loaded onto a flash silica column and eluted (30% EtOAc-hexane) to give a mixture of heptabenzoyl and octabenzoyl aglycone (123 mgH in 298 mgWt). Further purification on a second flash silica column (EtOAc-hexane) afforded a mixture of hepta and octabenzoyl aglycone (119 mgH in 121 mgWt).

m/z (+ve ES) 1478 (heptabenzoyl aglycone + water)⁺, 1583 (**57** + water)⁺

m/z (-ve ES) 1460 (heptabenzoyl aglycone).

6.4.3 Reaction product from wet loading column

The reaction was carried out as described in Section 6.4.1 using **22** (15 mgH in 103 mgWt; 0.02 mmol) for 60 h at RT. However, after the reaction and organic extractions, the product was wet loaded onto the flash silica column. Elution (25% EtOAc-hexane) gave octabenzoyl aglycone (8 mgH in 15 mgWt). ESMS data obtained was consistent with that obtained for **57** in Section 6.4.1.

6.4.4 Isolation of Octabenzoyl aglycone

The reaction was carried out as described in Section 6.4.1 using **22** (323 mg heptaene in 500 mgWt; 0.44 mmol) and left stirring at RT for 60 h. After organic extractions and washes as in Section 6.4.1, the crude product was purified on two flash silica columns and the heptaene eluted (30% EtOAc-hexane) to give **57** (325 mgH in 353 mgWt), which was analysed by Si-HPLC (20% EtOAc-hexane).

m/z (+ve) 1583.6671 (M + Na)⁺,

m/z (QTOF) Found 1583.6730 (M + Na)⁺ C₉₇H₉₉O₂₀ requires 1583.6671

λ_{max} (MeOH)/ nm 407, 384 and 365.

(ATR)/cm⁻¹ 2928 (w), 1787 (w), 1713 (s), 1690 (s), 1602 (m), 1584 (m), 1266 (s) and 706 (s).

δ_{H} (500.1 MHz; CDCl₃) 0.75 (3 H, d, *J* 7.2, 41-H), 0.90, 1.00 (3 H, *J* 6.5, 40-H), 1.03 (3 H, d, *J* 6.9, 39-H), 1.19 (3 H, d, *J* 6.5, 38-H), 1.30, 1.35, 1.60, 1.65 (2 H, m), 1.87 (1 H, ddd, *J* 15.0, 5.9 and 3.1), 2.02, 2.08, 2.14, 2.16, 2.31, 2.34, 2.65 (1 H, dd *J* 16.1, 6.5, 2-H), 2.67 (2-H), 2.72 (34-H), 2.74 (1 H, dd *J* 16.6, 3.5), 2.84 (1 H, dd, *J* 16.6, 9.2), 2.89 (1 H, dd, *J* 18.2, 6.8), 3.05 (1 H, dd, *J* 18.2, 4.3), 5.00 (2 x 1 H, 2 x *ca* d), 5.16, 5.24, 5.40, 5.42, 5.45 (33-H), 5.47 (37-H), 5.48 (19-H), 5.55, 5.80 (1 H, dd *J* 9.3 and 9.1, 20-H), 6.22–6.54 (12 H, m, 21 to 32-H), 7.22–7.35 (8 H, m, *Ar-meta*), 7.41–7.52 (12 H, m, *ArH* 4 x *para* + 8 x *meta*), 7.55–7.62 (4 H, m, *para*), 7.78–7.82 (2 H, *ca* t, *ortho*), 7.88–7.92 (6 H, m, *ortho*), 8.01–8.08 (6 H, m, *ortho*), 8.13–8.17 (2 H, m, *ortho*).

δ_{C} (125.8 MHz; CDCl₃) 10.4 (q, 39-C), 11.1 (q, 41-C), 16.3 (q, 38-C), 18.2 (q, 40-C), 21.0(t, 7-C), 34.3 (t, 6-C), 34.5 (t, 18-C), 34.8 (t, 10-C), 38.21 (t, 2-C), 38.24 (t, 4-C), 38.8 (t, 14-C), 39.0 (d, 36-C), 40.6 (d, 16-C), 41.2 (d, 34-C), 46.7 (t, 12-C), 47.1 (t, 8-C), 68.6 (d, 17-C), 68.7 (d, 15-C), 69.0 (d, 3-C), 69.7 (d, 11-C), 71.3 (d, 37-C), 71.46 (d, 5-C), 71.50 (d, 9-C), 73.7 (d, 19-C), 79.3 (d, 35-C), 128.13 (d), 128.16 (d), 128.2 (d), 128.3 (d), 128.44 (d), 128.49 (d), 128.53 (d), 129.5 (d), 129.6 (d), 129.65 (d), 129.7 (d), 129.85 (d), 129.9 (d), 130.0 (d), 130.1 (d), 130.2 (s), 130.3 (s), 130.9 (d), 132.3 (d), 132.5 (d), 132.6 (d), 132.7 (d), 132.77 (d), 132.80 (d), 132.9 (d), 133.0 (2 C, d), 133.1 (d), 133.3 (2 C, d), 133.4 (2 C, d), 133.6 (d), 133.7 (d), 133.9 (d), 134.0 (d), 134.1 (d), 134.3 (d), 134.7 (d), 135.0 (d), 136.7 (d), 149.0 (d), 165.49 (s), 165.51 (s), 165.58 (s), 165.64 (s), 166.01(s), 166.02 (s), 166.19 (s), 166.35 (s) 169.0 (s, 1-C), 203.0 (s, 13-C).

m/z (+ve ES) 1582.7 (M+water)⁺

m/z (FAB) 1564.67 (M)⁺, 1442 (Heptabenzoyl-water)⁺.

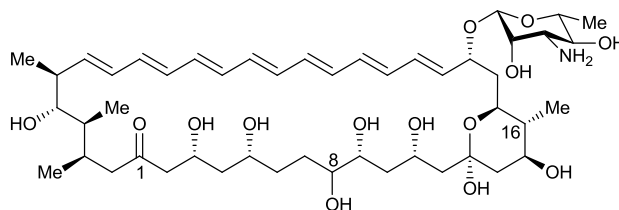
6.4.6 Crystallisation attempts

A portion of the product obtained from Section 6.4.5 was dissolved in ethyl acetate-hexane (30% v/v) to make a saturated solution at RT. The solution was stored in a cupboard for six weeks to allow the crystals to grow. The presence of light brown crystals were observed and checked by X-ray. These crystals did not diffract.

Another attempt to grow crystals of **57** was carried out by making a saturated solution of **58** in ethyl acetate. The vial was then placed in a bigger vial containing hexane to allow diffusion. After four weeks, no crystals were observed.

Growth of crystals was also attempted by dissolving **57** in warm methanol solution with slow cooling at RT. This produced some yellow crystals after 7 days. However, these crystals also did not diffract.

6.5 16-Descarboxyl-16-methyl-amphotericin B (**17**)



6.5.1 Extraction and Purification of 16-descarboxyl-16-methyl-amphotericin B from “ $\Delta amphNM+perDIDI$ ” mutant

6.5.1.1 Pre-culture and production media with thiostrepton

GYE preculture media with thiostrepton was inoculated with “ $\Delta amphNM+perDIDI$ ” mutant. After incubation (4 d), aliquots (5-10 mL) of the preculture was transferred to the production (FD) media (28 x 250 mL; with thiostrepton) and incubated (5 d). Harvesting and purification were carried out as described in Section 6.2.3. The yellow precipitate was recovered by centrifugation and dissolved in methanol. Volatiles were removed *in vacuo* and the resulting residue was water washed twice to afford a yellow precipitate. The precipitate obtained was dissolved in methanol to give **17** (72 mgH, 21 mgT in 298 mgWt).

6.5.1.2 Pre-culture with thiostrepton and production media without thiostrepton

GYE preculture (with thiostrepton), was inoculated with “*Δ amphNM+perDIDI*” and incubated (4 d). Aliquots of the preculture were transferred to production (FD) media (without thiostrepton) and incubated (5 d). Harvesting and purification were carried out as described in Section 6.2.3 to give a yellow precipitate (196 mgH, 141 mgT in 2371 mgWt) which was washed (2 x 50 mL water) to afford a yellow precipitate (107 mgH, 62 mgT in 590 mgWt).

6.5.1.3 Pre-culture and production media without thiostrepton

In another experiment GYE preculture (without thiostrepton) was inoculated with “*Δ amphNMper+DIDI*” and grown for two days. Aliquots of the preculture were transferred into FD media and incubated (5 d). Harvesting and purification and water washing were carried out as described in Section 6.5.1.2 to give a yellow precipitate (113 mgH, 56 mgT in 662 mgWt)

6.5.1.4 Duration of incubation

Preculture (without thiostrepton) was inoculated with “*Δ amphNM+perDIDI*” and incubated (2 d). Aliquots were then transferred

to the production media. Four flasks each of production media were incubated for five and fourteen days. Centrifugation and subsequent methanolic extraction of the broths gave 70 mgH, 150 mgH and 100 mgH for the first, second and third extractions, respectively, for the 14 d incubation whilst 50 mgH, 90 mgH and 80 mgH was recovered from the first, second and third extractions respectively for the 5 d incubation.

RP-HPLC showed the presence of **17**, **22** and **54** in the crude methanolic extracts, irrespective of the duration of incubation. The ratio of **17:22** in the methanolic extracts from 5 d incubation was 8:1 while the ratio from 14 d incubation was 16:1

The crude methanolic extracts (from both 5 d and 14 d growths) were then combined and purified as described in Section 6.2.3. The yellow precipitate was recovered by centrifugation and dissolved in methanol to give crude **17** (335 mgH, 333 mgT in 2864 mgWt). Volatiles were removed *in vacuo* and the resulting residue was water washed twice to afford a yellow precipitate. The precipitate obtained was dissolved in methanol to give **17** (287 mgH, 93 mgT in 1062 mgWt).

6.5.2 Other methods used to optimise yield

6.5.2.1 Purification using ethyl acetate wash

FD media was inoculated without thiostrepton. Purification was carried out as described in Section 6.2.3 to give a yellow precipitate (260 mgH, 160 mgT in 3318 mgWt) that was washed with water (2 x 80 mL) to give a yellow precipitate (126 mgH, 52 mgT in 890 mgWt). The resulting precipitate was dissolved in methanol (20 mL) and ethyl acetate (200mL) was added and stored for about 18 hours at 4 °C. The yellow precipitate (99 mgH, 35 mgT in 463 mgWt) was recovered by centrifugation. RP-HPLC confirmed the presence of **17** and **22**.

6.5.2.2 Purification using partial dissolution in methanol

Crude methanolic extract of "*ΔamphNM+perDIDI*" (689 mgH, 653 mgT) was purified as described in Section 6.2.3 to give a yellow precipitate that was water washed (2 x 100 mL) to give crude **17** as a yellow precipitate (588 mg H, 235 mgT). Methanol (60 mL) was added to the yellow precipitate with stirring and sonication. The resulting supernatant (143 mgH, 224 mgT) and precipitate (445 mgH, 10 mgT) were separated by centrifugation. The yellow precipitate was re-suspended in methanol (14 mL) and the resulting supernatant was concentrated *in vacuo* to give **17** (125 mgH, <1 mgT)

6.5.2.3 Purification using ether

GYE and FD media (both without thiostrepton) was inoculated and incubated. Purification was carried out as described in Section 6.2.3. The yellow precipitate (613 mgH, 867 mgT in 7425 mgWt) was water washed (2 x 20 mL) to afford a yellow precipitate (547 mgH, 502 mgT in 3518 mgWt). The precipitate was suspended in methanol (10 mL) and the supernatant (309 mgH, 325 mgT) obtained by centrifugation. Diethyl ether (100 mL) was added in portions to the supernatant with stirring. The resulting suspension (256 mgH, 100 mgT in 883 mgWt) was separated by from the supernatant (51 mgH, 205 mgT) by centrifugation.

6.5.3 Extraction and purification of 16-descarboxyl-16-methyl amphotericin B (**17**) from the 'new' *amphNM* mutant

GYE preculture media were inoculated with *amphNM* (without thiostrepton). After two days, aliquots were added to the production media and incubated (14 d). Methanolic extraction of the sediment gave a yield of 37 mgH L⁻¹.

6.5.3.1 Cultures from the *amphNM* mutant

Inoculation of GYE preculture media was routinely from deeps ('pc1'). A spore or colony from the remaining preculture of a high yielding growth

were aseptically selected, using a wire loop, and inoculated into fresh GYE preculture media ('pc2'). The precultures ('pc1' and 'pc2') were inoculated in separate FD media. The extracts from the culture broth were compared and the yield of **17** was observed to be higher (by how much) when 'pc2' was used to inoculate FD media.

6.5.3.2 Extraction of 16-descarboxyl-16-methyl amphotericin B (**17**) from the *amphNM* mutant

Sedimented mycelial and XAD16 beads from the production culture broth were obtained using either the 'Erlenmeyer flask' or 'muslin cloth' method as described in Section 6.2.2. It was observed that the muslin cloth method required only three extractions to deplete the broth of **17** whilst the Erlenmeyer method required about five extractions.

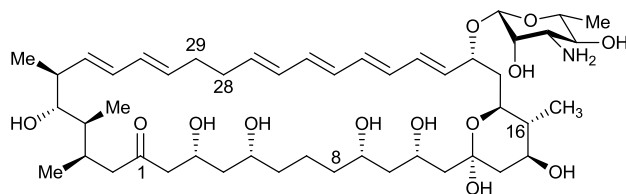
RP-HPLC analysis of the methanolic extracts from the Erlenmeyer flask method was observed to contain a higher ratio of aglycone (**22**) (31% of the total heptaene) than extracts from the 'muslin cloth' method (18% of the total heptaene).

6.5.3.3 Purification of 16-descarboxyl-16-methyl-amphotericin B from *amphNM* mutant

The combined methanolic extracts (421 mgH, 600 mgT) from the *amphNM* disruptant were reduced *in vacuo* and the resulting brown viscous solution was stored overnight at 4 °C. The yellow precipitate was separated by centrifugation and water washed (2 x 100 mL). The resulting yellow precipitate was partially suspended in methanol (100 mL) and the resulting supernatant (262 mgH, 255 mgT) was concentrated *in vacuo*.

Further purification was carried out by partial dissolution in methanol as described in Section 6.5.1.5 to give **17** (185 mgH in 465 mgWt).

6.6 8-Deoxy-16-descarboxyl-16-methyl-amphotericin A (**54**)



6.7.1 Fmoc protection of yellow precipitate after water washes

Methanolic extract from "*ΔamphNM+perDIDI*" mutant was reduced *in vacuo* and the resulting precipitate was water washed (as in Section 6.5.1.2) and dried. The yellow precipitate (180 mgH, 88 mgT in 930 mgWt; 0.20 mmol) was re-suspended in methanol (15 mL) and cooled to 0 °C. Pyridine (32 μL, 2 eq.) and Fmoc-OSu (135 mg, 2 eq.) were added and the reaction was left stirring at 0 °C for about 30 min and allowed to warm to RT with stirring for 16 h.

The reaction mixture was dry loaded onto flash silica flushed with ethyl acetate (3 x column volumes) and a gradient (MeOH/EtOAc) was then passed through the column. The product (70 mgH, 36 mgT in 340 mgWt) was eluted (10% MeOH/EtOAc) and wet loaded onto a second flash column. The column was flushed with DCM (2 x column volume) and a gradient (1-10% MeOH-DCM) was then passed through the column to give **61** (31 mgH, <1 mgT in 45 mgWt) which eluted (7% MeOH-DCM). More residual product contaminated with tetraene (35 mgH, 20 mgT) was eluted (8% MeOH-DCM).

6.7.2 Fmoc protection of yellow precipitate after water washes and initial partial dissolution in methanol

Methanolic extracts from the " $\Delta amphNM+perDIDI$ " mutant was reduced *in vacuo*, water washed and the resulting precipitate (75 mgH, 21 mgT in 220 mgWt) partially dissolved in methanol (10 mL) and the supernatant dried. The crude **17** was derivatised using Fmoc-OSu and pyridine as described in Section 6.7.1. After 17 h, the reaction mixture was concentrated *in vacuo* and extracted (x 2) with 10% MeOH-EtOAc. The supernatant (73 mgH, 20 mgT) obtained was reduced *in vacuo* and wet loaded onto a flash silica column. The column was flushed (EtOAc: 5 x column volume) and then eluted (1-10% MeOH-EtOAc). The product **61** (70 mgH, 11 mgT in 159 mgWt) was obtained (5% MeOH-EtOAc). This fraction was concentrated *in vacuo* and then loaded onto a second flash silica column (DCM). Elution with 7% MeOH-DCM gave **61** (65 mgH, 7 mgT in 78 mgWt).

6.7.3 Fmoc protection on *amphNM* extract free of tetraenes

Methanolic extract from the *amphNM* mutant was reduced *in vacuo* and purified as described in Section 6.5.1.5. The resulting yellow precipitate (95 mgH in 330 mgWt) was suspended in methanol and reacted with Fmoc-OSu and pyridine as described in Section 6.7.1. After 17 h, the

reaction mixture was concentrated *in vacuo* and extracted (x 2) with 10% MeOH-EtOAc to give a supernatant (92 mgH) which was reduced *in vacuo* and loaded onto a flash silica column. The column was flushed with copious amount of EtOAc and **61** (90 mgH in 193 mgWt) was eluted with 5% MeOH-EtOAc. The product obtained was loaded onto a second flash silica column (EtOAc) and **61** (85 mgH in 93 mgWt) eluted with 4% MeOH-EtOAc.

ν_{\max} (ATR)/ cm^{-1} 3398 (w), 2922 (w), 2591 (w), 1716, 1501, 1450, 1180, 1068 (s), 1020 (s), 848 (s), 762 (s), 740 (s).

Partial δ_{H} (500 MHz; d^4 -MeOH) 1.03 (d, J 7.44, 41-H), 1.13 (d, J 6.4, 40-H), 1.21 (d, J 6.4, 38-H), 1.47 (4-H), 1.83 (d, J 7.1, 18b-H), 1.97 (d, J 3.8, 36-H), 2.00 (d, J 4.7, 18a-H), 2.18 (s, 29b-H), 2.40 (s, 34-H), 3.22 (s, 35-H), 3.74 (9-H), 3.82 (5-H), 3.99 (15-H), 4.20 (17-H), 4.25 (9"-H), 4.35 (11-H), 4.38 (10"ab-H), 4.45 (t, 19-H), 4.62 (s, 1'-H), 5.40 (2 H, d, J 9.77, 33-H and 37-H), 6.02 (20-H), 7.33 (t, J 7.24, 3"-H and 6"-H), 7.41 (t, J 7.24, 2"-H and 7"-H), 7.70 (t J 6.51, 4"-H and 5"-H), 7.81 (d, J 6.88, 1"-H and 8"-H)

Partial δ_{H} (500 MHz; d^6 -DMSO) 0.99 (39-H), 1.05 (41-H), 1.10 (40-H), 1.15 (38-H), 1.30 (6'-H), 1.35 (7-H), 1.40-1.60 (4, 8, 10, 12-H), 1.70 (6b-H), 1.85 (18b-H), 2.0, 2.10, 2.15 (29b-H), 2.30, 2.35 (34-H), 2.65, 2.70, 2.85, 3.1, 3.2, 3.4, 3.45, 3.55 (15-H), 3.65 (17-H), 4.45 (19-H), 4.5, 4.53, 4.6 (1'-H), 4.65, 4.75, 4.8, 5.2, 5.3, 5.45 (33-H), 5.75 (27-H), 5.95 (20-H), 6.05 (31-H), 6.1 (32-H), 6.13, 6.17 (26-H), 6.2-6.5 (heptaene), 7.35 (2"-H and 7"-H), 7.45 (3"-H and 6"-H), 7.75 (1"-H and 8"-H), 7.9 (4"-H and 5"-H)

Partial δ_C (125.8 MHz, d^6 -DMSO) 12 (41-C), 18 (38-C), 29 (6'-C), 39 (6-C), 42 (29ab-C), 45 (18-C), 47, 58 (15-C and 4'-C), 68 (37-C), 72, 78 (39-C), 120 (4"-C and 5"-C), 126 (1"-C and 8"-C), 128 (2"-C and 7"-C), 129 (3"-C and 6"-C)

m/z (+ve ES) 1138.57 ($M+Na$)⁺

m/z (QTOF) Found 1116.6028 (MH)⁺ $C_{62}H_{86}NO_{17}$ requires 1116.5896

6.8 Optimisation of the method for the Fmoc derivatisation of 16-descarboxyl-16-methyl-amphotericin B (**17**)

6.8.1 Adding more Fmoc after an hour

Methanolic extract from the " *Δ amphNM+perDIDI*" mutant was reduced *in vacuo*, water washed and purified by partial dissolution in methanol. The resulting yellow precipitate (39 mgH in 138 mgWt) was suspended in methanol and reacted with Fmoc-OSu (1.6 eq.) and pyridine (1.3 eq.). The Fmoc-OSu (14 mg; 1.0 eq.) was added at the start of the reaction, and after an hour of reaction more Fmoc-OSu (9 mg; 0.6 eq.) was added and left stirring at RT. After 14 h of reaction, the reaction mixture was precipitated with diethyl ether (100 mL). The resulting yellow precipitate (23 mgH) was purified on two flash silica columns (EtOAc and then DCM) to give **61** (13 mgH in 19 mgWt).

6.8.2 Ether precipitation

Yellow precipitate from water washed sample of **17** from “*ΔamphNM+perDIDI*” mutant, was purified by repeated partial dissolution in methanol to give a yellow precipitate (146 mgH in 512 mgWt). This was reacted with Fmoc-OSu and pyridine as described in Section 6.7.1. After 16 h, the reaction mixture was poured onto stirred diethyl ether (0 °C, 300 mL) to give a suspension. The supernatant (71 mgH) was separated from the precipitate (70 mgH) by centrifugation. The resulting precipitate was purified on two flash silica columns (0-7% MeOH-EtOAc) to give **61** (68 mgH in 75 mgWt) which eluted at 5% MeOH-EtOAc.

Analysis by NP-HPLC showed the presence of 2 main peaks. These peaks were further purified and collected by semi-preparative NP-HPLC. *m/z* (+ve ES) 1138.2 (**61** + Na)⁺, 1153.3 (**62** + Na)⁺

6.8.3 Purification using chromatotron instead of a second flash silica column

Crude methanolic extracts (421 mgH, 600 mgT in 9248 mgWt) from the *amphNM* mutant, were reduced *in vacuo* and the resulting precipitate was water washed and the partially dissolved in methanol to give a yellow precipitate (232 mgH, 33 mgT in 958 mgWt). This was the reacted with

Fmoc-OSu and pyridine as described in Section 6.7.1. After 16 h, the reaction mixture was concentrated *in vacuo*, extracted (x2) in 10% MeOH-EtOAc and the resulting supernatant (202 mgH, 32mgT) was concentrated *in vacuo* and purified on a flash silica column (1-10% MeOH-EtOAc) to give **61** (152 mgH, 21 mgT in 435 mgWt) which was then loaded onto the chromatotron (in 10% MeOH-DCM) and after 90 min, **61** (148 mgH in 159 mgWt) eluted with 5% MeOH-DCM.

Proton NMR sample (in MeOH-d₆) left at RT overnight were observed to contain some crystals. The crystals were examined under a microscope and were observed to be very fibrous. However, the crystals did not diffract.

The supernatant from the NMR sample was separated from the crystals. Proton NMR of the supernatant from the crystals showed no lipids present while the ¹HNMR of the crystals (re-dissolved) showed the presence of lipids with the heptaene.

6.9 8-Deoxy-16-descarboxyl-*N*-fluorenylmethyloxycarbonyl-16-methyl amphotericin A (**63**)

16-Descarboxyl-16-methylamphotericin A (**54**) isolated from the supernatant from the partial dissolution of the water washed yellow precipitate of *amphNM* as described in Section 6.6.1. The supernatant

obtained was reduced *in vacuo* and the resulting yellow precipitate (179 mgH, 309 mgT in 2128 mgWt) was dissolved in methanol (10 mL) and reacted with Fmoc-OSu (2 eq.) and pyridine (2 eq.) as described in Section 6.7.1. After 16 h, the reaction mixture was concentrated *in vacuo*, extracted (x 2) with 10% MeOH-EtOAc and the resulting supernatant (113 mgH, 344 mgT) was wet loaded onto a flash silica column. The column was flushed (1-10% MeOH-EtOAc) and elution at 6% MeOH-EtOAc gave **63** (39 mgH, 296 mgT in 601 mgWt).

6.9.1 Purification using chromatotron

Further purification of **63** (39 mgH, 296 mgT in 601 mgWt) obtained from Section 6.9 was carried out on a chromatotron (in 10% MeOH-DCM). Elution of **63** (10 mgH, 282 mgT in 304 mgWt) was at 6% MeOH-DCM.

6.9.2 Purification using a second flash silica column

The supernatant obtained from the partial dissolution of the water washed precipitate from the *amphNM* mutant was concentrated *in vacuo* to give a yellow precipitate that was mainly **54** (58 mgH, 250 mgT in 912 mgWt). Fmoc-OSu (2 eq.) and pyridine (2 eq.) were added to the resulting precipitate and left stirring for 16 h. The reaction mixture was concentrated *in vacuo*, extracted (x 2) with 10% MeOH-EtOAc and the resulting super

natant (57 mgH, 248 mgT) was purified on a flash silica column. The column was flushed with copious amounts of ethyl acetate (4 x column volume) and then 1-10% MeOH-EtOAc to give **63** (25 mgH, 242 mgT in 664 mgWt) which eluted with 7% MeOH-EtOAc. This product was further purified using a second flash silica column (0-9% MeOH-EtOAc) to give **63** (9 mgH, 240 mgT in 258 mgWt).

Further purification of **63** was carried out by semi-preparative NP-HPLC to give 50 mgT in 52 mgWt.

δ_{H} (500 MHz; d^4 -MeOH) 0.99 (d, J 7.4, 39-H), 1.07 (d, J 6.8, 40-H), 1.22 (d, J 6.4, 38-H), 1.24 (16-H), 1.30 (br d, J 5.0, 6'-H), 1.35 (14b-H), 1.38 (7b-H), 1.42 (8b-H), 1.44 (6b-H), 1.55 (6a-H and 8a-H), 1.59 (4b-H and 10b-H), 1.61 (4a-H and 10a-H), 1.65 (7a-H), 1.76 (12a-H), 1.83 (18b-H), 1.94 (36-H), 2.01 (18a-H), 2.02 (14a-H), 2.15 (2ab-H), 2.24 (28ab-H and 29a-H), 2.36 (t, 34-H), 2.43 (d, 2b-H), 2.45 (d, 2a-H), 3.28-3.30 (2'-H, 5'-H and 35-H), 3.57 (15-H), 3.59 (4'-H), 3.73 (17-H), 3.76 (9-H), 3.83 (3'-H), 3.84 (5-H), 4.22 (3-H), 4.26 (t, 9"-H), 4.37 (11-H), 4.38 (d, 10"b-H), 4.40 (d, 10"a-H), 4.46 (br s, 19-H), 4.61 (br s, 1'-H), 5.47 (dd, 33-H), 5.57 (30-H), 5.72 (27-H), 5.79 (dd, 20-H), 6.01 (d, 31-H), 6.05 (d, 32-H), 6.14 (26-H), 6.22-6.29 (21-25-H), 7.33 (t, 3"-H and 6"-H), 7.41 (t, 2"-H and 7"-H), 7.70 (t, 4"-H and 5"-H), 7.82 (d, 1"-H and 8"-H).

Partial δ_C (125.8 MHz; d^6 -DMSO) 12.69 (39-C), 13.36 (41-C), 17.37 (38-C), 17.48 (40-C), 18.35 (6'-C), 22.64 (7-C), 33.52 (28-C and 29-C), 38.61-38.88 (8-C and 6-C), 38.72 (10-C), 41.98 (36-C), 42.28 (34-C), 43.56 (2-C), 44.59 (4-C), 44.72 (16-C), 45.30 (12-C), 45.71 (14-C), 48.3 (18-C), 48.5 (9"-C), 58.32 (4'-C), 67.98 (10"a-C), 68.62 (3-C), 68.81 (11-C), 70.32 (15-C), 71.38-71.56 (3'-C, 5-C, 9-C and 17-C), 71.88 (2'-C), 72.82 (37-C), 74.94-78.71 (35-C and 5'-C), 79.34 (19-C), 98.75 (13-C), 100.19 (1'-C), 120.93 (1"-C and 8"-C), 126.26-126.29 (4"-C and 5"-C), 128.19 (3"-C and 6"-C), 128.81 (2"-C and 7"-C), 131.73 (32-H), 132.17 (31-H), 132.53 (30-H), 132.66 (26-C), 132.8-134.66 (21-25-C), 134.92 (20-C), 135.52 (27-C), 135.90 (33-C), 142.61 (1"a-C and 8"a-C), 145.3, 145.43, 158.82 (11"-C), 170.1 (1-C) 1.00 (d, 39-H), 1.06 (d, 40-H), 1.22 (d, 38-H), 1.30 (d, 6'-H), 2.36 (34H) 4.20 (tt, 17-H), 4.35 (t, 11-H) 4.43 (t, 19-H), 4.60 (d, 1'H), 5.08 (t), 5.22 (q), 5.44 (dd, 33-H, 37-H), 5.56 (q), 5.70 (q), 5.77 (dd, 20-H)

m/z (+ve ES) 699.45 (M-sugar-water)⁺, 1124.59 (M+Na)⁺

m/z (QTOF) Found 1102.6311 (MH)⁺ $C_{62}H_{88}NO_{16}$ requires 1102.6103

6.10 Deprotection of 16-descarboxyl-N-fluorenylmethyloxycarbonyl-16-methyl amphotericin B (**61**)

6.10.1 Deprotection of N-Fmoc NM heptaene (**61**) containing some tetraenes

The deprotection of a mixture of **61** and **63** (4 mgH, 2 mgT) from Section 6.7.1 was carried out by reaction with piperidine (2 eq.) in DMSO. After an hour, the reaction mixture was poured onto stirred ether (18 mL). The resulting precipitate (2 mgH, 1 mgT) was separated from the supernatant (1 mgH, 1 mgT) by centrifugation. Analysis of precipitate obtained by HPLC showed deprotection.

6.10.2 Deprotection of hemi acetal (**61**) and methyl ketal (**62**) products

The deprotection of a mixture of **61** and **62** (13 mgH) obtained from Section 6.7.2 was dissolved in methanol (1 mL) and reacted with piperidine (2 eq.). After an hour, the reaction was stopped by adding water (2 mL) and the pH was adjusted from 8 to 6 with 5% HCOOH/H₂O (1 mL). XAD16 (2 g) was added to the solution and the volatiles were removed *in vacuo*. After an hour, the product was extracted from the XAD16 with

methanol. RP-HPLC showed the presence of two peaks corresponding to **17** and the methyl ketal analogue.

In another experiment, a mixture of **61** and **62** (20 mgH) from Section 6.7.2 was dissolved in methanol (1 mL) and reacted with piperidine (2 eq.) at RT for an hour. Water (2 mL) was added to the reaction mixture, the pH was adjusted from 8 to 6 with 5% HCOOH/ H₂O (1 mL), XAD16 was added and the volatiles were removed *in vacuo*. After an hour, the product was extracted from the XAD16 with methanol. The methanolic extract was concentrated *in vacuo* and then extracted with DCM. The resulting precipitate was dried *in vacuo* and the product obtained was analysed by RP-HPLC. Two peaks were observed by HPLC with elution at 22 min and 26 min.

6.10.3 Deprotection of N-Fmoc NM heptaene (**61**) without tetraenes

The deprotection of **61** obtained from Section 6.7.3, was carried out by dissolving the yellow precipitate (16 mgH in 18 mgWt) in DMSO (1 mL) and piperidine (2 eq.) was added at RT. The reaction was left stirring for an hour after which the reaction mixture was poured very slowly onto ether (35 mL) (dropwise). The suspension obtained was separated by centrifugation and the resulting precipitate (15 mgH) was further washed with ether (10 mL), suspended in methanol and concentrated *in vacuo*

before extraction with water (10 mL). The resulting precipitate (12 mgH in 13 mgWt) was suspended in methanol, dried *in vacuo* to give **17**.

m/z (+ve ES) 917 (M+Na)⁺

In another experiment, **61** (10 mgH in 11 mgWt) from Section 6.7.3, was dissolved in DMSO (1 mL) and reacted with piperidine (2 eq.) for an hour at RT. Ether (10 mL) was added dropwise to the reaction mixture to give a yellow oily suspension. The yellow oil was separated from the clear supernatant using a pipette. The yellow oil was further washed with ether (10 mL) and the resulting residue was suspended in methanol (3 mL) and dried *in vacuo* to give **17** as a fine yellow precipitate (9 mgH in 9.5 mgWt).

ν_{\max} (ATR)/cm⁻¹ 3367 (w), 2476 (w), 2245 (m), 2072 (s), 1595, 1120 (s), 950 (s), 821 (s).

Partial δ_{H} (500 MHz; d⁴-MeOH) 1.025 (41-H), 1.045 (39-H), 1.15 (40-H), 1.21 (38-H), 1.30 (6'-H), 1.35, 1.40, 1.42, 1.45, 1.50, 1.60, 1.70, 1.75, 1.85 (d, 36-H), 1.95 (d), 2.00 (dd), 2.20 (2-H), 2.25 (2b-H), 2.30, 2.40 (34-H), 2.65, 2.75, 2.90 (s), 3.05 (s, 8-H), 3.20, 3.30, 3.38 (9-H), 3.62 (d), 3.66 (d), 3.74 (t), 3.87 (s), 3.92 (d), 4.00, 4.15, 4.20 (tt), 4.35 (t), 4.50 (t, 19-H), 4.65 (br s, 1'-H), 4.90, 5.40 (33-H and 37-H), 6.05 (20-H), 6.15-6.55 (12H, m).

Partial δ_{C} (d⁶-DMSO) 12 (39-C and 41-C), 18 (38-C, 6'-C and 40-C), 32 (18-C), 42 (36-C), 44 (34-C), 58 (8-C), 70 (9-C and 37-C), 72, 74 (5'-C), 80 (19-C and 35-C), 100 (1'-C), 130-136, 137

m/z (+ve ES) 713.43 (M-sugar-water)⁺, 876.50 (M-water)⁺, 916.50 (M+Na)⁺

m/z (QTOF) Found 894.5193 (MH)⁺ C₄₇H₇₆NO₁₅ requires 894.5215

6. 11 Deprotection of 8-deoxy-16-descarboxyl-N-fluorenylmethyloxycarbonyl-16-methyl amphotericin A (**63**)

The deprotection of **63** obtained from Section 6.9.1, was carried out by dissolving **63** (9 mgH, 50 mgT in 64 mgWt) in DMSO (1 mL) and reacting with piperidine (2 eq.) for an hour at RT. Ether (10 mL, x 2) was added very slowly to the reaction mixture and the resulting precipitate (8 mgH, 44 mgT) was suspended in methanol, dried *in vacuo* and then extracted with water (10 mL, x 2). The resulting precipitate (7 mgH, 25 mgT) was dissolved in methanol and dried *in vacuo*.

Further purification was carried out by semi-preparative RP-HPLC to give **54** (5 mgT in 6 mgWt).

Partial δ_{H} (500 MHz; d⁴-MeOH) 0.95 (41-H), 0.99 (39-H), 1.05 (40-H), 1.10, 1.20 (38-H), 1.25 (16-H), 1.30 (br, 6'-H), 1.60 (4-H and 10-H), 2.00 (18-H and 14-H), 2.15 (2ab-H), 2.20 (28-H and 29-H), 2.35 (34-H), 2.40 (2-H), 2.90, 3.02, 3.04, 3.08, 3.15, 3.2, 3.26, 3.55 (15-H), 3.75 (17-H and 19-H), 3.80 (3'-H and 5'-H), 4.20 (t, 3-H), 4.35 (11-H), 4.45 (19-H), 4.55 (s, 1'-H), 5.21 (t), 5.45 (33-H), 5.55 (30-H), 5.65, 5.70 (27-H), 5.80 (20-H), 5.95, 6.00 (31-H), 6.05 (32-H), 6.10 (26-H), 6.22-6.30 (21-25-H).

6.12.2 Duration of incubation

GYE media (with thiostrepton) was inoculated with *amphNMDIIpHap2* and grown for two days. Aliquots were transferred into FD media and a batch of media was incubated for five days whilst another batch was incubated for fourteen days. All the conditions of growth of the media were the same apart from the duration of incubation.

Analyses of the methanolic extracts obtained from the broths incubated for five days showed 200 mg, 160 mg, 100 mg and 100 mg as the total heptaene from the first, second, third and fourth extractions respectively. Methanolic extracts from the broths incubated for fourteen days contained 200 mg, 100 mg, 80 mg and 60 mg of total heptaene from the first, second, third and fourth extractions respectively.

6.12.3 Harvest of mycelia

The mycelia and resin were separated from the broth (FD media) by two methods: centrifuge followed by soaking of the sediment in an Erlenmeyer flask; and filtration by gravity using 'muslin cloth' to collect the 'sediment', followed by soaking of the cloth in a bowl.

6.12.3.1 Erlenmeyer flask method

The mycelia and beads were harvested by centrifugation and the resulting sediment was finely dispersed in methanol (5 L) and left to soak overnight in a large Erlenmeyer flask. The methanolic extract in the supernatant was decanted and the sedimented mycelia and beads were re-extracted (4 x 2 L) with methanol.

6.12.3.2 Muslin cloth method

In another method, the culture was decanted into a muslin cloth on a colander and left to drain into a bucket overnight. The mycelial residue left on the cloth was sedimented by centrifugation and placed back in the cloth. The cloth was tied loosely at the ends and whilst suspended, soaked in methanol (1 L). After 3 h, the methanolic extract was decanted and the sediment were re-extracted (2x) with fresh methanol.

6.12.4 Comparison of the methanolic extracts from *amphNM* and *amphNMDIIpHap2* disruptants

The crude methanolic extract of **67** was analysed by RP-HPLC. An aliquot of the crude methanolic extract of **67** was added to a solution containing some **17**. Analysis of a solution of the mixture by RP-HPLC showed the presence of a new peak at 22.5 min.

6.12.5 Purification of 16-descarboxyl-16-methyl-19-(O)-perosaminyl amphoteronolide B (**67**)

The combined methanolic extracts of **67** were reduced *in vacuo* until a yellow precipitate formed (ca. 200 mL). The suspension was stored overnight at 4 °C and separated by centrifugation. RP-HPLC and LC-MS of the resulting precipitate showed **67** (19 min), deoxyhexosylated polyenes (28-34 min) and aglycone **22** (35 min).

6.12.5.1 Purification using partial dissolution in methanol

The yellow precipitate obtained by concentrating the crude methanolic extract of **67** was recovered by centrifugation and suspended in methanol. The volatiles from the resulting supernatant (104 mgH, 47 mgT) were removed *in vacuo*, and the precipitate obtained was re-suspended in methanol to give a supernatant (20 mgH, 32 mgT). The resulting precipitate was further suspended in methanol and dried *in vacuo* to give **67** (80 mgH, 11 mgT) as the main heptaene.

The precipitate obtained after partial dissolution in methanol was further purified by semi preparative RP-HPLC to give **67** (7 mgH in 15 mgWt).

Partial δ_{H} (500 MHz; d^4 -MeOH) 0.99 (39-H), 1.0 (41-H), 1.15 (40-H), 1.18, 1.22 (38-H), 1.65, 2.05, 2.15, 2.25 (2b-H), 2.30 (2a-H), 2.35, 2.75, 2.84, 3.18 (8-H), 3.30 (5'-H), 3.46, 3.72, 3.76 (9-H), 4.0 (5-H), 4.10, 4.14, 4.20 (3-H), 4.24, 4.28, 4.30 (11-H), 4.34, 4.38, 5.40 (33-H and 37-H), 6.00 (20-H), 6.15-6.55 (12H, m)

m/z (+ve ES) 697.43 (M-sugar-2H₂O)⁺, 713.41 (M-sugar-water)⁺, 876.49 (M-water)⁺, 916.49 (M+Na)⁺

6.12.5.2 Purification using water washes and extraction in ethyl acetate

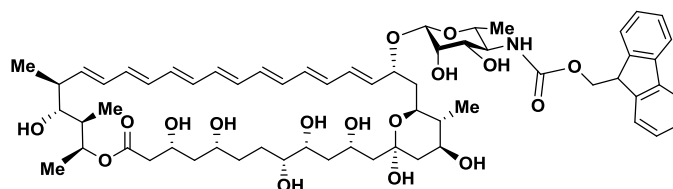
Yellow precipitate obtained from the crude methanolic extract (265 mgH, 105 mgT) of **67** after concentrating *in vacuo* was separated by centrifugation and suspended in methanol. The resulting supernatant (84 mgH, 67 mgT) was reduced *in vacuo* and water washed to give a yellow precipitate (80 mgH, 28 mgT) which was then suspended in methanol and concentrated *in vacuo*. The resulting precipitate was extracted with ethyl acetate and centrifuged to give **67** (59 mgH, 8 mgT).

6.12.5.3 Purification using extraction in water

Crude methanolic extract of **67** (113 mgH, 23 mgT) was reduced *in vacuo* and the yellow precipitate was recovered by centrifugation and suspended in methanol. The resulting supernatant (50 mgH, 10 mgT) was concentrated *in vacuo* and water washed to give a yellow precipitate (3 mgH) and supernatant (25 mgH, 8 mgT). XAD16 beads (5 g) was added to the aqueous supernatant and left to stand for an hour. Methanolic extract of the XAD16 gave **67** (20 mgH) as a yellow precipitate.

m/z (+ve ES) 916 (M+Na)⁺

6.13 16-descarboxyl- *N*-fluorenylmethyloxycarbonyl-16-methyl-19-(*O*)-perosaminyl-amphoteronolide B (**69**)



6.13.1 Fmoc protection of yellow precipitate obtained from partial dissolution in methanol

Yellow precipitate (80 mgH, 11 mgT in 420 mgWt) obtained from Section 6.12.5.1 was dissolved in methanol and reacted with Fmoc-OSu (2 eq.) and pyridine (2 eq.) for 16 h at RT. The reaction mixture was concentrated

in vacuo, extracted (x2) with 10% MeOH-EtOAc and dry loaded onto a flash silica column (0-7% MeOH-EtOAc). Elution at 5% MeOH-EtOAc gave **69** (26 mgH, 5 mgT in 73 mgWt). Further purification was carried out on a second flash silica column to give **69** (23 mgH, 3 mgT in 38 mgWt). Proton NMR showed the presence of lipids in **69** obtained.

6.13.2 Fmoc protection of the yellow precipitate from the supernatant during water wash

Yellow precipitate obtained from Section 6.12.5.3 (20 mgH in 57 mgWt), was dissolved in methanol and reacted with Fmoc-OSu (2 eq.) and pyridine (2 eq.) for 17 h at RT. The reaction mixture was concentrated *in vacuo*, extracted (x2) with 10% MeOH-EtOAc, and the resulting supernatant (18 mgH) was reduced *in vacuo* and wet loaded onto a flash silica column (0-7% MeOH-EtOAc) to give **69** (17 mgH in 33 mgWt) eluted with 5% MeOH-EtOAc. Further purification of the product obtained was carried out using a second flash silica column (0-10% MeOH-EtOAc) to give **69** (15 mgH in 20 mgWt). Proton NMR showed the presence of some lipids in the **69** obtained.

Partial δ_{H} (500 MHz; d^4 -MeOH) 0.99 (39-H), 1.15 (40-H), 1.18, 1.22 (38-H), 1.65, 2.05, 2.15, 2.25 (2b-H), 2.3 (t, 2a-H), 2.35, 2.75, 2.84, 3.18 (8-H), 3.30 (5'-H), 3.46, 3.72, 3.76, 4.00, 4.10 (t), 4.14 (t), 4.20, 4.24 (q), 4.28 (d), 4.30 (d), 4.34, 4.38, 5.40 (33-H and 37-H), 5.50 (s), 6.00 (dd, 20-H), 6.1-

6.5 (12H, m), 7.35 (t, 3"-H and 6"-H), 7.45 (t, 2"-H and 7"-H), 7.70 (d, 4"-H and 5"-H), 7.80 (d, 1"-H and 8"-H),
m/z (+ve ES) 1140 (M + Na)⁺, 1155 (M + Na + water)⁺.

6.13.3 Purification using a third flash silica column

Crude methanolic extracts from **67** (252 mgH, 105 mgT) was concentrated *in vacuo* and the yellow precipitate was recovered by centrifugation and purified as described in Section 6.12.5.1. The resulting yellow precipitate (78 mgH in 320 mgWt) was dissolved in methanol and reacted with Fmoc-OSu (2 eq.) and pyridine (2 eq.) for 17 h at RT. The reaction mixture was concentrated *in vacuo*, extracted (x2) with 10% MeOH/EtOAc and the resulting supernatant (72 mgH in 201 mgWt) was concentrated *in vacuo* and wet loaded onto a flash silica column (0-7% MeOH-EtOAc) to give **69** (66 mgH in 133 mgWt). A second flash silica column (0-7% MeOH-EtOAc) was used to further purify the product to give **69** (60 mgH, 87 mgT) which eluted at 5% MeOH-EtOAc. The product obtained was loaded onto a third flash silica column. The column was flushed with copious amounts of ethyl acetate (6 x column volume) and the 0-6% MeOH-EtOAc was flushed through the flash column to give **69** (49 mgH in 52 mgWt).

m/z (+ve ES) 1138.48 (M+Na)⁺.

6.14 Deprotection of 16-descarboxyl-N-fluorenyl-16-methyl-19-(O)-perosaminyl amphoteronolide B (**69**)

Deprotection of **69** was carried out using product from Section 6.12.5.3. The product (15 mgH in 20 mgWt) was dissolved in DMSO (1 mL) and reacted with piperidine (2 eq.) at RT for an hour. Diethyl ether (10 mL) was added very slowly to the reaction mixture to give a yellow oily layer which was separated from the clear supernatant with a pipette. The yellow oil was washed with more ether (10 mL) and separated from the resulting supernatant. The precipitate was dissolved in methanol and dried *in vacuo* to give a yellow precipitate (12 mgH in 17 mgWt). Proton NMR showed deprotection but the presence of large DMSO peaks. The yellow precipitate was resuspended in methanol, dried *in vacuo* and the DMSO was extracted with water (2 mL, x2). The resulting precipitate was dissolved in methanol, dried *in vacuo* to give a yellow precipitate (11 mgH in 14 mgWt). Analysis by RP-HPLC showed the presence of **67** at 19 min and **22** at 35 min. Further purification by semi-preparative RP-HPLC resulted in the isolation of **22** but no **67**.

Partial δ_{H} (500 MHz; d^4 -MeOH) 0.85 (41-H), 0.99 (39-H), 1.1 (40-H), 1.20 (38-H), 1.30 (6'-H), 1.40, 1.70, 1.80, 2.00, 2.15, 2.60, 3.00 (8-H), 3.60 (15-H), 3.75 (9-H), 3.90 (5-H), 4.00, 4.45 (19-H), 4.60 (1'-H), 5.15, 5.35, 5.45 (33-H and 37-H), 5.80 (20-H), 6.15-6.55 (21-32-H).

m/z (+ve ES) 757 (M-sugar-water)⁺, 895.47 (MH)⁺

Appendices

- Appendix One Supplementary data for 8-deoxy-16-descarboxyl-16-methyl-amphoterolide B
- Appendix Two Supplementary data for 16-descarboxyl-16-methyl-amphotericin B and its tetraene analogue from the “*ΔamphNM+perDIDI*” and ‘*amphNM*’ disruptants
- Appendix Three Supplementary data for 16-descarboxyl-16-methyl-19-(O)-perosaminyl-amphoterolide B

Appendix One: Supplementary data for 8-deoxy-16-descarboxyl-16-methyl-amphoteronolide B

Octabenzoyl NMPer 090615
OOI334-2.5 (0.343) Cm (4:17)

18-Jun-2009
1: Scan ES+
3.77e4

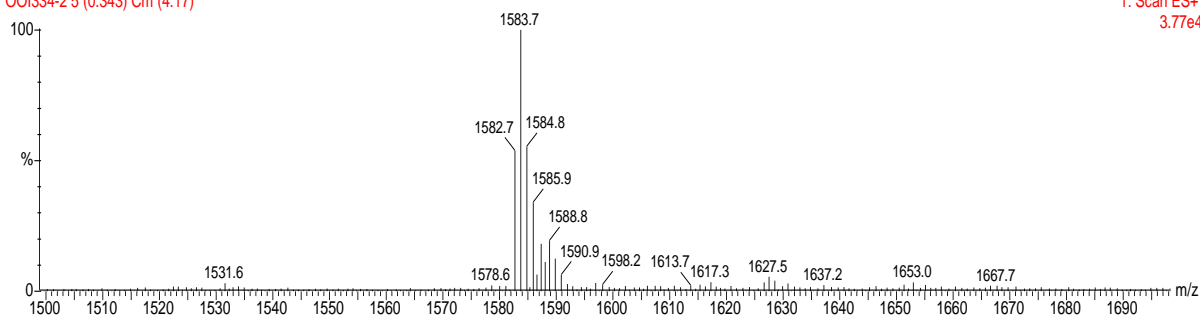


Figure 1 ESMS for octabenzoyl aglycone (57)

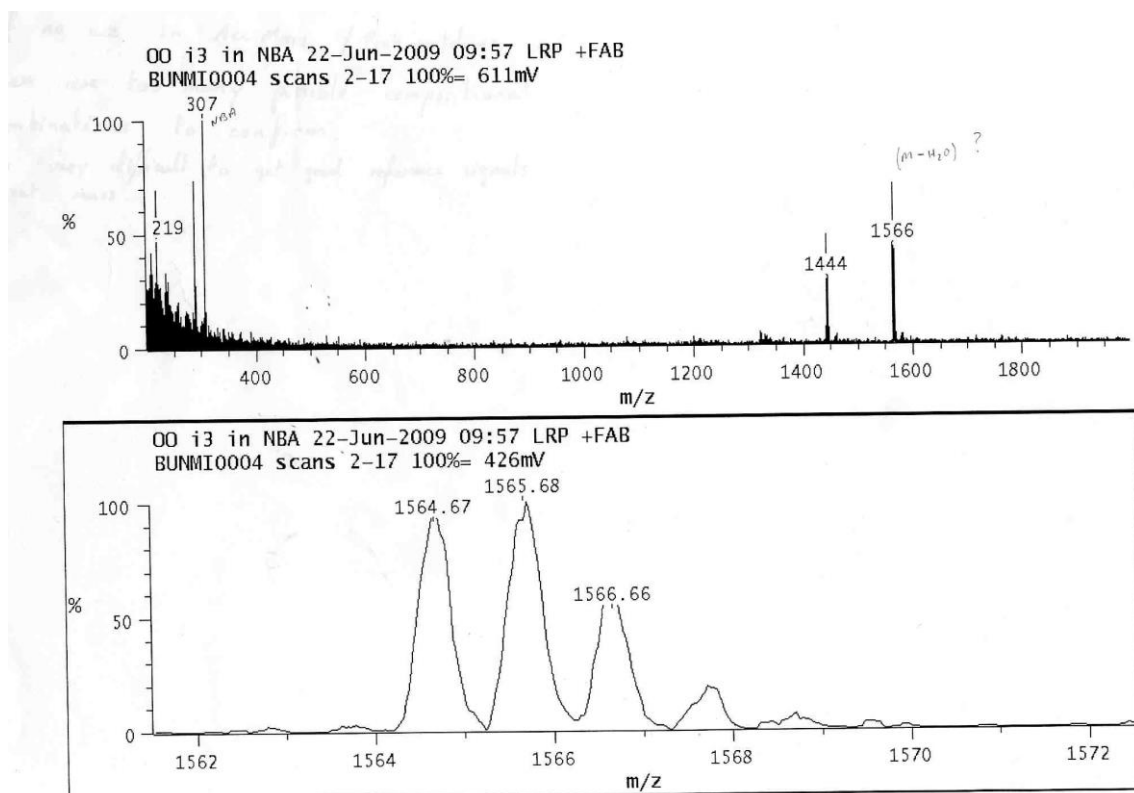


Figure 2 FAB-MS showing a mixture of heptabenzoyl and octabenzoyl aglycone

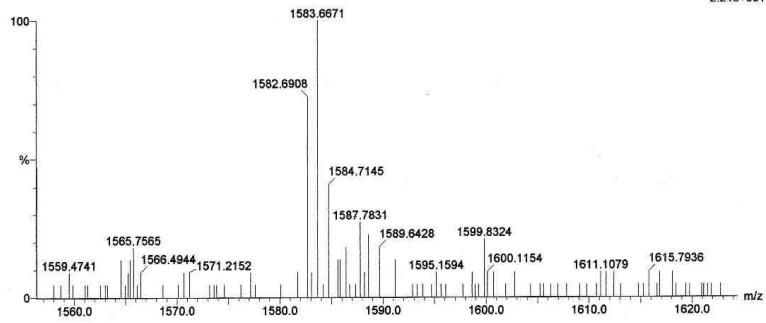
Elemental Composition Report

Single Mass Analysis

Tolerance = 10.0 PPM / DBE: min = -1.5, max = 50.0
 Element prediction: Off
 Number of isotope peaks used for i-FIT = 3

Monoisotopic Mass, Even Electron Ions
 54 formula(e) evaluated with 2 results within limits (all results (up to 1000) for each mass)
 Elements Used:
 C: 0-100 H: 0-100 O: 0-25
 Octabenzyl NMper
 GE Bunni 3 99 (1.562)

1: TOF MS ES+
 2.24e+001



Mass	Calc. Mass	mDa	PPM	DBE	i-FIT	i-FIT (Norm)	Formula
1583.6671	1583.6730	-5.9	-3.7	48.5	18.7	0.6	C97 H99 O20
	1583.6577	9.4	5.9	44.5	18.9	0.8	C93 H99 O23

Figure 3 Accurate mass/Elemental composition for octabenzoyl aglycone after HPLC prep

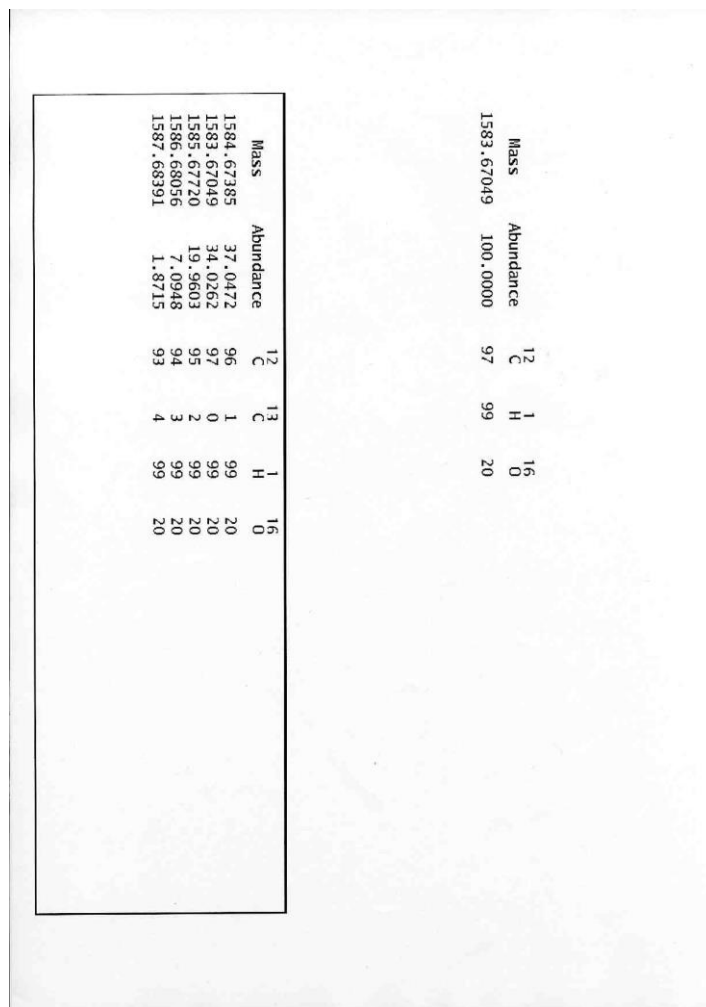


Figure 4 FAB-MS showing accurate mass for octabenzoyl aglycone

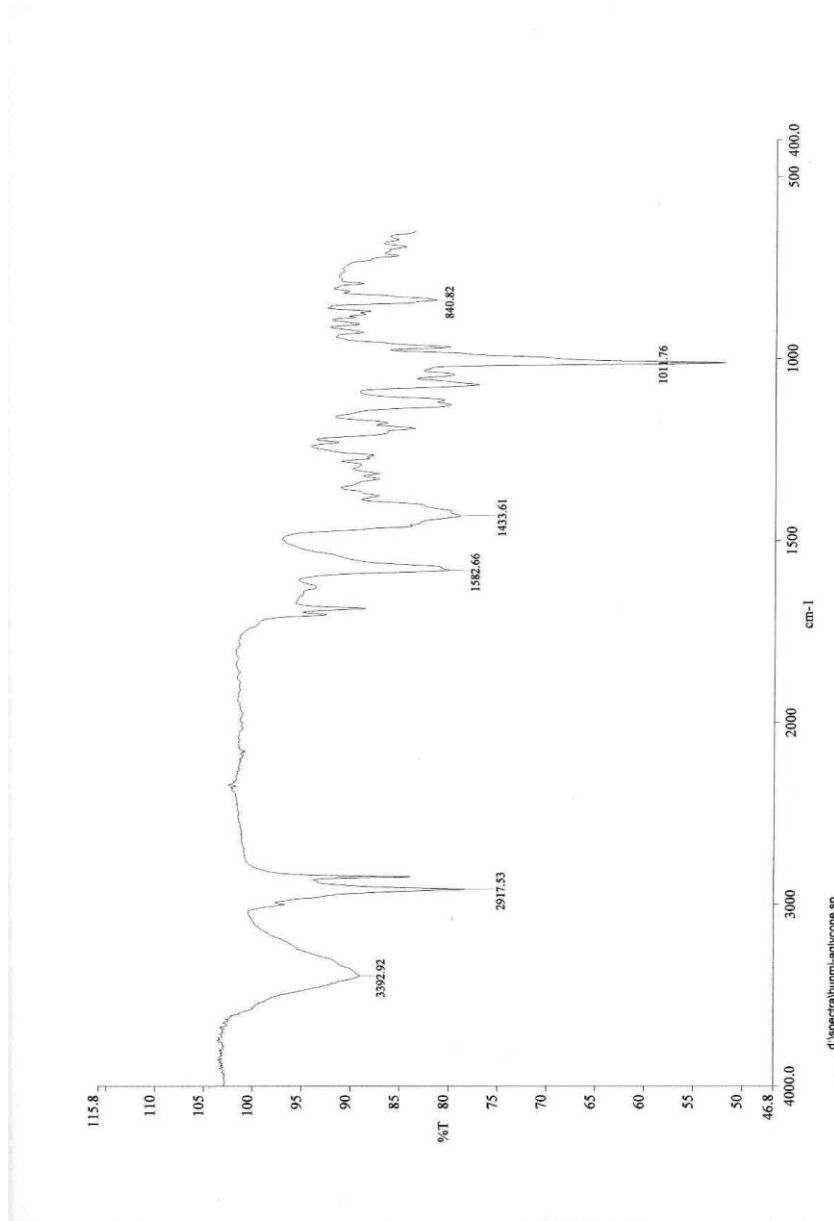


Figure 5 ATR-FTIR showing octabenzoyl aglycone

Preran	1.000 ml/min	A=85.00% B=15.00%
2.0 min	1.000 ml/min	A=85.00% B=15.00%
30.0 min	1.000 ml/min	A=75.00% B=25.00%
31.0 min	1.000 ml/min	A=20.00% B=80.00%
35.0 min	1.000 ml/min	A=20.00% B=80.00%
36.0 min	1.000 ml/min	A=85.00% B=15.00%

Figure 6 Method used for analytical HPLC for octabenzoyl aglycone

Prerun	14.800 ml/min	A=85.00% B=15.00%
2.0 min	14.800 ml/min	A=85.00% B=15.00%
30.0 min	14.800 ml/min	A=75.00% B=25.00%
31.0 min	14.800 ml/min	A=20.00% B=80.00%
35.0 min	14.800 ml/min	A=20.00% B=80.00%
36.0 min	14.800 ml/min	A=85.00% B=15.00%

Figure 7 Method used for Semi-preparative HPLC for octabenzoyl amphoteronolide B

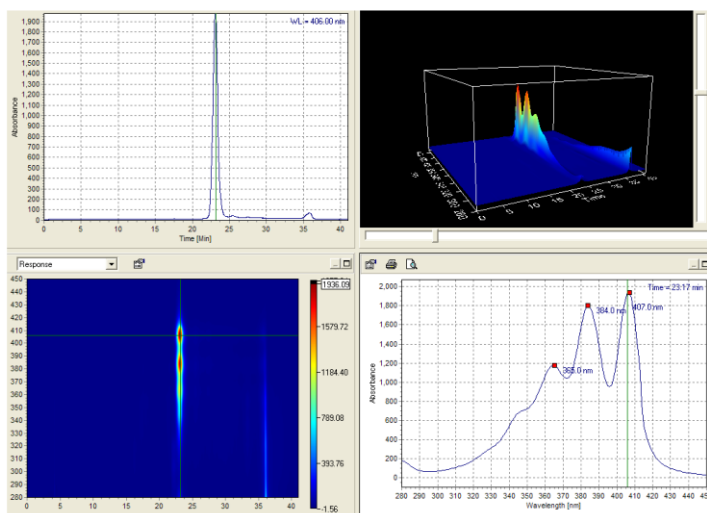


Figure 10 Si-HPLC on octabenzoyl amphoteronolide B

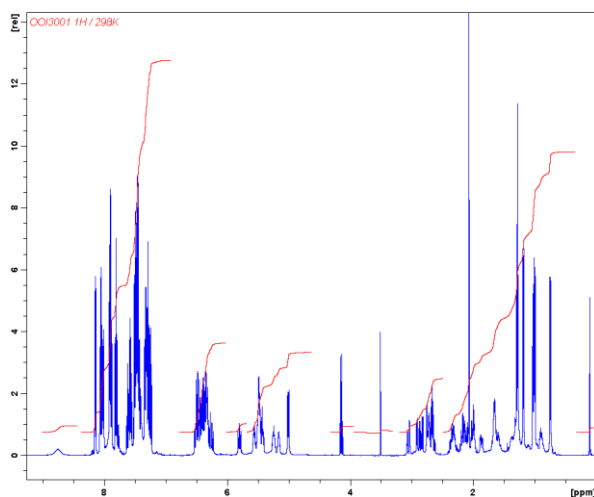


Figure 11 Proton NMR of octabenzoyl amphoteronolide B

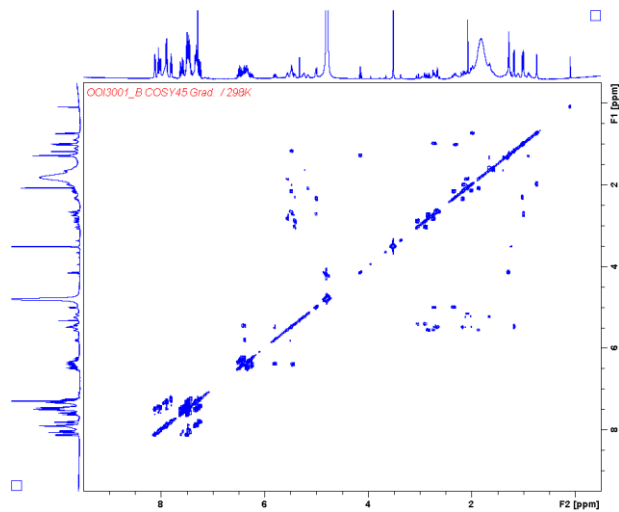


Figure 12 COSY for octabenzoyl amphoteronolide B

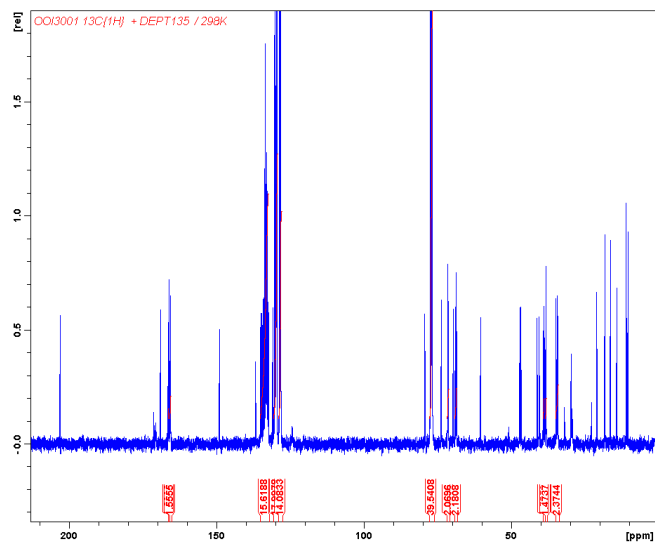


Figure 13 Carbon NMR of octabenzoyl amphoteronolide B

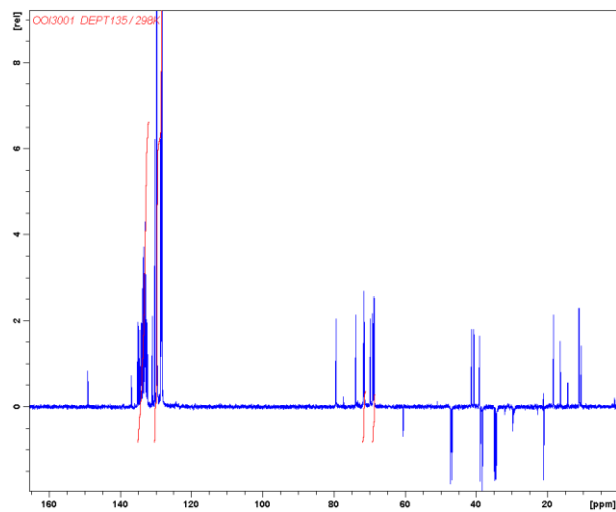


Figure 14 DEPT NMR of octabenzoyl amphoteronolide B

Appendix Two: Supplementary data for 16-
 descarboxyl-16-methyl-amphotericin B and its tetraene
 analogue from the “*Δ amphNM+perDIDI*” and
 ‘*amphNM*’ disruptants

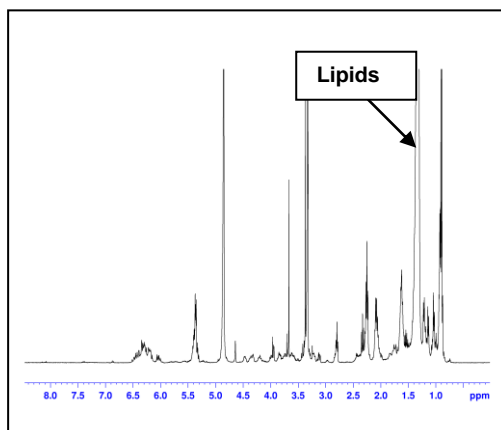


Figure 1 Proton NMR of 16-descarboxyl-16-methyl-
 amphotericin B (**17**) after water washes

Prerun	1.000 ml/min	A=50.00% B=50.00%
5.0 min	1.000 ml/min	A=50.00% B=50.00%
30.0 min	1.000 ml/min	A=5.00% B=95.00%
31.0 min	1.000 ml/min	A=0.00% B=100.00%
34.0 min	1.000 ml/min	A=0.00% B=100.00%
37.0 min	1.000 ml/min	A=50.00% B=50.00%
42.0 min	1.000 ml/min	A=50.00% B=50.00%

Figure 2 Method used for analytical RP-HPLC

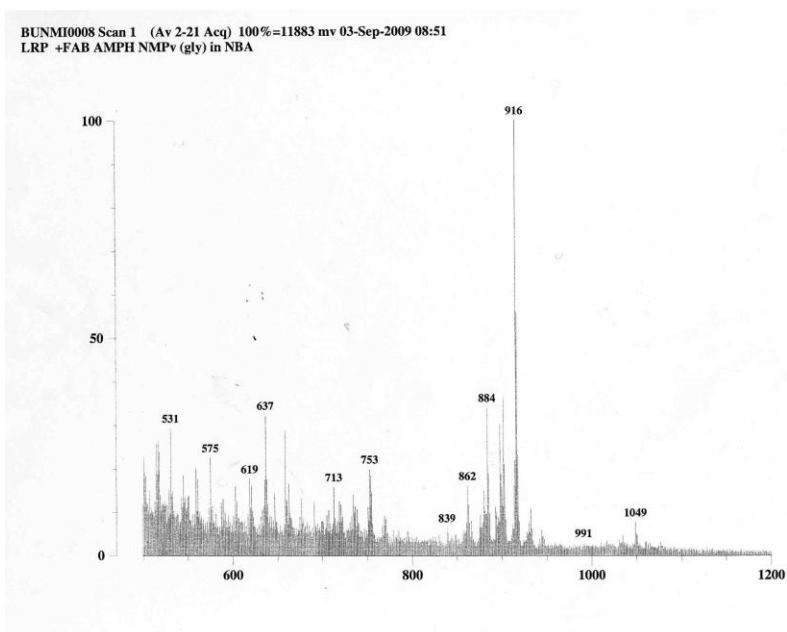


Figure 3 FAB-MS of 16-descarboxyl-16-methyl-amphotericin B (17)

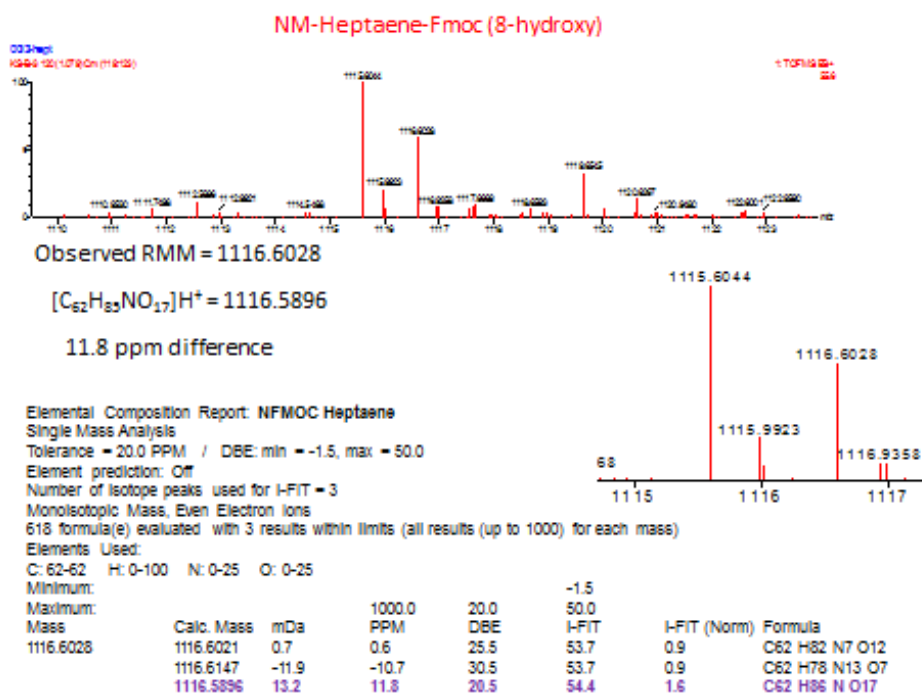


Figure 4 Elemental composition of N-Fmoc derivative of 16-descarboxyl-16-methyl-amphotericin B (17)

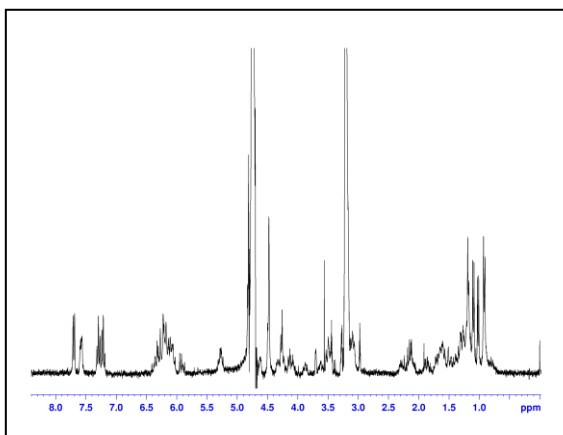


Figure 5 N-Fmoc NM (**61**) after HPLC prep

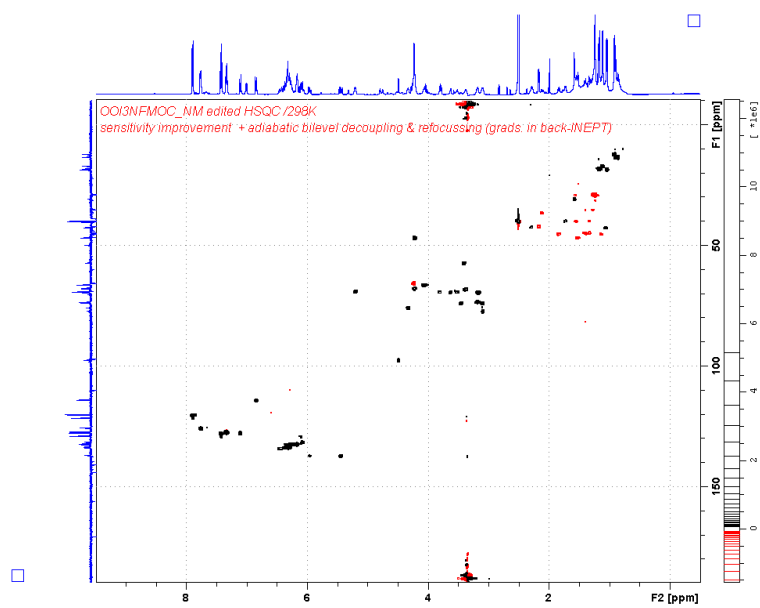


Figure 6 HSQC for N-Fmoc NM (**61**) after HPLC prep

Elemental Composition Report: NFMOC Tetraene						Observed RMM = 1124.5927	
Single Mass Analysis						[C ₆₂ H ₈₇ NO ₁₇] ^{Na} = 1124.5923	
Tolerance = 5.0 PPM / DBE: min = -1.5, max = 50.0						0.4 ppm difference	
Element prediction: Off							
Number of isotope peaks used for I-FIT = 3							
Monoisotopic Mass, Even Electron Ions							
1238 formula(e) evaluated with 2 results within limits (all results (up to 1000) for each mass)							
Elements Used:							
C: 62-62	H: 0-100	N: 0-25	O: 0-25	Na: 0-1			
Minimum:						-1.5	
Maximum:						50.0	
Mass	Calc. Mass	mDa	PPM	DBE	I-FIT	I-FIT (Norm)	Formula
1124.5927	1124.5923	0.4	0.4	19.5	47.3	0.2	C62 H87 N O16 Na
	1124.5947	-2.0	-1.8	33.5	48.9	1.8	C62 H74 N15 O6

NM-Tetraene-Fmoc

Elemental Composition Report: NFMOC Tetraene						Observed RMM = 1102.6311	
Single Mass Analysis						[C ₆₂ H ₈₇ NO ₁₆] ^H = 1102.6103	
Tolerance = 20.0 PPM / DBE: min = -1.5, max = 50.0						18.9 ppm difference	
Element prediction: Off							
Number of isotope peaks used for I-FIT = 3							
Monoisotopic Mass, Even Electron Ions							
621 formula(e) evaluated with 4 results within limits (all results (up to 1000) for each mass)							
Elements Used:							
C: 62-62	H: 0-100	N: 0-25	O: 0-25				
Minimum:						-1.5	
Maximum:						50.0	
Mass	Calc. Mass	mDa	PPM	DBE	I-FIT	I-FIT (Norm)	Formula
1102.6311	1102.6355	-4.4	-4.0	29.5	72.3	0.9	C62 H80 N13 O6
	1102.6229	8.2	7.4	24.5	72.5	1.0	C62 H84 N7 O11
	1102.6480	-16.9	-15.3	34.5	73.5	2.0	C62 H76 N19 O
	1102.6103	20.8	18.9	19.5	73.8	2.3	C62 H88 N O16

Figure 7 Elemental composition of N-Fmoc derivative of 8-deoxy-16-descarboxyl-16-methyl-amphotericin A (**54**)

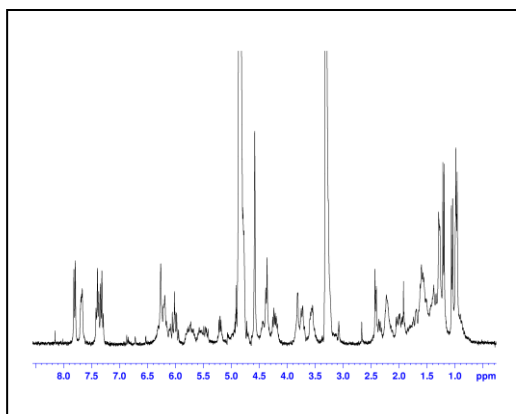


Figure 8 N-Fmoc NM tetraene (**63**) after HPLC prep

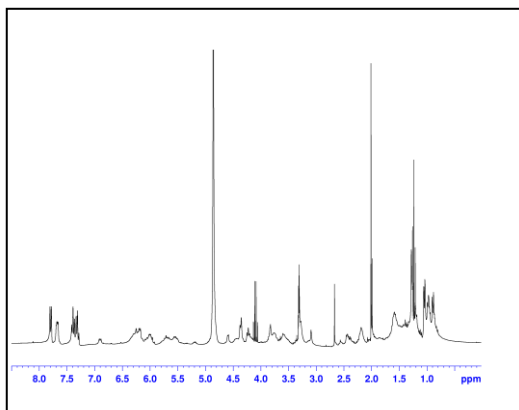


Figure 9 Proton NMR for N-Fmoc NM tetraene (**63**) after column x2

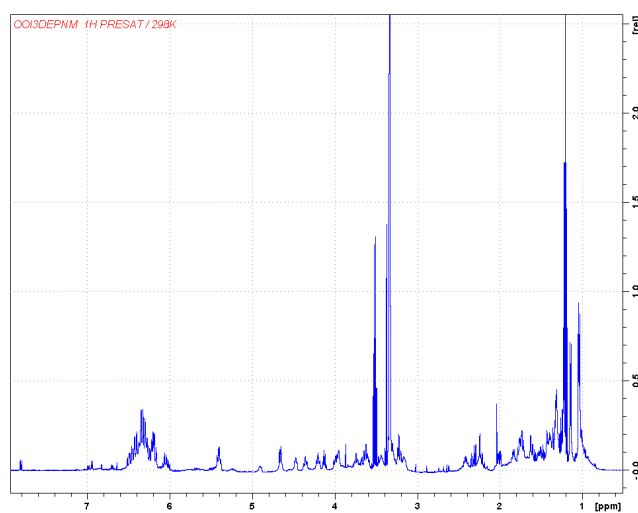


Figure 10 16-descarboxy-16-methyl-amphotericin B (**17**) after deprotection and HPLC prep

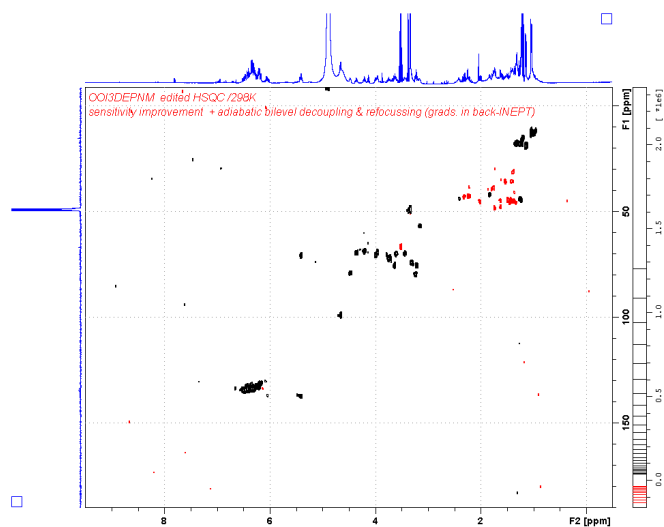


Figure 11 HSQC for **17** after deprotection and HPLC prep

Appendix Three: Supplementary data for 16- descarboxyl-16-methyl-19-(O)-perosaminyl- amphoteronolide B

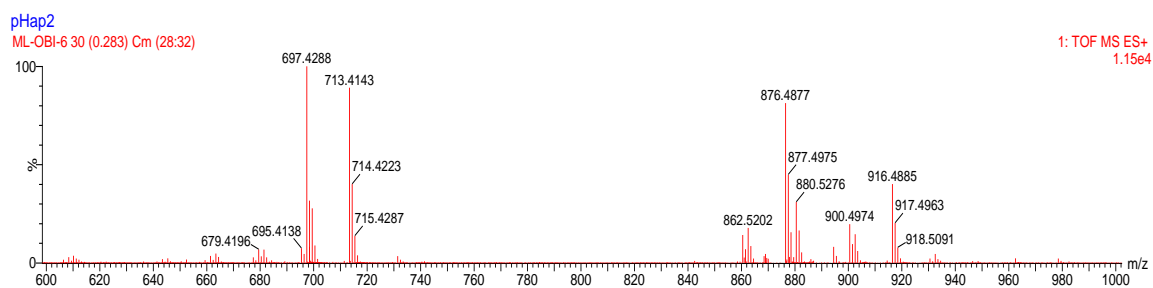


Figure 1 ESMS of pHap2 (**67**) after HPLC prep

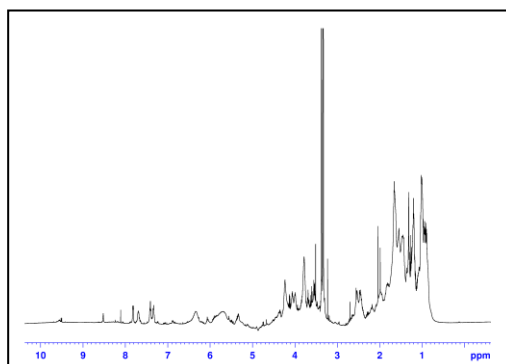


Figure 2 Proton NMR for the N-Fmoc pHap2 (**69**) after purification on three flash column

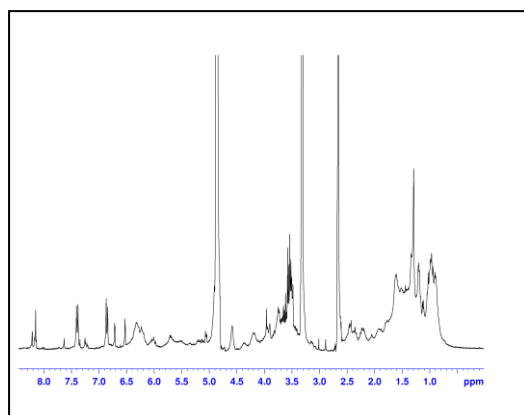


Figure 3 Deprotected pHap2 (**67**)

References

1. S. Ball, C. J. Bessell, and A. Mortimer, *J. Gen. Microbiol.*, 1957, **17**, 96–103.
2. F. Chappuis, S. Sundar, A. Hailu, H. Ghalib, S. Rijal, R. W. Peeling, J. Alvar, and M. Boelaert, *Nature Rev. Microbiol.*, 2007, **5**, 873–82.
3. L. Soler, P. Caffrey, and H. E. M. McMahon, *Biochim. Biophys. Acta*, 2008, **1780**, 1162–7.
4. M. Schafer-Korting and J. Blechschmidt, *Mycoses*, 1996, **39**, 329–339.
5. G. W. Gould, *Int. Biodeter. Biodegr.*, 1995, 267–277.
6. J. Brajtburg and J. Bolard, *Clin. Microbiol. Rev.*, 1996, **9**, 512–31.
7. P. Kovacic and A. Cooksy, *Med. Chem. Comm.*, 2012, **3**, 274.
8. K. C. Gray, D. S. Palacios, I. Dailey, M. M. Endo, B. E. Uno, B. C. Wilcock, and M. D. Burke, *P. Natl. Acad. Sci. USA*, 2012, **109**, 2234–9.
9. A. Czerwiński, W. A. König, P. Sowiński, L. Falkowski, J. Mazerski, and E. Borowski, *J. Antibiot.*, 1990, **43**, 1098–100.
10. M. Baginski, *BBA- Biomembranes*, 2002, **1567**, 63–78.
11. J. F. Aparicio, P. Caffrey, J. A. Gil, and S. B. Zotchev, *Appl. Microbiol. Biot.*, 2003, **61**, 179–88.
12. C. M. McNamara, S. Box, J. M. Crawforth, B. S. Hickman, T. J. Norwood, and B. J. Rawlings, *J. Chem. Soc., Perkin Trans. 1*, 1998, 83–88.
13. J. Mazerski, J. Grzybowska, and E. Borowski, *Eur. Biophys. J.*, 1990, **18**, 159–64.
14. T. Ehrenfreund-Kleinman, T. Azzam, R. Falk, I. Polacheck, J. Golenser, and A. J. Domb, *Biomaterials*, 2002, **23**, 1327–35.
15. R. D. Sloboda, G. Van Blaricom, W. A. Creasey, J. L. Rosenbaum, and S. E. Malawista, *Biochem. Biophys. Res. Co.*, 1982, **105**, 882–888.

16. A. Vermes, H. J. Guchelaar, and J. Dankert, *J. Antimicrob. Chemoth.*, 2000, **46**, 171–9.
17. R. B. Diasio, J. E. Bennett, and C. E. Myers, *Biochem. Pharmacol.*, 1978, **27**, 703–707.
18. F. Karst and F. Lacroute, *Molec. Gen. Genet.*, 1977, **154**, 269–277.
19. J. K. Volkman, *Appl. Microbiol. Biot.*, 2003, **60**, 495–506.
20. F. C. Odds, A. J. P. Brown, and N. A. R. Gow, *Trends Microbiol.*, 2003, **11**, 272–9.
21. S. Kelly, D. Lamb, D. Kelly, N. Manning, J. Loeffler, H. Hebart, U. Schumacher, and H. Einsele, *FEBS Lett.*, 1997, **400**, 80–82.
22. M. A. Pfaller, L. Boyken, R. J. Hollis, J. Kroeger, S. A. Messer, S. Tendolkar, and D. J. Diekema, *J. Clin. Microbiol.*, 2008, **46**, 150–6.
23. M. P. Arevalo, *J. Antimicrob. Chemoth.*, 2002, **51**, 163–166.
24. D. S. Perlin, *Drug Resist. Update*, 2007, **10**, 121–130. DOI: 10.1016/j.drug.2007.04.002
25. S. E. Orosz and D. L. Frazier, *J. Avian Med. Surg.*, 1995, **9**, 8–18.
26. J. Brajtburg, W. G. Powderly, G. S. Kobayashi, and G. Medoff, *Antimicrob. Agents Ch.*, 1990, **34**, 183–8.
27. A. Lemke, A. F. Kiderlen, and O. Kayser, *Appl. Microbiol. Biot.*, 2005, **68**, 151–62.
28. A. Chattopadhyay and M. Jafurulla, *Biochem. Biophys. Res. Co.*, 2011, **416**, 7–12.
29. D. Sacks and N. Noben-Trauth, *Nat. rev. Immunol.*, 2002, **2**, 845–58.
30. B. L. Herwaldt, *Lancet*, 1999, **354**, 1191–9.
31. P. Desjeux, *Comp. Immunol. Microbiol.*, 2004, **27**, 305–18.
32. S. Sundar and J. Chakravarty, *Expert Opin. Invest. Drugs*, 2008, **17**, 787–94.
33. G. Carneiro, D. C. M. Santos, M. C. Oliveira, A. P. Fernandes, L. S. Ferreira, G. A. Ramaldes, E. A. Nunan, and L. A. M. Ferreira, *J. Lipos. Res.*, 2010, **20**, 16–23.

34. H. W. Murray, J. D. Berman, C. R. Davies, and N. G. Saravia, *Lancet*, 2005, **366**, 1561–77.
35. P. Olliaro, S. Darley, R. Laxminarayan, and S. Sundar, *Trop. Med. Int. Health*, 2009, **14**, 918–25.
36. R. Demaimay, R. Race, and B. Chesebro, *J. Virol.*, 1999, **73**(4), 3511–3513.
37. S. J. Collins, V. Lewis, M. Brazier, A. F. Hill, A. Fletcher, and C. L. Masters, *Ann. Neurol.*, 2002, **52**, 503–506.
38. H. Rudyk, S. Vasiljevic, R. M. Hennion, C. R. Birkett, J. Hope, and I. H. Gilbert, *J. Gen. Virol.*, 2000, **81**, 1155–64.
39. A. Mange, N. Nishida, O. Milhavet, H. E. M. McMahon, D. Casanova, and S. Lehmann, *J. Virol.*, 2000, **74**, 3135–3140.
40. R. Demaimay, K. Adjou, C. Lasmézas, F. Lazarini, K. Cherifi, M. Seman, J. P. Deslys, and D. Dormont, *J. Gen. Virol.*, 1994, **75** (Pt 9), 2499–503.
41. M. Pocchiari, S. Schmittinger, and C. Masullo, *J. Gen. Virol.*, 1987, **68** (Pt 1), 219–23.
42. T. M. Folks, S. W. Kessler, J. M. Orenstein, J. S. Justement, E. S. Jaffe, and A. S. Fauci, *Science*, 1988, **242**, 919–22.
43. Y. D. Korin, D. G. Brooks, S. Brown, A. Korotzer, and J. A. Zack, *J. Virol.*, 2002, **76**(16), 8118–8123. DOI: 10.1128/JVI.76.8118-8123.2002
44. J. Kulkosky, *Blood*, 2001, **98**, 3006–3015.
45. J. P. Sheridan, *Science*, 1997, **277**, 818–821.
46. C. Van Lint, S. Emiliani, M. Ott, and E. Verdin, *EMBO J.*, 1996, **15**, 1112–1120.
47. G. Krupitza, H. Harant, E. Dittrich, T. Szekeres, H. Huber, and C. Dittrich, *Carcinogenesis*, 1995, **16**, 1199–205.
48. G. Jones, Y. Zhu, C. Silva, S. Tsutsui, C. A. Pardo, O. T. Keppler, J. C. McArthur, and C. Power, *Viol.*, 2005, **334**, 178–93.
49. A. Volmer, A. M. Szpilman, and E. M. Carreira, *Nat. Prod. Rep.*, 2010, **27**, 1329–49.

50. P. Kovacic, and A. Cooksy, *Med. Chem. Commun.*, 2012, **3**, 274–280.
51. M. M. Weber and S. C. Einsky, *J. Bacteriol.*, 1965, **89**, 306–312.
52. L. N. Ermishkin, K. M. Kasumov, and V. M. Potseluyev, *BBA - Biomembranes*, 1977, **470**, 357–367.
53. S. D. Rychnovsky and D. E. Mickus, *J. Org. Chem.*, 1992, **57**, 2732–2736.
54. M. J. Driver, A. R. Greenlees, W. S. Maclachlan, D. T. Macpherson, and A. W. Taylor, *Tetrahedron Lett.*, 1992, **33**, 4357–4360.
55. M. P. Croatt and E. M. Carreira, *Org. Lett.*, 2011, **13**, 1390–3.
56. Y. Umegawa, Y. Nakagawa, K. Tahara, H. Tsuchikawa, N. Matsumori, T. Oishi, and M. Murata, *Biochem.*, 2012, **51**, 83–9. DOI: 10.1021/bi2012542
57. B. de Kruijff, *Bioscience Rep.*, 1990, **10**, 127–30.
58. B. de Kruijff, W. Gerritsen, A. Oerlemans, R. Demel, and L. Vandeenen, *BBA - Biomembranes*, 1974, **339**, 30–43.
59. N. Matsumori, Y. Sawada, and M. Murata, *J. Am. Chem. Soc.*, 2005, **127**, 10667–10675.
60. J. Mazerski, J. Bolard, and E. Borowski, *BBA - Biomembranes*, 1995, **1236**, 170–176.
61. N. Matsumori, N. Yamaji, S. Matsuoka, T. Oishi, and M. Murata, *J. Am. Chem. Soc.*, 2002, **124**, 4180–1.
62. A. M. Szpilman, J. M. Manthorpe, and E. M. Carreira, *Angew. Chem. Int. Edit.*, 2008, **120**, 4411–4414.
63. D. S. Palacios, T. M. Anderson, and M. D. Burke, *J. Am. Chem. Soc.*, 2007, **129(45)**, 13804–13805. DOI:10.1021/ja075739o.
64. M. Baginski, K. Sternal, J. Czub, and E. Borowski, *Acta Biochim. Pol.*, 2005, **52**, 655–8.
65. N. Matsumori, Y. Umegawa, T. Oishi, and M. Murata, *Bioorg. Med. Chem. Lett.*, 2005, **15**, 3565–7.
66. M. Chéron, B. Cybulska, J. Mazerski, J. Grzybowska, A. Czerwiński, and E. Borowski, *Biochem. Pharmacol.*, 1988, **37**, 827–836.

67. P. Kovacic and A. Cooksy, *Med. Chem. Comm.*, 2012, **3**, 274.
68. K. C. Nicolaou, T. K. Chakraborty, Y. Ogawa, R. A. Daines, N. S. Simpkins, and G. T. Furst, *J. Am. Chem. Soc.*, 1988, **110**, 4660–4672.
69. H. Resat and M. Baginski, *Eur. Biophys. J.*, 2002, **31**, 294–305.
70. J. Szlinder-Richert, B. Cybulska, J. Grzybowska, E. Borowski, and R. Prasad, *Acta Biochim. Pol.*, 2000, **47**, 133–40.
71. K. Moribe, K. Maruyama, and M. Iwatsuru, *Int. J. Pharm.*, 1999, **193**, 97–106.
72. I. Blanc, M. Bueno Da Costa, J. Bolard, and M. Saint-Pierre Chazalet, *Biochim. Biophys. Acta*, 2000, **1464**, 299–308.
73. P. Caffrey, S. Lynch, E. Flood, S. Finnan, and M. Oliynyk, *Chem. Biol.*, 2001, **8**, 713–23.
74. T. Brautaset, O. N. Sekurova, H. Sletta, T. E. Ellingsen, A. R. Strøm, S. Valla, and S. B. Zotchev, *Chem. Biol.*, 2000, **7**, 395–403.
75. A. B. Campelo and J. A. Gil, *Microbiol.*, 2002, **148**, 51–59.
76. D. J. Bevitt, J. Staunton, and P. F. Leadlay, *Biochem. Soc. T.*, 1993, **21**, 30S.
77. E. De Poire, N. Stephens, B. Rawlings, and P. Caffrey, *Appl. Environ. Microb.*, 2013, **79**, 6156–9.
78. C. Méndez and J. A. Salas, *Trends Biotechnol.*, 2001, **19**, 449–56.
79. J. Aparicio, R. Fouces, M. Mendes, N. Olivera and J. Martin, *Chem. Biol.*, 2000, **7**, 895–905.
80. T. Brautaset, H. Sletta, A. Nedal, S. E. F. Borgos, K. F. Degnes, I. Bakke, O. Volokhan, O. N. Sekurova, I. D. Treshalin, E. P. Mirchink, A. Dikiy, T. E. Ellingsen, and S. B. Zotchev, *Chem. Biol.*, 2008, **15**, 1198–206.
81. S. E. F. Borgos, P. Tsan, H. Sletta, T. E. Ellingsen, J. M. Lancelin, and S. B. Zotchev, *J. Med. Chem.*, 2006, **49**, 2431–9.
82. T. Brautaset, H. Sletta, K. F. Degnes, O. N. Sekurova, I. Bakke, O. Volokhan, T. Andreassen, T. E. Ellingsen, and S. B. Zotchev, *Appl. Environ. Microb.*, 2011, **77**, 6636–43.

83. A. N. Tevyashova, E. N. Olsufyeva, S. E. Solovieva, S. S. Printsevskaya, M. I. Reznikova, A. S. Trenin, O. A. Galatenko, I. D. Treshalin, E. R. Pereverzeva, E. P. Mirchink, E. B. Isakova, S. B. Zotchev, and M. N. Preobrazhenskaya, *Antimicrob. Agents Ch.*, 2013, **57**, 3815–22.
84. M. Carmody, B. Byrne, B. Murphy, C. Breen, S. Lynch, E. Flood, S. Finnan, and P. Caffrey, *Gene*, 2004, **343**, 107–115.
85. B. Murphy, K. Anderson, C. Borissow, P. Caffrey, G. Griffith, J. Hearn, O. Ibrahim, N. Khan, N. Lamburn, M. Lee, K. Pugh, and B. Rawlings, *Org. Biomol. Chem.*, 2010, **8**, 3758–70.
86. P. Power, T. Dunne, B. Murphy, L. Nic Lochlainn, D. Rai, C. Borissow, B. Rawlings, and P. Caffrey, *Chem. Biol.*, 2008, **15**, 78–86.
87. B. Byrne, M. Carmody, E. Gibson, B. Rawlings, and P. Caffrey, *Chem. Biol.*, 2003, **10**, 1215–1224.
88. P. Power, T. Dunne, B. Murphy, L. Nic Lochlainn, D. Rai, C. Borissow, B. Rawlings, and P. Caffrey, *Chem. Biol.*, 2008, **15**, 78–86.
89. O. Volokhan, H. Sletta, T. E. Ellingsen, and S. B. Zotchev, *Appl. Environ. Microb.*, 2006, **72**, 2514–2519.
90. M. V Mendes, N. Antón, J. F. Martín, and J. F. Aparicio, *Biochem. J.*, 2005, **386**, 57–62.
91. P. M. Kells, H. Ouellet, J. Santos-Aberturas, J. F. Aparicio, and L. M. Podust, *Chem. Biol.*, 2010, **17**, 841–51.
92. M. Carmody, B. Murphy, B. Byrne, P. Power, D. Rai, B. Rawlings, and P. Caffrey, *J. Biol. Chem.*, 2005, **280**, 34420–6.
93. E. Hutchinson, B. Murphy, T. Dunne, C. Breen, B. Rawlings, and P. Caffrey, *Chem. Biol.*, 2010, **17**, 174–82.
94. J. A. Gil and A. B. Campelo-Diez, *Appl. Microb. Biot.*, 2003, **60**, 633–42.
95. E. M. Seco, F. J. Pérez-Zúñiga, M. S. Rolón, and F. Malpartida, *Chem. Biol.*, 2004, **11**, 357–66.
96. T. Brautaset, H. Sletta, A. Nedal, S. E. F. Borgos, K. F. Degnes, I. Bakke, O. Volokhan, O. N. Sekurova, I. D. Treshalin, E. P. Mirchink, A. Dikiy, T. E. Ellingsen, and S. B. Zotchev, *Chem. Biol.*, 2008, **15**, 1198–206.

97. J. Pawlak, P. Sowinski, E. Borowski, and P. Gariboldi, *J. Antibiot.*, **48**, 1034–1038.
98. K. C. Nicolaou, R. A. Daines, Y. Ogawa, and T. K. Chakraborty, *J. Am. Chem. Soc.*, 1988, **110**, 4696–4705.
99. H. Tsuchikawa, N. Matsushita, N. Matsumori, M. Murata, and T. Oishi, *Tetrahedron Lett.*, 2006, **47**, 6187–6191.
100. E. Atherton, C. Bury, R. C. Sheppard, and B. J. Williams, *Tetrahedron Lett.*, 1979, **32**, 3941–3942.
101. Y. Han, *J. Org. Chem.*, 1986, **37**, 3404–3409.
102. H. Tsuchikawa, N. Matsushita, N. Matsumori, M. Murata, and T. Oishi, *Tetrahedron Lett.*, 2006, **47**, 6187–6191.
103. K. Hostettmann, M. Hostettmann-Kaldas and O. Sticher, *J Chromatogr. A*, 1980, **202**, 154–156.
104. A. Carpino, *Accounts Chem. Res.*, 1987, 401–407.
105. A. Zumbuehl, D. Jeannerat, S. E. Martin, M. Sohrmann, P. Stano, T. Vigassy, D. D. Clark, S. L. Hussey, M. Peter, B. R. Peterson, E. Pretsch, P. Walde, and E. M. Carreira, *Angew. Chemie Int. Edit.*, 2004, **116**, 5293–5297.
106. C. J. Thibodeaux, C. E. Melançon, and H. Liu, *Angew. Chemie Int. Edit.*, 2008, **47**, 9814–59.
107. V. Kren and L. Martínková, *Curr. Med. Chem.*, 2001, **8**, 1303–28.
108. D. Hoffmeister, B. Wilkinson, G. Foster, P. J. Sidebottom, K. Ichinose, and A. Bechthold, *Chem. Biol.*, 2002, **9**, 287–295.
109. L. Nic Lochlainn and P. Caffrey, *Metab. Eng.*, 2009, **11**, 40–7.
110. Y. Sun, F. Zeng, W. Zhang, and J. Qiao, *Gene*, 2012, **499**, 288–96.
111. X. Mao, F. Wang, J. Zhang, S. Chen, Z. Deng, Y. Shen, and D. Wei, *Appl. Biochem. Biotech.*, 2009, **159**, 673–86.
112. S. Heia, S. E. F. Borgos, H. Sletta, L. Escudero, E. M. Seco, F. Malpartida, T. E. Ellingsen, and S. B. Zotchev, *Appl. Environ. Microb.*, 2011, **77**, 6982–90.
113. J. M. Winter and Y. Tang, *Curr. Opin. Biotech.*, 2012, **23**, 736–43.

- | |
|--|
| |
| |
114. S. Donadio, J. B. McAlpine, P. J. Sheldon, M. Jackson, and L. Katz, *P. Natl. Acad. Sci. USA*, 1993, **90**, 7119–23.
 115. S. Khaliq, K. Akhtar, M. Afzal Ghauri, R. Iqbal, A. Mukhtar Khalid, and M. Muddassar, *Microbiol. Res.*, 2009, **164**, 469–77.
 116. A. Freitag, C. Méndez, J. A. Salas, B. Kammerer, S. M. Li, and L. Heide, *Metab. Eng.*, 2006, **8**, 653–61.
 117. A. Trefzer, C. Fischer, S. Stockert, L. Westrich, E. Künzel, U. Girreser, J. Rohr, and A. Bechthold, *Chem. Biol.*, 2001, **8**, 1239–52.
 118. M. Kawabata, M. Onda, and T. Mita, *J. Biochem.*, 2001, **129**, 725–32.